INTERANNUAL VARIABILITY OF NORTH AMERICAN MONSOON

HYDROCLIMATE AND APPLICATION TO WATER MANAGEMENT IN THE

PECOS RIVER BASIN

by

KATRINA AMELIA GRANTZ

B.A., Grinnell College, 1997

M.S., University of Colorado, 2003

A thesis submitted to the faculty of the Graduate School of the

University of Colorado in partial fulfillment of the requirement for the degree of

Doctor of Philosophy

Department of Civil, Environmental, and Architectural Engineering

2006

This thesis entitled:

Interannual Variability of the North American Monsoon Hydroclimate and

Application to Water Management in the Pecos River Basin

written by Katrina A. Grantz

has been approved for the

Department of Civil, Environmental, and Architectural Engineering

_____

Balaji Rajagopalan

_____

Edith Zagona

_____

Kenneth Strzepek

Date _____

The final copy of this thesis has been examined by the signatories, and we find that

both the content and the form meet acceptable presentation standards of scholarly

work in the above mentioned discipline.

Grantz, Katrina A. (Ph.D., Civil, Environmental, and Architectural Engineering)

Interannual Variability of the North American Monsoon Hydroclimate and

Application to Water Management in the Pecos River Basin

Thesis directed by Professor Balaji Rajagopalan

The North American Monsoon (NAM) is the large-scale atmospheric circulation system responsible for up to 55% of the annual precipitation in the southwestern U.S. These summer thunderstorms, however, are highly variable and predicting the variability in the strength, location, and timing of monsoonal precipitation and streamflow is understandably very important for efficient water resources management.

This research, comprised of three main components, analyzes the spatial and temporal variability of NAM precipitation and streamflow; and using this information it develops a statistical forecasting framework which is then integrated with a decision support system to evaluate water management strategies on the Pecos River Basin. First, the interannual variability of precipitation and streamflow in the NAM region of southwest U.S. is studied and large-scale and local climate features that drive the variability are diagnosed using robust Spearman rank correlation analysis and Kendall Theil slope estimators. These analyses led to the proposal of the following hypothesis: antecedent Pacific sea surface temperatures (SSTs) modulate the winter/spring hydroclimatology and land conditions of the NAM region, thus playing an important role in setting up the land-ocean temperature gradient (the key driver of the NAM), and, consequently, in modulating monsoonal rainfall and precipitation. This offers increased hopes of long-lead forecasts of summer

hydrologic conditions in the NAM region. The second component of this study develops a framework for generating ensemble forecasts of spring and summer streamflow at five lead times using the large-scale climate information obtained from the diagnostics. In the third, and final, component of this study, streamflow exceedance probabilities calculated from the ensemble forecasts are used in a decision support system, modeled with RiverWare, to evaluate various water management options for reservoir releases, irrigation diversions and inter-state spill in the Pecos River Basin. The Pecos River receives a significant portion of its annual streamflow in the summertime from monsoon thunderstorms, however operations on the river do not utilize forecasts of this important moisture source. The research framework developed here demonstrates significant improvements to water management though decreased reservoir spills and increased irrigation water delivery.

ACKNOWLEDGEMENTS

CONTENTS

TABLES

FIGURES

CHAPTER 1

INTRODUCTION

Motivation

The southwestern United States and northwest Mexico receive a significant portion of their annual precipitation during the summer months of July, August, and September. This summertime precipitation phenomenon known as the North American Monsoon (NAM) accounts for up to 55% of the annual precipitation in the southwestern U.S. and up to 80% in northwest Mexico (Douglas et al. 1993). However, this important moisture source is highly variable, especially in the southwestern U.S. region comprising Arizona and New Mexico. Presently, water and agriculture managers largely ignore the influence of summer monsoon rainfall in planning and management due to its high variability. Nevertheless, the variability of the NAM is of particular concern for watershed managers, farmers, and planners in the arid region as too little summer rainfall has negative agricultural and environmental impacts and heavy summer thunderstorms present the danger of flash floods. Thus, understanding and predicting the variability in the strength and location of monsoonal precipitation and streamflow and planning the coordination with spring streamflows is key to efficient water resources management in the region.

NAM Background

The NAM is the large-scale atmospheric circulation system that drives the dramatic increase in rainfall experienced in the desert southwest U.S. and

northwestern Mexico during the summer months of July, August and September. These summer thunderstorms typically begin in early July and last until mid-September and can account for as much as 50-70 percent of the annual precipitation in the arid region (Carleton et al. 1990; Douglas et al. 1993; Higgins et al. 1997; Mitchell et al. 2002; Sheppard et al. 2002).

Geographically, the NAM is centered over the Sierra Madre Occidental, a mountain range in northwestern Mexico (Douglas et al. 1993; Barlow et al. 1998), however it extends into New Mexico, Arizona, and southern Colorado and Utah (e.g., Douglas et al. 1993; Hawkins et al. 2002; Lo and Clark 2002). Several researchers (e.g., Brenner 1974; Hales 1974; Houghton 1979; Tang and Reiter 1984; Reiter and Tang 1984) have defined the NAM region to be much larger, covering the entire plateau of western North America.

The NAM is established when the winds shift from a generally westerly direction in winter to southerly flow in summer. This shift is responsible for bringing moist air from the Gulf of California, the eastern Pacific Ocean and the Gulf of Mexico northward to the land during the summer months (Adams and Comrie 1997). The combination of moist air and warm land surfaces causes convective instability, thus producing frequent summer precipitation events (Adams and Comrie 1997; Barlow et al. 1998). The seasonal shift in the winds that brings in monsoonal moisture depends primarily upon the relative location of the subtropical jet during the summer months. The subtropical ridge typically migrates northward during the summer months. Several studies have shown that a more northward displacement of the subtropical ridge is associated with a wetter monsoon over the southwestern U.S..

In years when the ridge stays in a more southerly position, the transport of tropical moisture is inhibited (Carleton 1986; Carleton et al. 1990; Adams and Comrie 1997; Comrie and Glen 1998; Ellis and Hawkins 2001; Hawkins et al. 2002).

The source of moisture for the NAM, either the Gulf of Mexico or the Gulf of California, has been debated for decades (e.g., Bryson and Lowry 1955; Reitan 1957; Rasmussen 1967; Hales 1972; Brenner 1974; Mullen et al 1998). Determining the source of monsoonal moisture is particularly important for prediction purposes. The current consensus is that while the Gulf of California and eastern Pacific provide the majority of total monsoonal moisture, the Gulf of Mexico also provides an important contribution.

The complex nature of the moisture source and transport mechanism together with extremely varied topography in the region makes it difficult to understand the spatial variability of the NAM. Regionally, the intensity of the NAM decreases and the variability increases as one moves northward of the Sierra Madre Occidental into in the regions of Arizona, New Mexico, and southern Colorado.

Temporal variability of the NAM ranges from diurnal to seasonal, to interannual, to interdecadal. Diurnal variability is dominated by precipitation peaking in the afternoon and early evening (Dai et al. 1999; Berbery 2001; Trenberth et al. 2003; Anderson and Kanamaru 2004). On an intra-seasonal scale, particularly the northern parts of the monsoon region experience wet and dry spells within a monsoon season. This is likely related to a gulf surge phenomenon that brings moisture up the Gulf of California in intermittent bursts (Hales 1972; Brenner 1974). Carleton (1986, 1987) demonstrated that periods of convective activity across the

southwestern U.S. are associated with passing upper-level troughs in the westerlies. Also, as noted earlier, the position of the subtropical ridge significantly affects convective activity (Carleton 1986; Carleton et al. 1990; Adams and Comrie 1997; Comrie and Glen 1998; Ellis and Hawkins 2001; Hawkins et al. 2002).

Interannual variability is presumed to result from variability in certain synoptic-scale patterns as well as variability in the initial conditions of the landmass and Pacific Ocean Sea Surface Temperatures (SSTs). Carleton et al. (1990) observed that shifts in the subtropical ridge are related to the phase of the Pacific/North American (PNA) pattern (which is related to the El Niño-Southern Oscillation (ENSO)), where a positive (negative) PNA pattern in winter is typically followed by a northward (southward) displacement of the subtropical jet and a wet (dry) summer monsoon. Higgins et al. (1999) found that cold (warm) tropical Pacific SST anomalies appear near the dateline prior to wet (dry) monsoons and that the anomalies increase in amplitude during the spring. Other studies (Higgins and Shi 2000; Mo and Paegle 2000) found that anomalously cold SSTs in the northern Pacific and anomalously warm SSTs in the subtropical northern Pacific contribute to a wetter and earlier monsoon season. Castro et al. (2001) observed similar relationships with Pacific SSTs linking a high (low) Pacific Decadal Oscillation (PDO) phase and El Niño (La Niña) with a southward (northward) displaced monsoon ridge and a late (early) monsoon onset and below (above) average early monsoon rainfall. Mitchell et al. (2002) determined certain threshold SST values for the northern Gulf of California that are associated with the regional onset of the NAM.

Land surface conditions also play an extensive role in the onset and intensity of the NAM. Within a monsoon season increased soil moisture impacts evapotranspiration between storm events, thus enhancing future storm systems and precipitation (Matusi et al. 2003). On an interseasonal scale, several studies have demonstrated an inverse relationship between winter precipitation, particularly snowfall, and subsequent summer precipitation (Higgins et al. 1998; Gutzler 2000; Higgins and Shi 2000; Lo and Clark 2002; Zhu et al. 2005). This relationship is thought to result from snowfall acting as an energy sink. Greater amounts of snowfall in winter require more energy to melt and evaporate the moisture by summer. Larger snow cover areas also increase the albedo in spring, thus reinforcing the relationship. The resulting delayed and decreased warming of the North American landmass upsets the land-ocean heating contrasts necessary for monsoonal circulation patterns, thus delaying and decreasing the intensity of the NAM. The relationship between antecedent land conditions and monsoonal precipitation, however, appears to vary spatially and temporally (Lo and Clark 2002; Zhu et al. 2005) and the intensity of the monsoon may depend more on large-scale forcings than local antecedent soil moisture conditions (Zhu et al. 2005).

There have been few studies on understanding the spatio-temporal variability of monsoonal streamflow in the NAM region (e.g., Gochis et al., 2003). This is very important for improving water management in the region. Furthermore, the variability in the timing of the monsoon seasonal cycle is important, especially for crop planting and water management (Ray et al., 2005), though this aspect of the NAM is not well understood. Several recent studies have illustrated an earlier onset

of spring in the western United States (e.g., Dettinger and Cayan 1995; Cayan et al. 2001; Mote 2003; Stewart et al. 2004; Regonda et al. 2005), however this has not been studied in relation to the NAM.

Outline of the study

Given this motivation and background, there is a clear need to incorporate the understanding of interannual variability in NAM precipitation and streamflow into water resources management. Thus, three key questions emerge: (i) What is the spatial and temporal variability of NAM hydroclimatology (i.e. precipitation and streamflow and their seasonality) and its potential drivers? (ii) What is the potential for seasonal streamflow forecasting in the NAM region? (iii) How can this potential be realized to improve water resources management? An integrated framework, consisting of three inter-related components shown in Figure 1, is proposed to address the above questions. The thesis is outlined as follows.
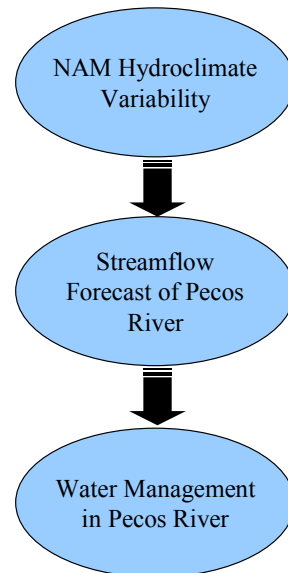
Figure 1. Flowchart of study.

In Chapter 2, a systematic analysis of daily and monthly precipitation in the NAM region is undertaken. The objective is to understand the spatial and temporal variability of NAM precipitation (both magnitude and seasonal cycle) at interannual and interdecadal time scales and also to discern the role of land-ocean-atmospheric features in modulating this variability.

A similar detailed analysis of the variability of streamflow (both spring and summer) in the NAM region is performed in Chapter 3. The understanding of the interannual variability of the streamflow will also shed light on the potential predictability of seasonal streamflow in the NAM region.

Chapter 4 develops a seasonal streamflow forecasting model. Water resources management on the Pecos River Basin is chosen to demonstrate the utility of the knowledge of hydroclimate variability acquired from the diagnostics efforts in Chapters 2 and 3. Based on operations and management in the Pecos Basin, the various seasonal streamflows of interest and the lead times of their desired prediction are established. Predictors of these seasonal flows and at the desired lead times are identified from large-scale land-ocean-atmosphere variables. Using the predictors, a nonparametric functional estimation model is developed to generate cross-validated ensemble seasonal streamflow forecasts and the skills of these forecasts are evaluated.

In Chapter 5, the ensemble forecasts are used to drive policy alternatives in a decision support model of the water resources management in the Pecos River Basin. Thus, improvements to management based on the streamflow forecasts are evaluated relative to current practices that do not consider seasonal streamflow forecasts. This

integration of hydroclimate variability knowledge and predictions with a decision support model constitutes a unique and important contribution.

A summary of the key findings and contributions from each component of the research along with recommendations for future extensions is presented in Chapter 6.

CHAPTER 2

PRECIPITATION ANALYSIS

Introduction

      This chapter presents a systematic analysis of the space-time variability of North American monsoon (NAM) precipitation over the southwestern U.S. and its land and oceanic drivers. An overview of the data sets and methodology is presented first. Next, the monsoon seasonal cycle is studied, followed by an analysis of rainfall volume trends. A hypothesis that explains the trends is proposed. The hypothesis is tested by investigating the links between antecedent land and oceanic conditions and the timing and strength of the monsoon. The chapter closes with a summary and conclusions.

Data

      The data sets used in this study are described below.

Climate Division Data

      Monthly precipitation, temperature, and Palmer Drought Severity Index (PDSI) data from 8 climate divisions covering New Mexico (NM) and 7 divisions for Arizona (AZ) for the years 1948-2004 were used. The climate divisions and data sets are obtained from www.cpc.ncep.noaa.gov.

Daily precipitation data were obtained from the National Weather Service (NWS) cooperative network (COOP). Most COOP stations have records beginning from the mid-1900s. Stations with continuous daily records from 1948-1999 across NM and AZ were selected amounting to 219 stations in total.

NCEP/NCAR Re-analysis Data

Monthly values of large-scale ocean and atmosphere variables, e.g., sea surface temperatures (SSTs), geopotential heights, precipitable water, winds, etc., from the NCEP/NCAR Re-analysis data set (Kalnay et al. 1996) were obtained from www.cdc.noaa.gov for the years 1948-2004.

Methodology

To understand the seasonal cycle and 'timing' of the monsoon, the Julian day when the 10th, 25th, 50th, 75th, and 90th percentile of the monsoonal (July to September) precipitation occurred is first identified for each year at all the COOP stations. The Julian day at these five thresholds helps capture the entire monsoon cycle. This provides an objective means for representing the monsoon cycle uniformly across all locations without resorting to subjective definitions for determining the monsoon onset or end. Various researchers (e.g., Higgins et al. 1998, 1999; Ellis et al. 2004) have used different methods to determine/define the onset and demise of the NAM. These typically involve analyses of detailed humidity and precipitation data and the development of different threshold criteria, some of which are location specific. The approach employed in this research is both simple and

unique in that it captures the entire seasonal cycle of the NAM, rather than just the onset or closing of the monsoon.

Nonparametric trend analysis based on Spearman rank correlation (Helsel and Hirsch 1995) is performed on the 10th, 25th, 50th, 75th, and 90th percentile Julian days at all the stations. The Spearman rank correlation is similar to the standard correlation coefficient (i.e., Pearson's R), except that it does not require that data be normally distributed and it is robust against outliers. To perform the Spearman rank correlation in this study, one station's time series of Julian days when 50 percent of monsoonal precipitation occurred is selected and these Julian day values are converted to ranks. These ranks are then plotted against the corresponding year in which the value occurred and a linear regression is fit. The robust Kendall Theil slope estimator (Helsel and Hirsch 1995) is used to calculate the magnitude (number of days) and direction (earlier or later) of the timing shift. The Kendall Theil method is robust to outliers and estimates slope by calculating the median of the slopes between all combinations of two points in the data. This process is repeated for each station and for the other percentiles (10th, 25th, 75th, and 90th) of precipitation. The estimated trends in 'timing' are then spatially mapped. Stations exhibiting a trend at the 90% significance level or above are highlighted. The spatial maps of the 90% and 95% significance results were found to be, largely, the same and almost all of them are field significant at the 95% significance level. However, the 90% significance figures are shown so as to better illustrate the spatial extent of the trends. Similar analyses are performed on the monsoon monthly and seasonal rainfall amounts as well as the precipitable water. It is recognized that the Spearman rank correlation

trend analysis, like other trend analyses, is sensitive to the data at the beginning and the end of the period of record. However, because the Spearman rank correlation trend analysis uses ranks and is thus robust against outliers, the trends are less sensitive to extreme wet periods and dry periods.

The field significance of the spatial patterns of the trends and correlations is determined using the method proposed by Livezey and Chen (1983). For a spatial map to be field significant at the 95% confidence level at least 16 locations (out of 219 coop stations) and 2 divisions (out of 15 climate divisions) should exhibit significant trends and correlations.

To understand the physical mechanisms driving the trends, the relationship between antecedent (Dec-May) land/ocean conditions and summer rainfall is analyzed. First, the Spearman rank correlation analysis is performed to detect trends in antecedent precipitation and soil moisture (PDSI is used as a proxy for this). The PDSI is used as a surrogate for soil moisture primarily because the quality and quantity of soil moisture data required for this study was unavailable. The PDSI is an integrated measure of rainfall and temperature and is thus a good indicator of the soil moisture. Simms et al. (2002) found good correspondence between PDSI and soil moisture in North Carolina and Guttman et al. (1992) suggested that the PDSI is best suited for semiarid and dry climate regions. Together, these studies suggest that PDSI is an appropriate proxy for soil moisture in the NAM region.

Next, the leading modes of timing and rainfall amounts from the summer season are correlated with the antecedent ocean, atmosphere and land conditions. The leading modes are obtained by performing principal component analysis (PCA) on

the Julian day and monthly rainfall time series. PCA, which is widely used in climate research, decomposes a space-time random field into orthogonal space and time patterns using Eigen decomposition and effectively reduces the dimensions of the data (von Storch and Swiers 1999). In PCA the patterns are automatically ordered according to the percentage of variance captured; that is, the first space-time pattern, also called the leading mode or first principal component (PC), captures the most variance present in the data, and so on. In this research, for example, the 50th percentile rainfall Julian days of the multivariate data is represented by a 52 by 219 matrix with the years in rows and the stations in columns. PCA is performed resulting in 219 PC time series, the first few of which capture most of the variance among the stations. This is repeated for the other Julian day time series (i.e., 10th, 25th, 75th, and 90th percentiles) and the monthly (i.e., July, August and September) rainfall time series. In all cases the first spatial pattern or Eigen vector was found to have similar magnitude and sign across the spatial locations and the first PC was highly correlated with the spatial average time series. Thus the first PC was used to represent the timing and amount across the region rather than a straight spatial average. This first PC, as an average spatial index, is then correlated with the antecedent ocean, atmosphere and land conditions.

Analysis of the rainfall amount is performed using the monthly climate division data since, unlike the COOP data, this data set extends until the present. The COOP and climate division data, however, are quite consistent, and a comparative analysis found that the results are insensitive to the data set. For the timing analysis, the daily COOP data is required.

Results

The results from the trend analysis of the timing and rainfall amounts are presented first, followed by the relationships to antecedent large-scale climate variables and the physical mechanisms. Based on these results a hypothesis for the monsoon variability is proposed.

Monsoon Cycle

Julian day trends at the five threshold levels (10th, 25th, 50th, 75th, and 90th percentile) significant at the 90% level are shown in Figure 2. It can be seen that there is a significant delay in the entire monsoon cycle (i.e., all five percentiles) over the monsoon region. With well over 21 stations exhibiting a statistically significant trend across the NAM region, the spatial trend maps are field significant at the 95% confidence level for all threshold percentiles. The shifts are on the order of 10 to 20 days, depending on the station. To put these shifts in perspective, the median Julian days, that is, the median of all historical data for all stations, for these thresholds are also shown in Figure 2. Climatologically, the monsoon begins in early July, reaching 10% of the total precipitation by (or on) July 19th; the peak of the monsoon (when 50% of the precipitation has fallen) occurs around August 13th (roughly a week earlier in Arizona than in New Mexico) and the monsoon typically nears its end (when 90% of the total precipitation has fallen) roughly at the end of August and into the beginning of September.
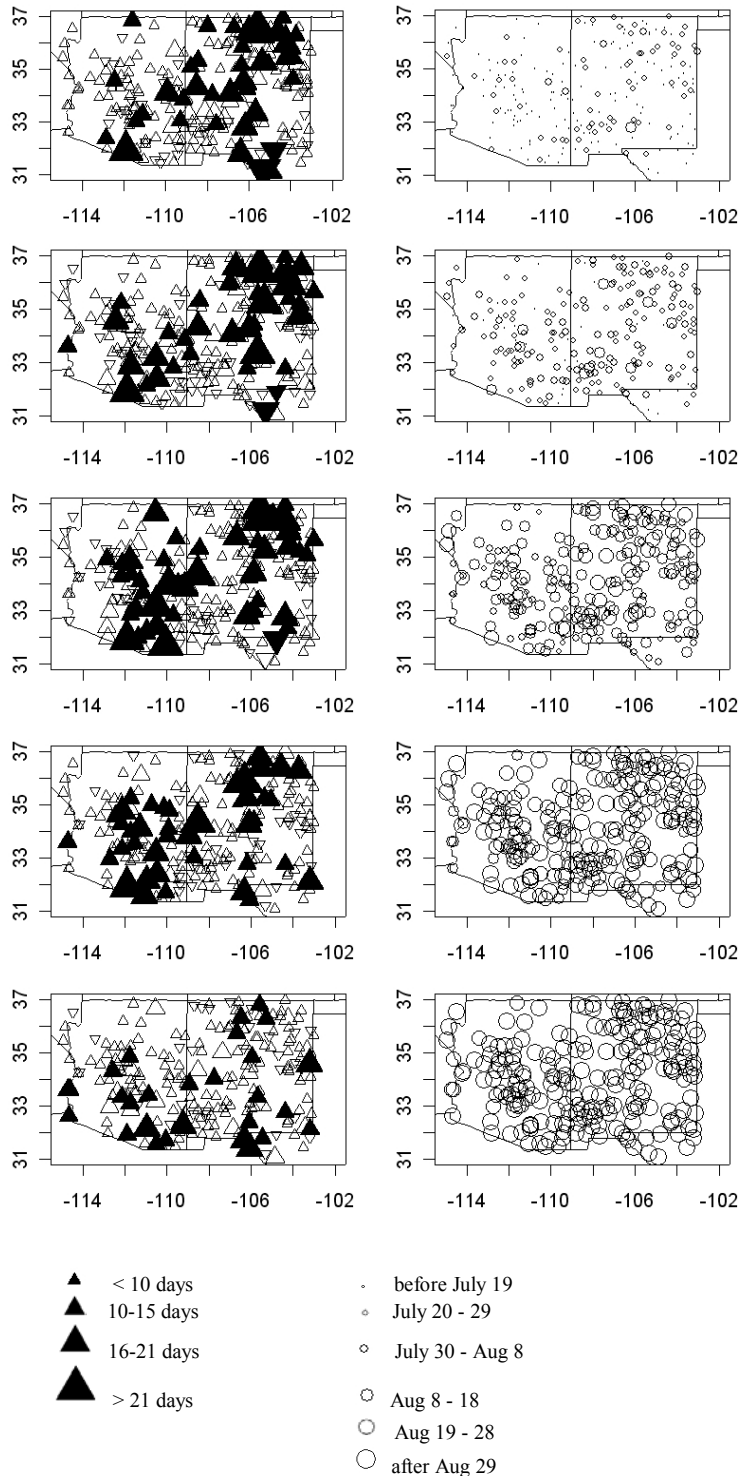
Figure 2. **Trends in Julian day of summer (Jul-Sep) seasonal rainfall accumulation at five thresholds (10th, 25th, 50th, 75th, and 90th percentile) (left column, top to bottom, respectively) and the corresponding climatological Julian days (right column, top to bottom, respectively). For the Julian day trends, point up triangles indicate delay and point down triangles indicate advancement. Filled triangles indicate 90% significance.**

Figure 3 shows the timeseries of the first PC for the 10th and 50th percentile Julian days. As described in the methodology section, these PCs can be thought of as a spatial average for the region. The trend line shown in the figures is the nonparametric Kendall Theil slope of the data. As can be seen, the timing PCs exhibit similar trends to those exhibited in the COOP station data presented in Figure 2.

(a) (b)
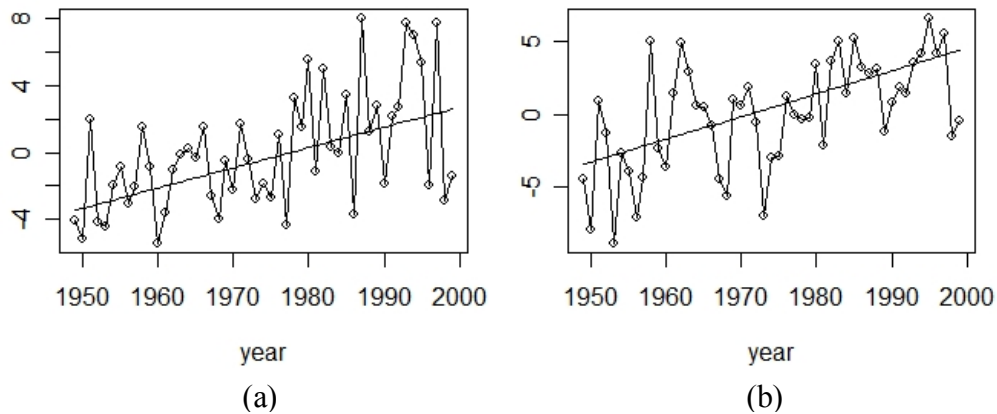
Figure 3. Timeseries of PC1 for the Julian day when the 10th (a) and 50th (b) percentile of the summer (Jul-Sep) seasonal rainfall has accumulated. The trend line is the nonparametric Kendall Theil slope of the data.

The timing shift that delays the monsoon cycle would suggest an increase in August and September rainfall and a corresponding decrease in July rainfall. For supporting evidence to the trends seen with the coop data in Figure 2 and the timing PCs in Figure 3, the annual cycle of the rainfall is analyzed using the monthly climate division data. The annual cycle of the rainfall at four representative climate divisions from the region for the period 1948-1975 and 1976-2004 are shown in Figure 4. A comparison of the two time periods shows a general decrease in precipitation in July and an increase in August and September from the first half of the period of record to the second. Other climate divisions, particularly those in the lower regions, show

16

similar changes to the annual cycle. These shifts are consistent with the shifts identified in Figure 2.

(a) (b)

(c) (d)
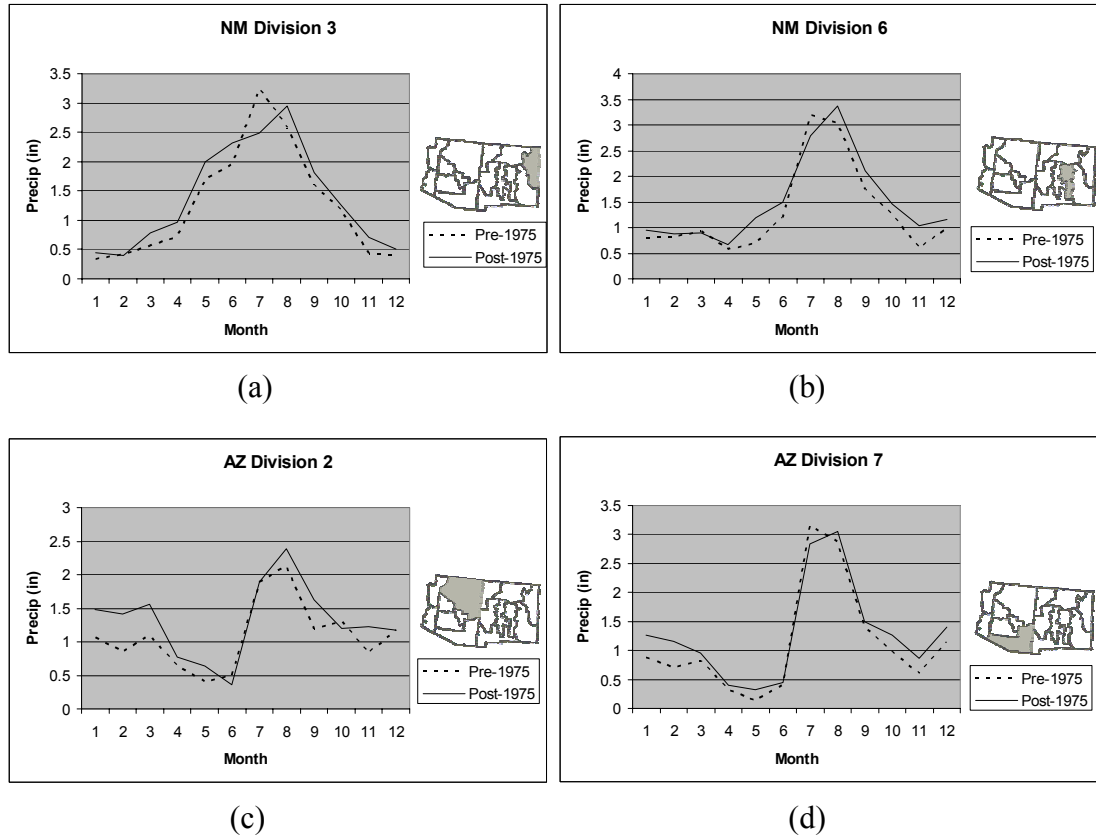
Figure 4. Annual cycle of precipitation during 1948-1975 (dashed line) and 1976-2004 (solid line) at two climate divisions in New Mexico (a, b) and two climate divisions in Arizona (c, d)

Monsoon Rainfall

Spatial trends in the monthly rainfall amount for July to September are shown in Figure 5. It can be seen that precipitation is generally decreasing in July and increasing in August and September, with NM exhibiting a stronger trend. Also, a general increase in total monsoonal precipitation (Jul-Sep) is evident largely for NM – consistent with the increasing trend in August and September. The spatial trend maps are field significant at the 95% confidence level. The daily COOP station data,

which has a shorter period of record, shows very similar trend results indicating that the trend is not dependent on the beginning and end of the data set (figure not shown). To further corroborate this result, the trends in the July to September precipitable water (Figure 6) are computed. The precipitable water shows trends similar to the rainfall results. It should be noted that the trends seen in the timing and rainfall amount should not be used for predictive purposes in and of themselves, but rather as a diagnostic tool to help shed light on the key drivers of monsoon variability.
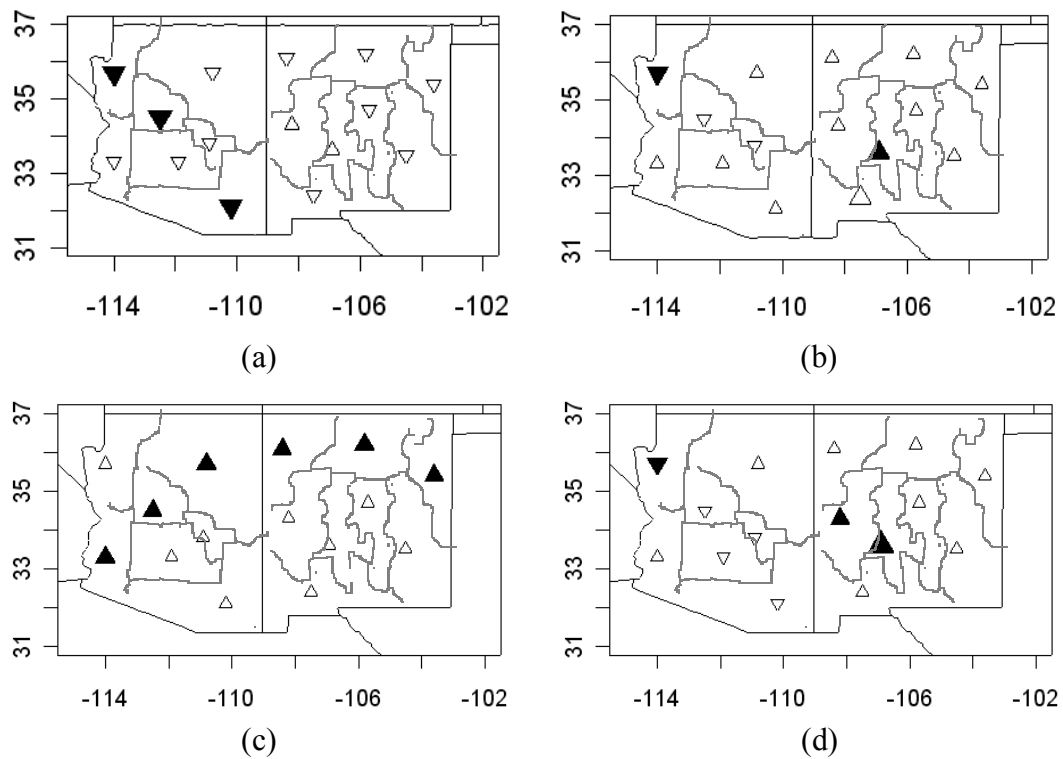
Figure 5. Trends in July (a), August (b), September (c) and July to September (d) rainfall. Point up triangles indicate an increasing trend and point down triangles indicate a decreasing trend. Size indicates the relative magnitude of the trend. For July, August and September, the triangle sizes correspond to approximately < 0.4 inches, 0.4-0.7 inches, and > 0.7 inches. Filled symbols indicate 90% significance.
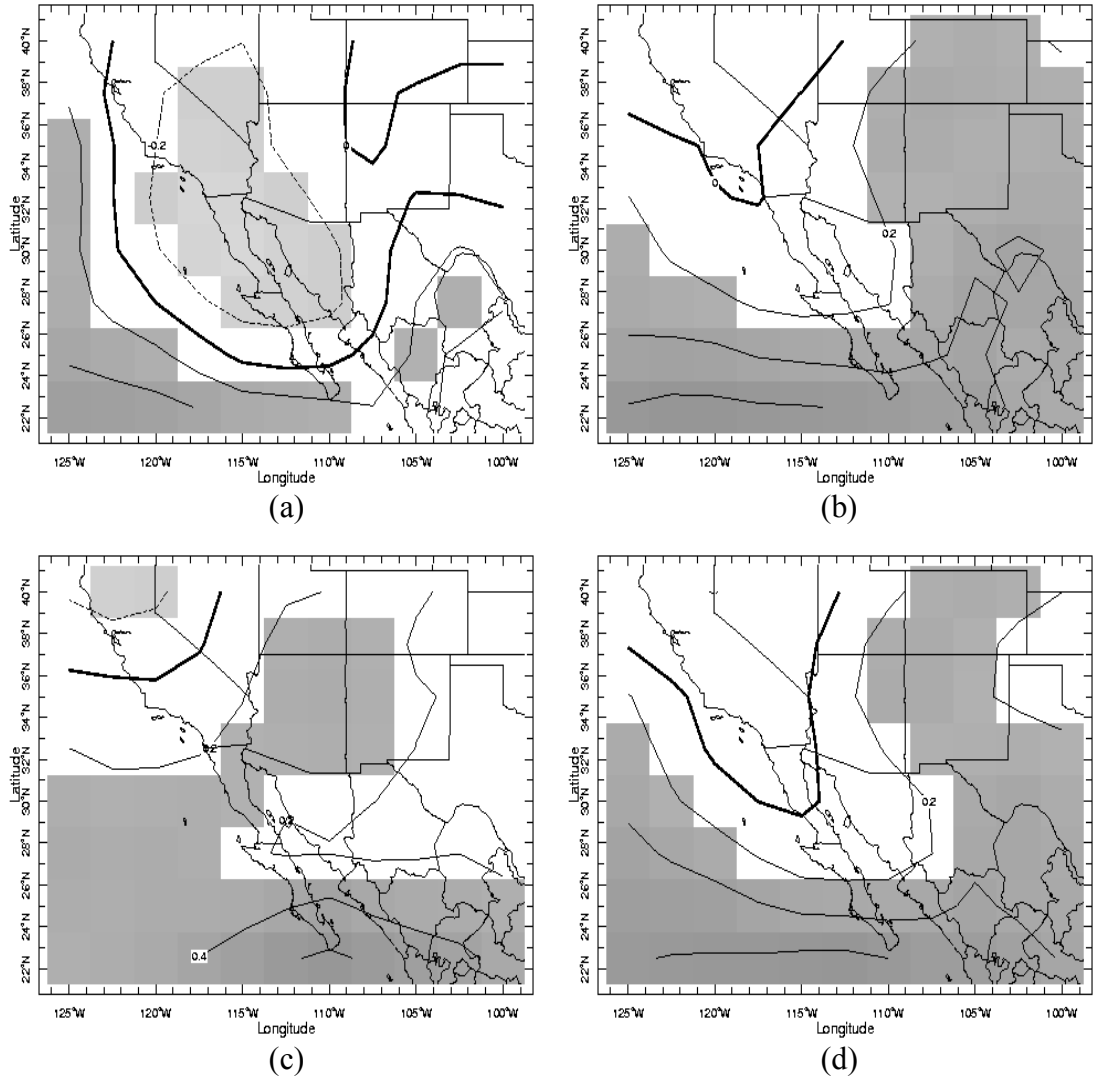
Figure 6. Trends in July (a), August (b), September (c) and July to September (d) precipitable water. Shaded regions indicate approximate 90% significance. Images provided by the International Research Institute for Climate and Society from the website at www.iridl.ldeo.columbia.edu.

Hypothesis

The key question that emerges from the above analysis is: what is driving the delay in the monsoon cycle? The basic driver the monsoon process, that is, the pre-monsoon land-ocean gradient, is explored for answers. This study hypothesizes that there is increased antecedent (pre-monsoon) soil moisture in the southwestern U.S.

that requires longer summer heating and delays the development of the necessary land-ocean temperature gradient, consequently delaying the summer monsoon. It is reasoned that the wetter winter and spring conditions in the southwestern U.S. are largely driven by winter ocean-atmosphere conditions, especially Pacific SSTs, the Pacific Decadal Oscillation (PDO)/ El Niño-Southern Oscillation (ENSO) pattern and the observed increase in ENSO activity in recent decades (Trenberth and Hoar 1996; Rajagopalan et al. 1997). Links to the antecedent land, ocean, and atmosphere conditions offer hope for long-lead forecasts of the summer monsoon. This hypothesis is tested in the following sections. A similar hypothesis was proposed by Zhu et al. (2005) though their hypothesis and analysis focused on the role of the antecedent land and atmosphere conditions (not ocean conditions) and monsoon precipitation in the Monsoon West region of western New Mexico and eastern Arizona. The results presented below generally corroborate those of Zhu et al. though the analysis and data sets are different.

Antecedent Land Conditions

To determine whether the antecedent land conditions are getting wetter, trends in the precipitation and PDSI for the December to May season are examined (Figure 7). A significant increasing trend in the winter/spring precipitation and PDSI over the desert southwest can be seen. Also, a corresponding decreasing trend over the Pacific Northwest is apparent. These trends are field significance at the 95% confidence level. Increased precipitation in the southwest and decreased precipitation in the northwest is typical of ENSO teleconnections in the western U.S. identified by

several researchers (Ropelewski and Halpert 1986; Redmond and Koch 1991; Cayan and Webb 1992; Cayan et al. 1999).

(a)   (b)
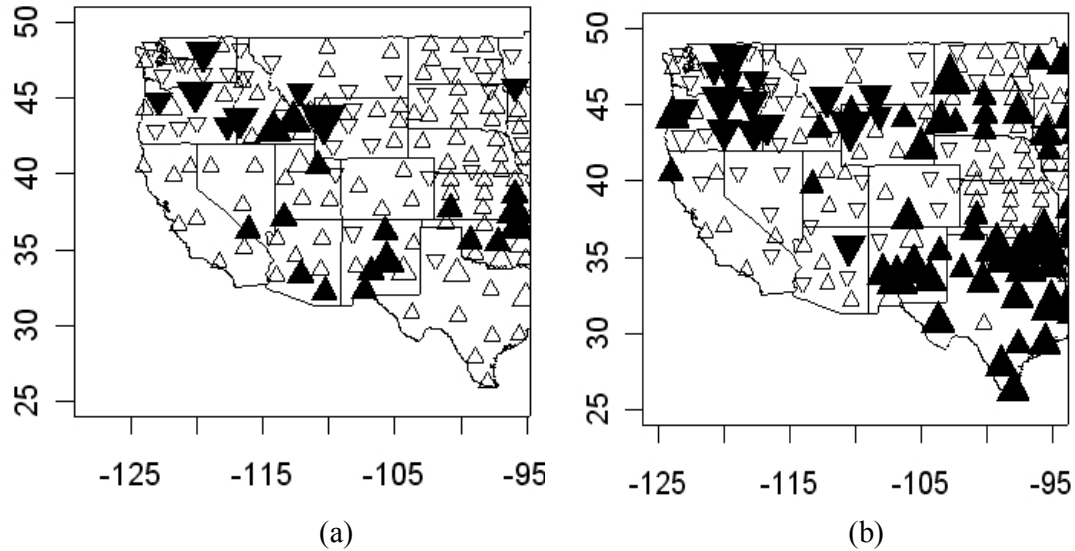
Figure 7. Trends in antecedent winter/spring (December-May) land conditions – precipitation (a) and PDSI (b). Point up triangles indicate an increasing trend, point down triangles, a decreasing trend. Symbol size indicates the relative magnitude of the trend and filled symbols indicate 90% significance.

To further demonstrate the strength of the link between antecedent land conditions and the timing of the monsoon, the leading mode of the monsoon timing is correlated with the pre-monsoon land conditions. The first PC explains 28% of the total variance and the first Eigen vector has similar magnitude and sign across all stations; hence the first PC can be regarded as the regional monsoon "timing index". Figure 8 (a, b) shows the correlations between the first PC for the monsoon peak, i.e., the Julian day when the 50th percentile of the total seasonal rainfall has occurred, and the winter/spring (Dec-May) precipitation and PDSI. Significant positive correlations exist between the regional monsoon timing index and antecedent precipitation and PDSI over the monsoon region. These positive correlations indicate that an increase

in the monsoon peak's Julian day (i.e., a late shift in the monsoon) occurs with

increased rainfall and soil moisture during the preceding winter/spring, thus

supporting the proposed hypothesis. When the timing of the onset of the monsoon is

considered, this correlation pattern becomes even stronger. Figure 8 (c, d) presents

the correlations between the first PC of the onset (i.e., the Julian day when the 10th

percentile of the seasonal rainfall has occurred) and the antecedent conditions. The

(a)　　　　　　　　　　　　(b)

(c)　　　　　　　　　　　　(d)
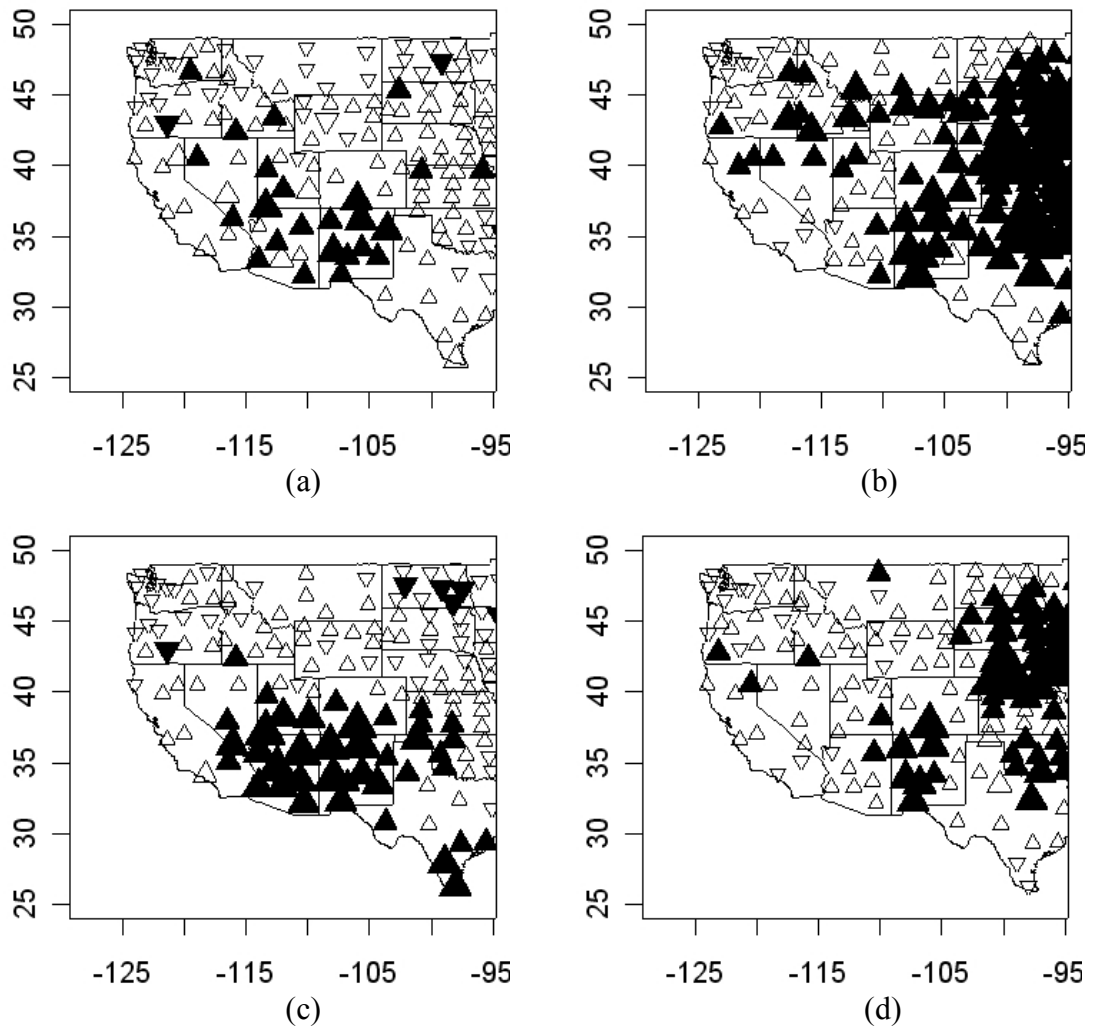
Figure 8. Correlation map of the 50th percentile (a,b) and 10th percentile (c,d) of the timing PC with antecedent winter/spring precipitation (a,c) and PDSI (b,d) Point up triangles indicate a positive correlation, point down indicate a negative correlation. Symbol size indicates the relative magnitude of the correlation and filled symbols indicate 90% significance.

10th percentile PC captures 31% of the total variance and can be thought of as the leading mode of the monsoon onset. It is noted that the relatively low values of 28% and 31% of the total variance accounted for by the first PCs can be explained by the noise in the daily data. The leading PC in all the cases, however, provides a robust measure of the spatial average.

Correlations between the leading mode of the summer (Jul-Sep) monsoon rainfall amount and antecedent precipitation (Figure 9a) show a negative correlation pattern over the monsoon region and positive pattern over the northwestern U.S. The results are similar for the antecedent PDSI (figures not shown). Interestingly, the correlation pattern for the leading mode of the July rainfall amount (Figure 9b) is even stronger, indicating that the onset of the monsoon is most affected by antecedent conditions. These results are consistent with the timing results presented above: as pre-monsoon land moisture increases the monsoon is delayed, thus decreasing

(a)   (b)

Figure 9. Correlation map of the rainfall amount's first PC for July to September (a) and July (b) with antecedent winter/spring precipitation. Point up triangles indicate a positive correlation, point down triangles indicate a negative correlation. Symbol size indicates the relative magnitude of the correlation and filled symbols indicate 90% significance.

23

monsoonal precipitation in July. The negative relationship between winter/spring precipitation and summertime precipitation over the southwestern U.S. has also been noted in previous studies (e.g., Gutzler 2000; Lo and Clark 2002). Similar results were obtained when the PCA was performed separately for Arizona precipitation and New Mexico precipitation and each of these leading PCs were correlated with antecedent land conditions. In general, correlations with Arizona tended to be slightly stronger. Table 1 shows the percent of total variance captured by all the leading PCs.

Table 1. Percent of total variance captured by each leading PC of monsoonal precipitation in varying months and regions.

State	Month	variance
NM and AZ	July	45%
NM and AZ	August	53%
NM and AZ	September	58%
NM and AZ	July-September	43%
AZ	July	80%
AZ	August	78%
AZ	September	75%
AZ	July-September	77%
NM	July	61%
NM	August	64%
NM	September	71%
NM	July-September	63%

These results indicate that the preceding winter/spring land conditions (i.e., precipitation and soil moisture) tend to most strongly affect the timing of the monsoon initiation and the early monsoon rainfall amount (i.e., July rainfall). That is, a wetter winter/spring tends to delay the monsoon cycle and decrease monsoon rainfall in July, and vice-versa.

It is generally accepted that the enhanced wet (dry) conditions over southwestern (northwestern) U.S. in winter and spring are largely due to warm ENSO (i.e., El Niño) conditions (Ropelewski and Halpert 1986; Redmond and Koch 1991; Cayan and Webb 1992; Cayan et al. 1999). Consequently, winter and spring ocean conditions should also be related to the following monsoon. To investigate this explicitly, the monsoon attributes (i.e., timing and rainfall amount) are correlated with antecedent ocean conditions.

Correlations between the winter/spring (Dec-May) SSTs and the leading mode of the following monsoon's peak Julian day exhibit strong negative values (between -0.5 and -0.6) in the northern Pacific Ocean (Figure 10a) around 30N, just east of the dateline. Weaker positive correlations are seen to the southeast of this region (around 10N) and in the tropical Pacific. This pattern is larger and stronger with the leading mode of the early monsoon Julian day (Figure 10b). Shaded regions are statistically significant at the 90% confidence level based on the normal test for correlation

<p align="center">(a)   (b)</p>
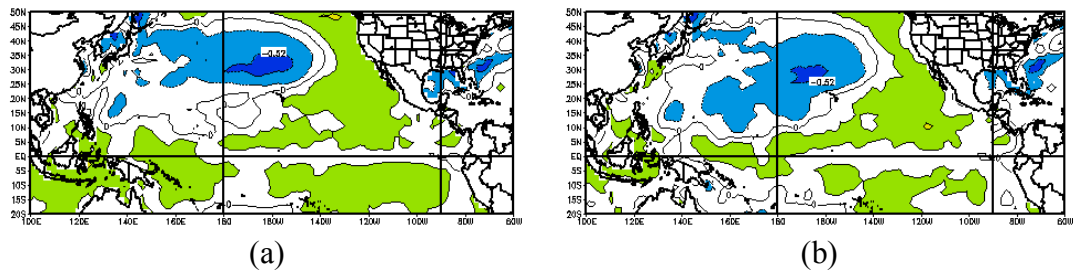
Figure 10. Correlations between the winter/spring (Dec-May) SSTs and the first PC of the Julian day of the 50th (a) and 10th (b) percentile. Shaded regions are statistically significant at the 90% confidence level. Blue indicates a negative correlation; green indicates a positive correlation. Images provided by the NOAA-CIRES Climate Diagnostics Center in Boulder, Colorado from their web site at www.cdc.noaa.gov.

coefficient (Helsel and Hirsch 1995). These correlations indicate that a dipole pattern of below average SSTs in the north Pacific and above average SSTs to the southeast and in the tropical Pacific in winter/spring tend to increase (i.e., delay) the monsoon timing. This study hypothesizes that this occurs via an increased winter/spring precipitation over the monsoon region resulting in a weaker land-ocean gradient which delays the monsoon cycle (Figure 2). Though ENSO activity has been shown to increase winter and spring precipitation in the southwest U.S., the SST correlation pattern with the monsoon timing is suggestive of ENSO, but does not show an explicit ENSO pattern.

The leading mode of the monthly and summer seasonal monsoon rainfall amounts are correlated with the antecedent ocean conditions (Figure 11). The SST patterns for the July rainfall (Figure 11a) show positive correlations (between +0.4 and +0.5) in the northern Pacific region (same as Figure 10) and negative correlations
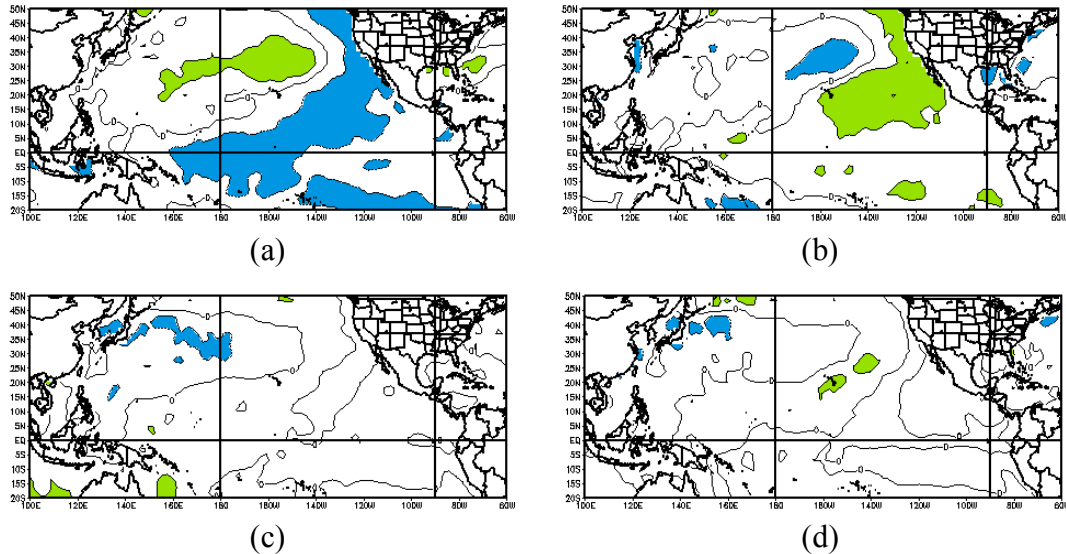
Figure 11. Same as Figure 9 except for correlations between the winter/spring (December-May) SSTs and the first PC of the July (a), August (b), September (c), and July-September (d) monsoon rainfall.

26

(between -0.3 and -0.4) to the southeast of this region extending down to the tropics. That is, warmer northern Pacific SSTs and cooler tropical Pacific SSTs during winter/spring are related to increased monsoon rainfall during July. It is hypothesized that these SST conditions result in decreased winter/spring precipitation over the southwest U.S. (e.g., Ropelewski and Halpert 1986) increasing the land-ocean temperature gradient and the resulting monsoonal precipitation in July.   The correlation pattern reverses and is much weaker (Figure 10b, c, d) for the August, September, and total seasonal precipitation. In August, the correlations are between +0.3 and +0.4 in the northern Pacific and between -0.2 and -0.3 to the south and east. By September the correlations are not statistically significant. This indicates that the antecedent winter/spring ocean conditions have a stronger impact on the early monsoon (July) rainfall.   This is consistent with the results obtained for the antecedent land conditions described in the previous section.

This leaves one to question what large-scale features, if any, affect the late monsoon (August to September) rainfall. To explore this, the leading modes of August and September rainfall were correlated with the near term and concurrent ocean conditions. The leading mode of rainfall in these months is related to SSTs near the California coast and Gulf of California, where correlations are above +0.4 and are stronger for August than for September. (Figures not shown.) These results generally corroborate those of Kim et al. (2005) who showed through modeling that increases in SSTs around the Gulf of California are linked with increased monsoonal precipitation after the onset of the monsoon.

Summary and Conclusions

A systematic analysis of the spatio-temporal attributes of NAM in Arizona and New Mexico was performed in this study. Trends in the Julian day of summer rainfall indicate a significant delay (approximately 10-20 days) in the entire cycle of the summer monsoon in Arizona and New Mexico. This delay in the monsoon cycle is manifested with a decrease in rainfall during the early monsoon (July) and corresponding increase during the later period (August and September). The antecedent (winter/spring) rainfall and PDSI show an increasing trend over the southwestern U.S. monsoon region and a decreasing trend over the northwestern U.S. − this is consistent with the well-known ENSO teleconnections in the western U.S. Combining these observations, the following hypothesis was proposed: increased antecedent (pre-monsoon) soil moisture in the monsoon region will take longer summer heating to set up the land-ocean gradient and consequently delay the monsoon cycle. The wetter antecedent conditions in the southwestern U.S. are largely driven by winter ocean-atmospheric conditions, especially ENSO. Correlations between antecedent SSTs and the leading modes of the monsoon timing and rainfall amount show that the monsoon (particularly the early monsoon) is related to winter/spring SSTs in the tropical/ extra-tropical Pacific, however, no explicit ENSO pattern emerged in this analysis. It is reasoned that the detected shift in the timing of the monsoon is a direct response to increased ENSO activity in recent decades and that future winter/spring SSTs anomalies and antecedent soil moisture will likewise modulate the timing of the monsoon via the proposed mechanism (i.e., later (earlier) monsoon with warm (cool) tropical SST anomalies) . These antecedent links to the land and ocean offer hope for long-lead forecasts of the summer

28

monsoon. The late season monsoon precipitation appears to be more related to SSTs

near the Gulf of California. Further analysis using climate models is needed to more

rigorously test the proposed hypothesis.

CHAPTER 3

STREAMFLOW ANALYSIS

Introduction

Understanding streamflow variability in the semi-arid western United States is important for efficient and sustainable water resources management and development. This is underscored by the increasing challenges of population and economic growth, environmental concerns together with climate variability and climate change. It is increasingly evident that large-scale climate features, particularly the El Niño-Southern Oscillation (ENSO) (Allan et al. 1996, Trenberth 1997) and the Pacific Decadal Oscillation (PDO) (Mantua et al. 1997, Mantua and Hare, 2002), have a strong influence on the variability of regional hydrology in the western U.S. In particular, warming in the central and eastern equatorial Pacific Ocean (i.e., El Niño) typically shifts the southern branch of the winter subtropical jet stream southward, increasing precipitation and streamflow in the southwestern U.S. and shifts the northern branch of the subtropical jet stream northward above the Pacific Northwest, decreasing precipitation and streamflow in that area (Cayan and Webb 1992). Almost the opposite hydroclimate response is realized, albeit with some asymmetry (Hoerling et al. 1997, Clark et al. 2001), during the cooling of the central and eastern Pacific Ocean (i.e., La Niña). The PDO has also been found to impact western U.S. hydroclimatology in conjunction with ENSO (Jain and Lall 2000, 2001; Pizarro and Lall 2002), although there is debate regarding its independent nature from ENSO

(Newmann 2003). Several studies (among others, Cayan and Peterson 1989; Redmond and Koch 1991; Kahya and Dracup 1993a,b, 1994a,b; Dracup and Kahya 1994; Piechota et al. 1997; Clark et al. 2001; Pizarro and Lall 2002; Tootle et al. 2005) have identified the origins of interannual streamflow variability in the western U.S. to be large-scale climate features such as ENSO and PDO. As would be expected, the use of large-scale climate information improves the skill in streamflow forecasts (e.g., Hamlet and Lettenmaier 1999; Clark et al. 2001) and water management (e.g., Hamlet et al. 2002).

These large-scale climate features have been shown to affect extreme hydrologic occurrences such as droughts and floods in the western U.S. For example, Piechota and Dracup (1996) found a significant relationship between El Niño and drought in Pacific Northwest and La Niña and drought in the southern U.S. (i.e., Texas). Pizarro and Lall (2002) found that El Niño years present an enhanced possibility of winter floods in California and Oregon, spring floods in S. Idaho, NE Utah and Colorado and summer floods in New Mexico and S. Colorado. In Washington, N Idaho, Montana and Wyoming the likelihood of flooding appeared reduced. However, when they considered the recent weakening of the negative PDO signal, the probability of floods decreased in California, N. Washington and S. Colorado, and increased in the other regions.

Other studies of streamflow variability seek to classify streamflow regions. For example, Lins (1997) used rotated principal component analysis (PCA) to classify streamflow regimes across the entire U.S. Among other patterns, the well documented Western Opposition (i.e., northwest-southwest opposition) pattern (e.g.,

Cayan and Peterson 1989; and Redmond and Koch 1991; Piechota et al. 1997) emerged. In the 1997 study Lins found this pattern to be strongest in the summer months of June, July, and August.

Most of the studies described above focus on winter and spring streamflows, which are generally driven by the stronger and more organized larger-scale climate patterns of winter and which are larger in magnitude relative to streamflows in other seasons. There have been relatively few studies on warm season streamflow variability, particularly that in the desert southwest driven by the North American Monsoon (NAM) system. One of the recent studies by Gochis et al. (2003) used the fifth-generation Pennsylvania State University—National Center for Atmospheric Research (PSU—NCAR) Mesoscale Model (MM5) with three different parameterization schemes to model, among other hydrologic responses, rainfall runoff in northwest Mexico. With all three schemes, the generation of surface runoff depended more on precipitation rates in individual local storms than on monthly total, basin-averaged precipitation. However, they also found large differences in the monthly total surface runoff between the three schemes, underscoring that model parameterization can significantly affect streamflow analyses. Though NAM streamflow studies are sparse, the variability of NAM precipitation has been studied quite extensively (as described in Chapter 1). Predicting the variability in the strength, location, and timing of monsoonal precipitation and streamflow is understandably very important for efficient water resources management.

The above background and needs motivate this research to investigate the space-time variability of streamflow in the NAM region of the southwestern U.S.

This chapter is organized as follows. The study area, data and methods are first described followed by a classification of the streamflow stations in the study area. Analysis of the winter/ spring streamflow is then presented, followed by space-time trends in summer streamflow and their relationship to antecedent land-ocean-atmosphere conditions. A physical hypothesis is then proposed for the streamflow variability in the region. A discussion and comparison of the results with those of the NAM precipitation analysis (Grantz et al. 2006 and Chapter 2) concludes the chapter.

Study Area

It is recognized that the center of NAM activity is in northwestern Mexico (Douglas, et al., 1993, Barlow et al., 1998), however, for this study the focus in on streamflow variability in the NAM region of Arizona and New Mexico. This was the study region in the recent NAM precipitation analysis (Grantz et al. 2006 and Chapter 2) and also this understanding will be used in a water management application in the Pecos River Basin in New Mexico.

Data

HCDN Streamflow Data

Daily streamflow data for the period 1948-2004 were obtained from U.S. Geological Survey (USGS) stations in the Hydro-climatic Data Network (HCDN). HCDN streamflow data are relatively free from such anthropogenic influences as regulation and diversion and meet certain measurement accuracy criterion outlined by Slack et al. (1993). This study used daily streamflow data for the period 1949-2004 from 43 stations across New Mexico and Arizona. For monthly analyses, the daily

data were summed to monthly values. The stations were filtered to include a minimum of 90% of total data. Missing values were filled in with the daily or monthly climatological value for that station. For the summer streamflow analyses, only stations that had at least 20% of the annual streamflow occurring in July to October were selected. Together these two filtering criteria resulted in 18 stations. The streamflow data were obtained from www.water.usgs.gov.

Climate Division Data

Monthly precipitation, temperature, and Palmer Drought Severity Index (PDSI) data from 8 climate divisions covering New Mexico and 7 divisions for Arizona for the years 1948-2004 were used. The climate divisions and data sets are obtained from www.cpc.ncep.noaa.gov.

NCEP/NCAR Re-analysis Data

Monthly values of large-scale ocean and atmosphere variables, e.g., sea surface temperatures (SSTs), geopotential heights, precipitable water, winds, etc., from the NCEP/NCAR Re-analysis data (Kalnay et al. 1996) were obtained from www.cdc.noaa.gov for the years 1948-2004.

Methodology

The annual hydrograph for each of the stations was computed to identify the peak streamflow month and to classify the stations as spring runoff dominated or summer monsoon dominated.

To understand the seasonal cycle and 'timing' of monsoonal streamflow, the Julian day when 10, 25, 50, 75, and 90 percent of the monsoonal (July to October)

streamflow occurred was identified for each year at each of the HCDN stations. The Julian day at these five thresholds helps capture the entire monsoon cycle. Nonparametric trend analysis based on Spearman rank correlation (Helsel and Hirsch 1995) is performed on these Julian days at all the stations. The Spearman rank correlation is similar to Pearson's correlation coefficient, R, except that it doesn't require that data be normally distributed, the values are converted to ranks before computing the correlation coefficient, and it is robust against outliers. To perform the Spearman rank correlation in this study one station's time series of Julian days when 50 percent of monsoonal streamflow occurred was selected and these Julian day values were converted to ranks. These ranks are linearly regressed against the corresponding year in which the value occurred. The Kendall Theil slope estimator (Helsel and Hirsch 1995) is then used to calculate the magnitude (number of days) and direction (earlier or later) of the timing shift. The Kendall Theil method is robust against outliers and estimates slope by calculating the median of the slopes between all combinations of two points in the data. This process is repeated for each station and for the other percentages (10, 25, 75, and 90) of streamflow. The estimated trends in 'timing' are then spatially mapped.

To understand the physical mechanisms driving the streamflow variability the leading mode of variability is correlated with large-scale land and ocean conditions. The leading modes are obtained by performing a principal component analysis (PCA) on the spatial streamflow timeseries. PCA, which is widely used in climate research, decomposes a space-time random field into orthogonal space and time patterns using Eigen decomposition, thus reducing the dimensions of the data (e.g., von Storch and

Swiers 1999).   In PCA the patterns are automatically ordered according to the percentage of variance captured, i.e., the first space-time pattern, also called the leading mode or first principal component (PC), captures the most variance present in the data, and so on.   Typically, the first few modes capture most of the variance present in the data.   In this research, the time component, or PC, of the leading mode was used.

Results

Streamflow Classification

From the annual hydrograph at each location, the peak streamflow month was identified and plotted in Figure 12.   Stations in the north have a late spring (April to June) peak indicating that they are snowmelt dominated.   Stations in the central region have an early spring (March) peak suggesting that they are winter snow and rain dominated, melting earlier relative to stations further north, likely because of warmer temperatures in the region.   For stations in the south or at lower elevations, the streamflow peak occurs during late summer (August to October), likely due to monsoon rainfall runoff.   Given the variation in peak runoff timing, the streamflow stations were grouped into three categories based on the peak runoff month: north, central, and south.   The "northern" stations are stations that peak in April to June, "central" stations peak in March, and "southern" stations peak in August to October. The hydrographs at all the stations in each of the three categories are shown in Figure 12 (b). It can be seen that station hydrographs may have two peaks, one due to runoff from winter snow/precipitation and another due to runoff from summer monsoon rainfall.   For several northern stations the spring peak lasts into summer making it

difficult to differentiate between spring snowmelt and summer monsoon runoff – this aspect will be further investigated and discussed later. The central stations, too, have a peak in spring and in summer. The southern stations have very little spring runoff and peak only in summer.
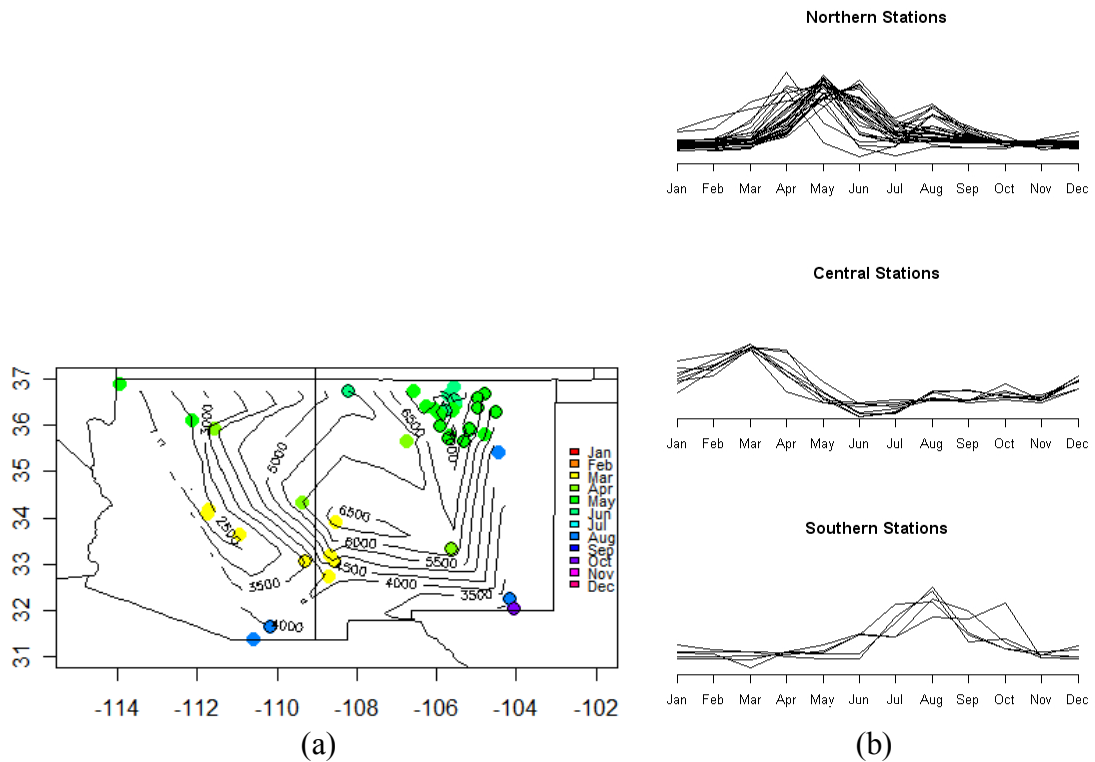
Figure 12. (a) Peak streamflow month. Color indicates the month when the most streamflow occurs. Circled stations contained enough data to be included in this study. (b) Scaled hydrographs of northern, central, and southern stations.

The relationship between monsoon precipitation (Jul-Sep) and the resulting streamflow (Jul-Oct) is shown in Figure 13. The relationship is generally linear, however streamflow variability is greater for the larger precipitation seasons. This could be due, in part, to runoff resulting in streamflow only after ponding takes place. During intense events, this can occur before the soil is completely wetted; during less intense events, the rainfall will soak into the soil before eventually contributing to

37

runoff. The philosophy taken here is that years of high seasonal precipitation are made up of more of the large monsoon precipitation events.
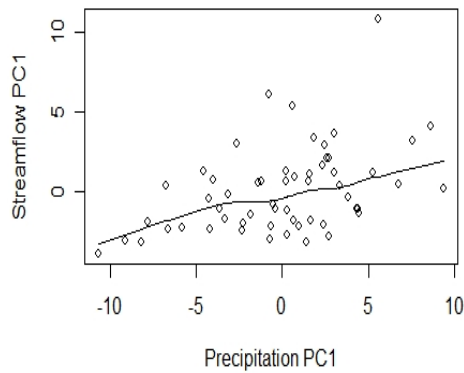
Figure 13. July to October precipitation PC1 versus streamflow PC1.

Winter / Spring Streamflow Analysis

Spatial maps of robust trend estimates of the winter/spring streamflow volume and precipitation from the Spearman rank correlation and Kendall-Theil slope estimator are shown in Figure 14. It can be seen that the winter and spring streamflow in the NAM region has been increasing over the past half century (Figure 14(a)) which is consistent with the increasing precipitation trend (Figure 14(b)) in the region. A simultaneous decrease in winter/spring precipitation over the Pacific Northwest (Figure 14(b)) is consistent with well-known ENSO teleconnection patterns (e.g., Cayan and Webb 1992). The spatial trend maps are field significant (Livezey and Chen 1983) at the 95% confidence level. These results are consistent with those of Regonda et al. (2005), who found significant increasing trends in the April 1st snow water equivalent (SWE) over northern New Mexico and decreasing trends over the Pacific Northwest. Winter/spring streamflows in this NAM region are strongly related to ENSO (e.g., Redmond and Koch 1991 and Dracup and Kahya

1994). Recent decades have experienced enhanced ENSO activity (Trenberth and Hoar 1996, Rajagopalan et al. 1997) and hence, an increased winter moisture (Figure 2b, Grantz et al., 2006) and consequently, increased streamflow.
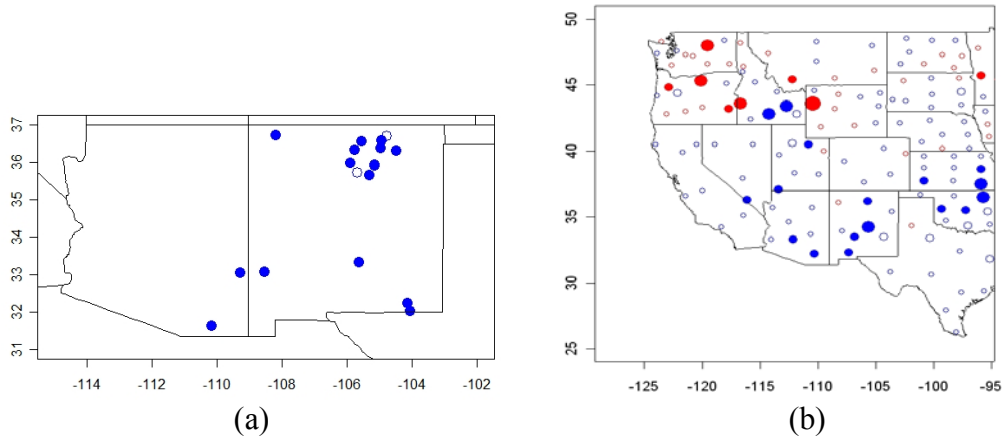
Figure 14. (a) Trends in the December to June streamflow volume. (b) Trends in the December to May precipitation. Blue indicates increasing trend, red indicates decreasing trend. Filled circles are significant at the 90 percent confidence level and circle size indicates relative magnitude of the trend.

To investigate the relationship between the streamflow variability in the NAM region and large-scale ocean and atmosphere features, the leading PC of the December to June streamflow is correlated with the coincident (Dec-May) Pacific SSTs and winds. The December to June time period was used because the central streamflow stations can have flow in both winter and the early spring months, and the other regions are not affected by including the winter months because they have very little flow during this time. PCA was performed separately on streamflows in the three regions and also on the entire NAM region. The leading (first) PC, henceforth referred to as PC1, of north, central, and southern regions, captured 78, 90, and 46 percent of the variance, respectively. Table 2 to Table 5 show the percent variance explained by PC1 for the three regions and for different monthly and seasonal

streamflows, and also their correlation with the regional averaged streamflow. The PC1s are highly correlated with the regional averaged streamflow in all the regions, suggesting that they are a good representation of the regional streamflow.

Table 2. Percent variance explained by streamflow PC1

	North	Central	South	Regional
Winter	78	90	46	61
July	61	66	44	42
August	59	61	65	41
September	56	68	53	40
October	60	68	55	40
Summer	61	61	58	41

Table 3. Correlation of area average and streamflow PC1

	North	Central	South	Regional
Winter	0.95	0.98	0.42	0.96
July	0.90	0.93	0.92	0.87
August	0.83	0.95	0.82	0.86
September	0.73	0.96	0.75	0.80
October	0.73	0.93	0.40	0.43
Summer	0.82	0.92	0.87	0.78

Table 4. Percent variance explained by timing PC1

	North	Central	South	Regional
10%	45	50	50	50
25%	52	51	47	51
50%	51	57	50	57
75%	47	67	44	67
90%	46	60	44	60

Table 5. Correlation of timing area average and timing PC1

	North	Central	South	Regional
10%	0.97	0.98	0.99	0.98
25%	0.99	0.99	0.87	0.99
50%	0.99	0.99	0.71	0.99
75%	0.98	0.99	0.89	0.99
90%	0.96	0.99	0.76	0.99

A positive correlation exists between equatorial Pacific SSTs and the PC1 of winter/spring streamflow of the NAM (New Mexico and Arizona) region (Figure 15a). This suggests that above normal equatorial Pacific SSTs (i.e., El Niño conditions) tend to result in higher winter/spring streamflows over the NAM region, and vice-versa. This result corroborates the well documented ENSO teleconnection pattern of an El Niño (La Niña) event resulting in above (below) normal winter precipitation in the southwestern United States (Ropelewski and Halpert 1986; Redmond and Koch 1991; Cayan and Webb 1992; Cayan et al. 1999).

When streamflows are considered by region, the northern region (Figure 15b) shows the strongest ENSO correlation pattern, with the central stations (Figure 15c) showing a somewhat weaker connection, and the southern stations (Figure 15d) showing no significant correlation with equatorial Pacific SSTs. It is presumed that the weak correlation for the southern stations is due to the insignificant amount of winter/spring streamflow in the southern region. Consistent correlations were seen between the PC1 of streamflow and atmospheric variables such as geopotential heights, etc. As an illustration, the correlation pattern of December to May 200mb zonal winds and the NAM regional streamflow PC1 is shown in Figure 15e, corroborating the SST correlations. Negative correlations along the equator indicate a decrease in the normal east to west tropical winds (i.e., El Niño) which is linked with increased streamflow (from the enhanced jet stream) in the southwestern U.S.
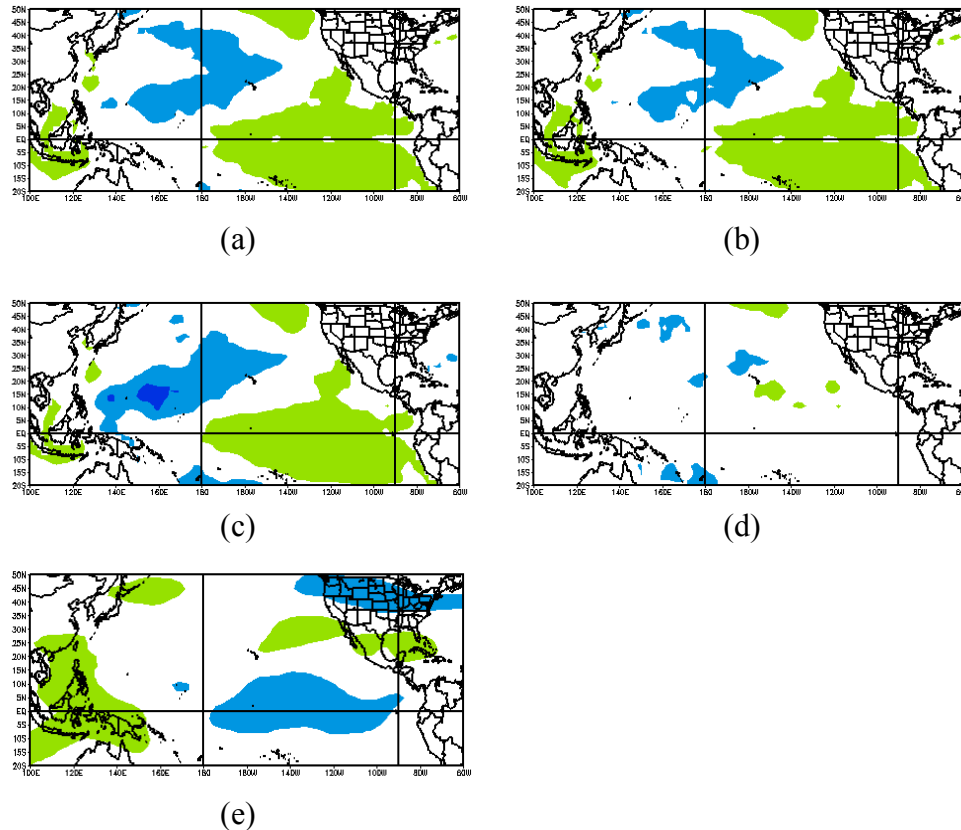
Figure 15. Correlations between December to May SSTs and PC1 of December to June streamflow in (a) New Mexico and Arizona, (b) northern stations, (c) central stations, and (d) southern stations. Correlations between December to May 200mb zonal winds and PC1 of December to June streamflow in New Mexico and Arizona (e). Shaded regions are statistically significant at the 95% confidence level. Green indicates a positive correlation, blue indicates a negative correlation. Image provided by the NOAA-CIRES Climate Diagnostics Center in Boulder, Colorado from their web site at www.cdc.noaa.gov.

The relationship between the winter/spring streamflows in the NAM region and ENSO and PDO is further corroborated by its correlation with one of the standard ENSO indices, NINO3 (Mann et al. 2000), and the PDO index (Mantua et al. 1997). The NAM regional PC1 correlations with NINO3 and PDO are statistically significant at 0.36, and 0.37, respectively. The correlations of the North, Central and Southern regional PC1 are 0.35, 0.38, -0.01, respectively, with NINO3 and 0.38, 0.26, 0.24, respectively, with PDO.

Summer Streamflow Analysis: Volume Trends

Trends in monthly summer (Jul-Oct) streamflow at all the stations in the NAM region are shown in Figure 16. In general, it can be seen that the early monsoon months show a decreasing trend and the later monsoon months show an increasing trend. The July and October trends pass field significance (Livezey and Chen 1983). It could be surmised that the decreasing trend in streamflow during the early monsoon month of July is related to the trend of late arrival of the monsoon precipitation as found in Grantz et al. (2006). They proposed the hypothesis that increased winter/spring moisture over the southwestern U.S. monsoon region requires more time and solar energy to heat up the land and set up the necessary land-ocean gradient to drive the monsoon, thus delaying the monsoon cycle. Accordingly, they
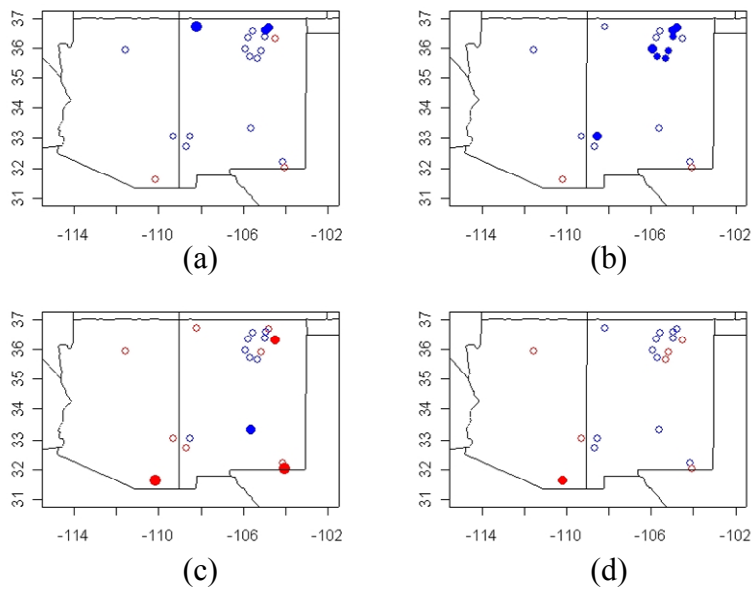
Figure 16.   Same as Figure 14, except for trends in the July (a), August (b), September (c) and October (d) streamflow volume.

found a decreasing rainfall trend over the NAM region in July (see their Figure 4) consistent with Figure 16 here. The validity of applying this hypothesis to the streamflow variability is investigated below.

The PC1 of streamflows in each of the summer months for the three regions are correlated with the antecedent winter/spring precipitation over the western U.S. (Figure 17). Results for the correlation with antecedent PDSI were similar (figures not shown). The southern regional streamflow PC1 of the early summer months shows a negative correlation with the antecedent precipitation over the NAM region while the central region exhibits no statistically significant correlation. The negative correlation between the early monsoon streamflow in the southern region and the antecedent precipitation is consistent with the hypothesis described above and proposed by Grantz et al. (2006) for the monsoon rainfall variability. In this, a wetter winter/spring tends to delay the monsoon initiation and consequently leads to lower streamflow during early monsoon months. This corroborates previous studies (e.g., Gutzler 2000; Higgins and Shi 2000; Lo and Clark 2002; and Zhu et al. 2005) that show an inverse relationship between winter precipitation, particularly snowfall, and subsequent summer monsoon precipitation. Again, the correlations are strongest for the early monsoon period (i.e., July) when the antecedent soil moisture will have the strongest affect. Results for the central streamflow stations are not statistically significant, presumably because the monsoon driven streamflow in this region is relatively small.
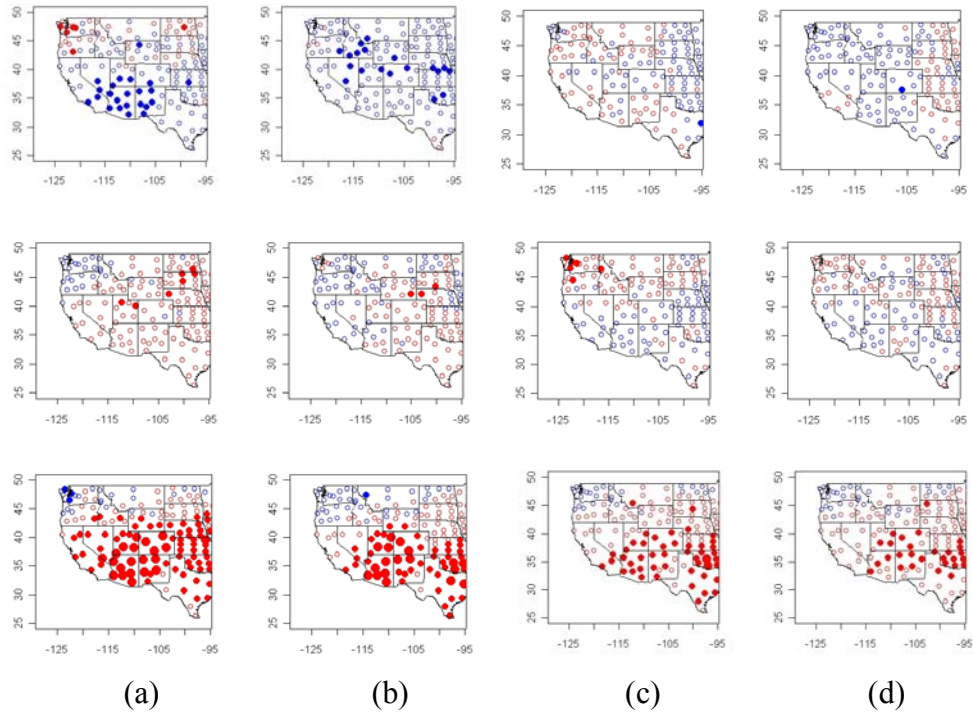
Figure 17. Correlations between December to May precipitation each climate division in the western U.S. and the PC1 of July (a), August (b), September (c), and October (d) streamflow for southern (top), central (middle) and northern (bottom) stations. Red circles indicate a positive correlation, blue circles indicate a negative correlations. Filled circles are significant at the 95 percent confidence level and circle size indicates relative magnitude of the correlation.

On the contrary, and interestingly so, the PC1 of the northern regional streamflows (Figure 17, bottom) exhibits a positive correlation with the antecedent winter/spring precipitation over the NAM region. Streamflows in the northern region are largest during the spring season due to snowmelt, as seen in Figure 12. In years of high winter precipitation the ensuing spring runoff lasts well into the typical monsoon time period, thus increasing the July to October streamflow and consequently resulting in the positive correlation with antecedent precipitation. The correlations are strongest for the early monsoon months when the effects of the spring

45

runoff are most evident. To test this deduction, the spring flow component was removed from the summer streamflow in the northern region.

Separating the spring and summer components of streamflow is not trivial, thus a simplified method was utilized to obtain a sense of the summer streamflow in the northern region. The method is represented as:

$$MonsoonStreamflow \Pr oxy = \sum_{n=i}^{N} Q_i \geq Q_{i-1}$$

where Q is streamflow for day i for N total days in the monsoon season July 1st to October 31st. The premise is that the spring streamflow due to snowmelt appears as baseflow in the summer months and, thus, removing the baseflow component leaves the streamflow component due to summer rainfall. The method adds up all the daily increases in streamflow; these are presumed to be the rising limb of the streamflow response to individual rainfall events. It is recognized that this method does not actually calculate the exact volume of monsoon streamflow and that there are other comprehensive methods for subtracting out baseflow (e.g., Chow et al. 1988). That said, the value obtained from this method is proportional to monsoon rainfall driven streamflow and can be used as a good proxy for monsoon streamflow.

Figure 18 shows the correlation between the monsoon streamflow proxy, obtained from the above method, for one of the northern stations and the antecedent precipitation. The northern station chosen was the one that exhibited the highest correlation with streamflows at all other northern stations. With the baseflow (i.e., the effect of spring streamflow) subtracted out, the early summer flow shows a negative correlation with the antecedent precipitation in the monsoon region, consistent with that of the southern regional streamflow (Figure 17, top).

(a) (b) (c) (d)
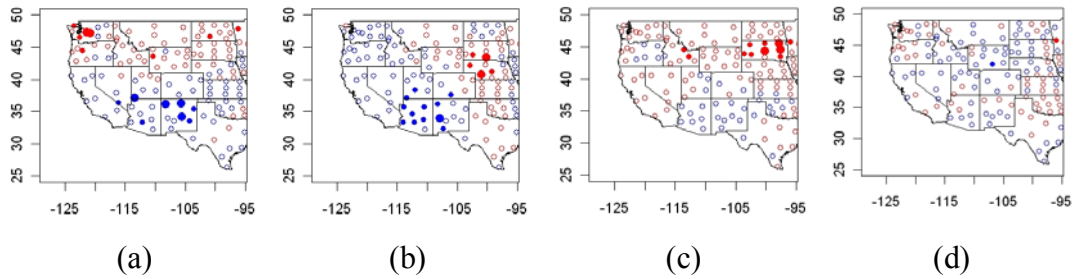
Figure 18. Same as Figure 17, except for correlations between the monsoon streamflow proxy for a northern station and December to May precipitation.

To investigate the relationship between the early summer streamflow and antecedent ocean conditions, the PC1 of July streamflow from the three regions is correlated with December to May Pacific SSTs (Figure 19). The southern regional streamflow exhibits a negative correlation with equatorial Pacific SSTs. In this, warmer SSTs in this region of the Pacific (i.e., El Niño conditions) lead to a wetter winter/spring in the NAM region, thus reducing the land-ocean temperature gradient. This in turn delays the initiation of the following summer monsoon, resulting in reduced early monsoon rainfall and streamflow. The central region shows no significant correlations. The northern region is positively correlated with equatorial Pacific SSTs. It is proposed that this is because the winter/spring streamflow impacts the early summer flow: higher streamflows in winter/spring (due to El Niño) lead to higher early summer streamflow, thus the positive correlations. However, the northern monsoon streamflow proxy (as calculated using the method described earlier) exhibits a negative correlation with equatorial Pacific SSTs (Figure 19d) consistent with results obtained for the southern region. The positive correlations along the equator for the northern stations suggest that above average tropical SSTs in winter (i.e., El Niño) are followed by above average streamflow in the early summer

47

months. This relationship weakens for streamflow in the later summer (August to October) months (figures not shown).

(a)

(b)

(c)

(d)
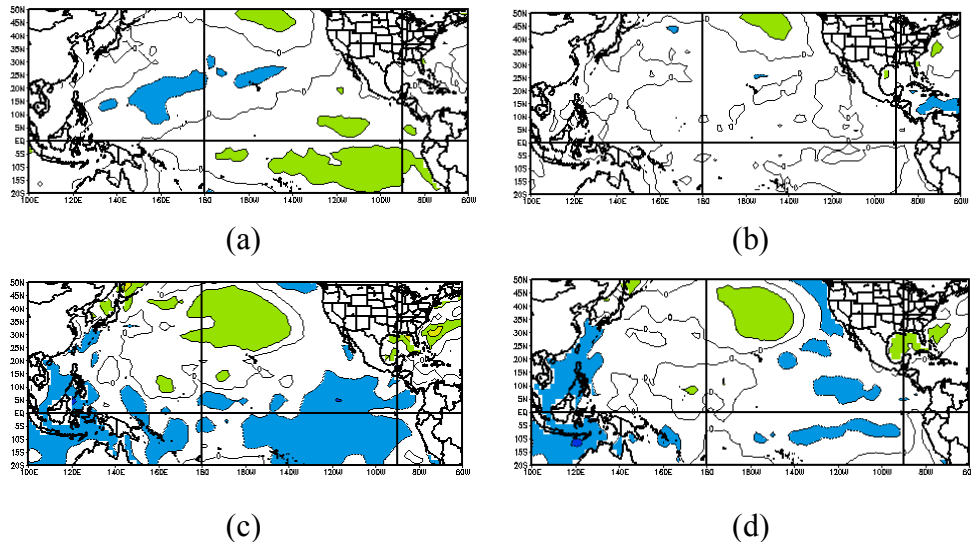
Figure 19. Same as Figure 15, except for the PC1 of northern (a), central (b), and southern (c) stations July streamflow and northern monsoon (Jul-Oct) streamflow proxy (d).

It thus seems apparent that winter tropical Pacific SSTs impact the winter/spring moisture (i.e., precipitation) and land conditions over the NAM region which, in turn, modulate the timing and the strength of the early monsoon rainfall and streamflow.   This connection between the large-scale land-ocean-atmospheric conditions in the antecedent winter/spring and the early monsoon rainfall and streamflow is very interesting and offers hope for long-lead forecasts of at least the state of the summer streamflow in the NAM region. This information could be very useful to water managers in the region.

Summer Streamflow Analysis: Timing Trends

As mentioned earlier, Grantz et al. (2006) found a late shift in the monsoon precipitation cycle in the NAM region and hypothesized this to be related to

antecedent land-ocean-atmospheric features. To investigate the validity of the hypothesis in relation to the timing of summer streamflow, analysis was performed on the time series of the Julian day when 10, 25, 50, 75, and 90 percent of the monsoon (Jul-Oct) streamflow accrued in each year at each of the stations. The five percentage thresholds are used to capture the entire cycle of monsoonal streamflow. Trends in the Julian day for these thresholds at each location are shown in Figure 20. It can be seen that the early stage of the monsoon (i.e., the Julian day when 10 percent of the seasonal streamflow occurred) shows no significant trend while the middle and later stages of the monsoon show a late shift. It is speculated that the insignificant results for the early stage of the monsoon are due to the arbitrary assignment that the "start" of the monsoon is July 1st. Though precipitation may generally start in early July, the resulting streamflow may not be realized until several weeks later. Thus, the 10 percent results shown in Figure 20 (left) may not accurately reflect the beginning of monsoonal streamflow for all stations across the region. To address this, the same analysis was performed on the Julian day time series for the August to October streamflow period (Figure 20, right). Results for the August to October period show a late shift in all stages (i.e., percentage thresholds) of the monsoon streamflow cycle. This is consistent with the findings of Grantz et al. (2006) (see their Figure 1) for the NAM precipitation.
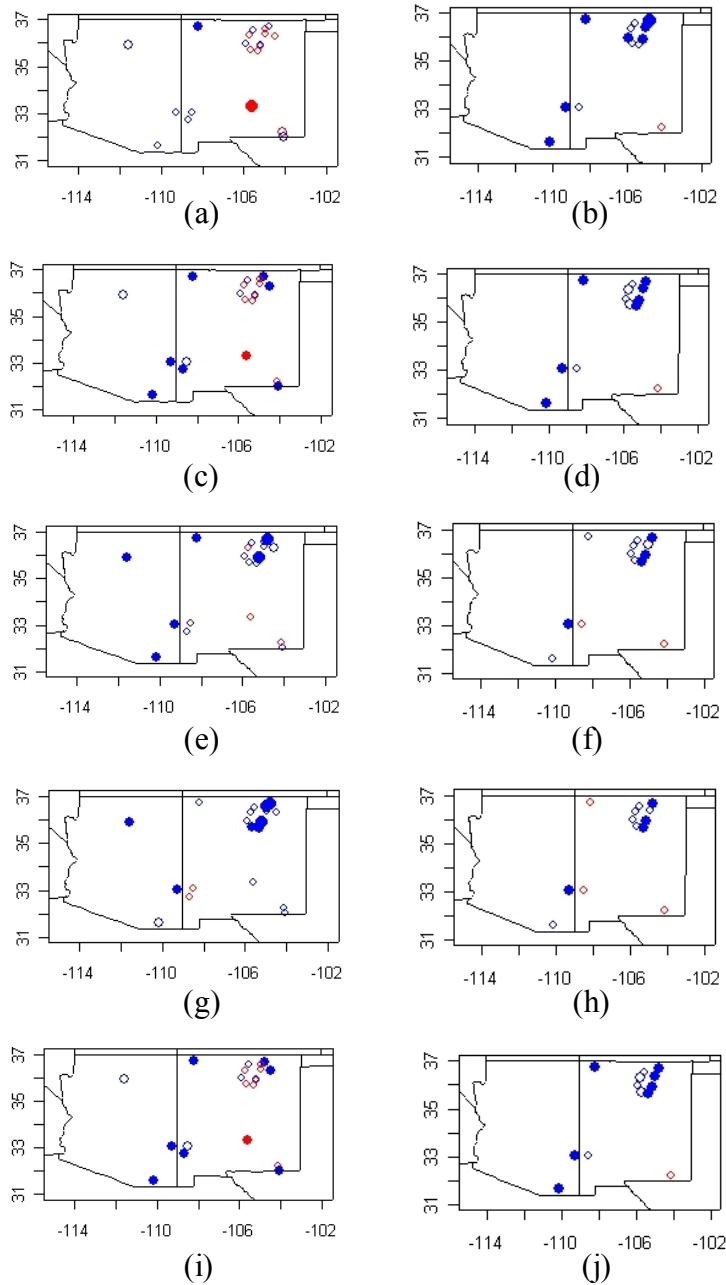
Figure 20. Same as Figure 14 except for trends in the Julian day when 10 (a,b), 25 (c,d), 50 (e,f), 75 (g,h), and 90 (i,j) percent of July to October (left column) and August to October (right column) streamflow occurred.

To investigate the relationship between the shifts in the streamflow cycle seen above and antecedent land conditions, the PC1 of the Julian days at each of the thresholds and for each of the three regions is correlated with the December to May

precipitation across the western U.S. (Figure 21). The positive correlations between the PC1 for the southern stations and the antecedent NAM regional precipitation corroborate the findings from the precipitation analysis of Grantz et al. (2006). In

(a)   (b)   (c)
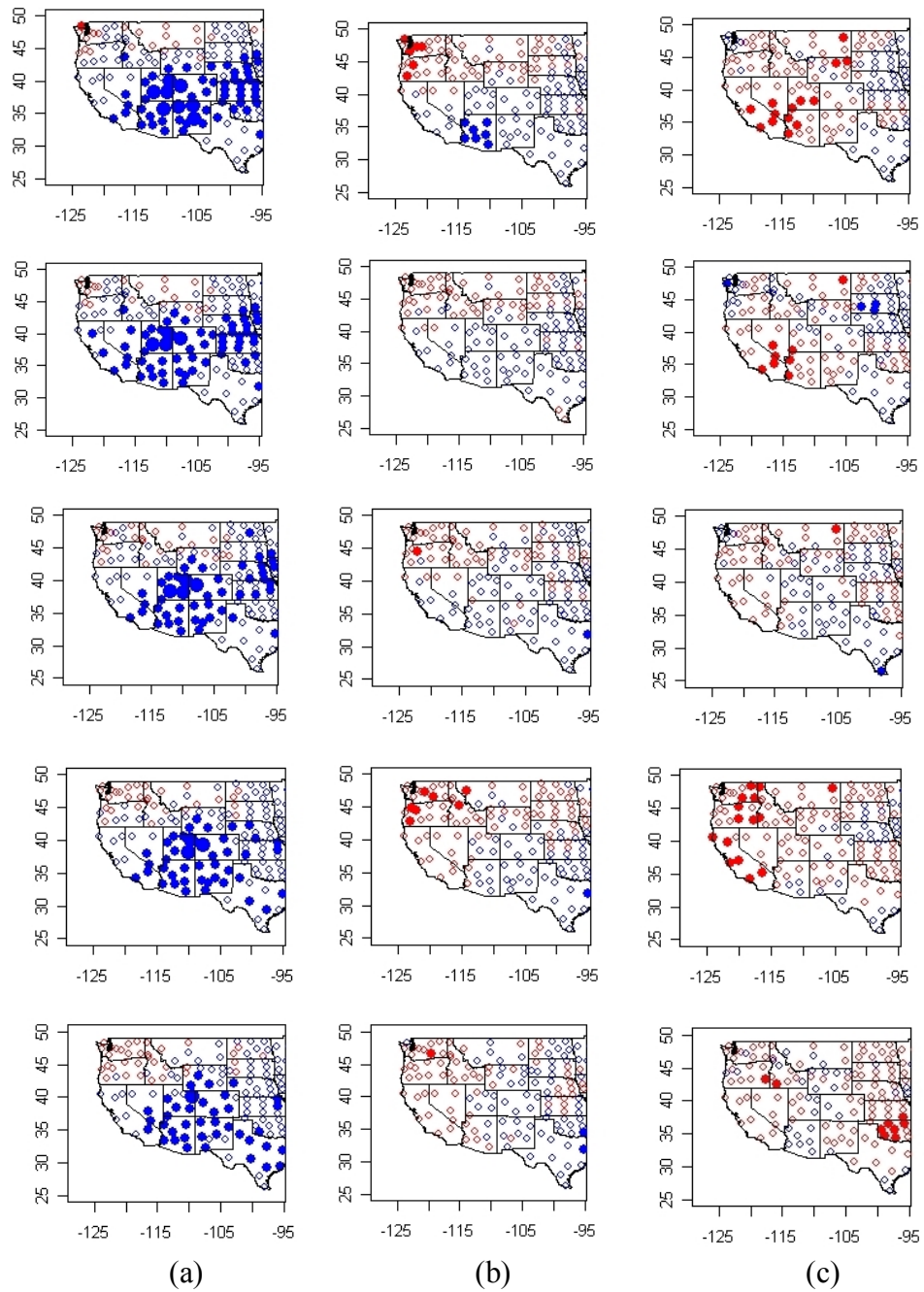
Figure 21. Same as Figure 17 except for the summer streamflow timing PC1 (10, 25, 50, 75, and 90 percent, top to bottom) for the northern (a), central (b) and southern (c) stations.

this, above average antecedent precipitation decreases the land-ocean gradient thus delaying the initiation of the monsoon and the Julian day of the early streamflow (i.e., the 10 percent threshold). Northern and central stations, as expected, show the opposite correlation, presumably because of the influence of snowmelt. The correlations become weaker for the PC1s of the other thresholds, indicating that the early stages of the monsoon are most affected by antecedent precipitation. Results for correlation with the antecedent PDSI were similar (figures not shown).

To check the sensitivity of the above results to the definition of monsoon initiation, the same analysis is performed on the August to October (rather than July to October) monsoon streamflow. The results are similar to those seen for the July to October streamflow (Figure 21), however, the negative correlations are not quite as strong (figures not shown).

To investigate the role of ocean conditions in modulating the monsoon streamflow cycle, the PC1s of the timing are correlated with antecedent winter/spring SSTs (Figure 22). The early timing (i.e., 10th percent) of the streamflow in the southern region exhibited a significant positive correlation, albeit small, with tropical Pacific SSTs. This suggests that a warmer equatorial Pacific (i.e., El Niño conditions) tends to delay the timing of early monsoon streamflow, and vice-versa for cooler SSTs, via the mechanism proposed earlier. The northern region early monsoon flow timing shows negative correlations with the antecedent equatorial Pacific SSTs. This is likely due to the winter/spring flows impacting the early monsoon flow in this region, as seen earlier. The later timing (e.g., 50th percent) PCs show decreased correlations.

(a)   (b)   (c)
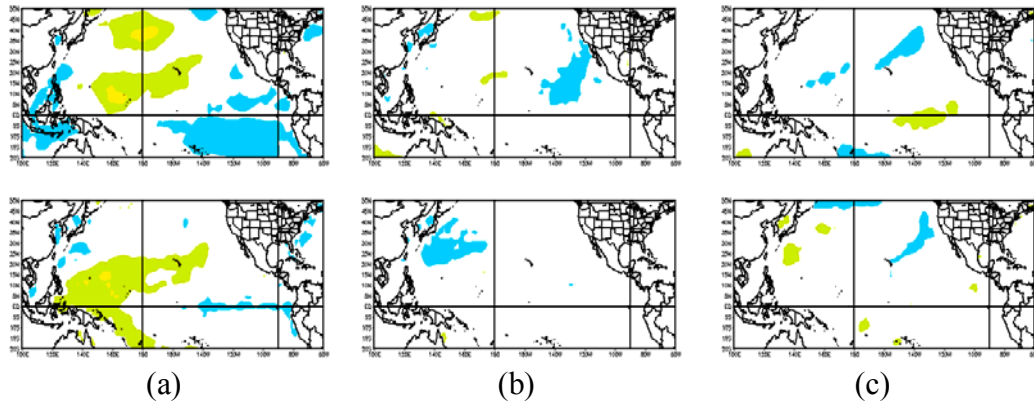
Figure 22. Same as Figure 17, except for PC1 of northern (a), central (b), and southern (c) stations 10% (top) and 50% (bottom) of monsoon season streamflow.

Caution is advised when interpreting these and other streamflow timing results and it is emphasized that the timing of streamflow is complex due, in part, to baseflow and the delayed nature of runoff. The timing of precipitation, in contrast, is much more direct to interpret: whenever it rains, the data indicate an accumulation of precipitation. Nevertheless, in a broad sense, these streamflow timing results do support the hypothesis and the previous precipitation results (Grantz et al 2006).

Summary and Conclusions

A systematic spatial and temporal analysis was performed on winter, spring and summer streamflows in the NAM region consisting of New Mexico and Arizona. Based on streamflow climatology and peak flow months, the stations were grouped into north (snowmelt dominated), central (early snowmelt and rain dominated), or south (summer rainfall dominated) regions. A significant increasing trend in the winter/spring streamflow was observed for recent decades. This trend is likely driven largely by enhanced ENSO activity. Both the magnitude and timing of early summer streamflows showed a significant relationship with antecedent winter/spring

53

precipitation in the NAM region with increased precipitation favoring a weaker and later streamflow cycle, and vice-versa. Summer streamflows in the northern region are largely impacted by the antecedent spring runoff. A simple approach was applied to remove this influence.

The results of this study motivated the following hypothesis to describe streamflow variability in the NAM region. Warmer than average equatorial Pacific SSTs and cooler than average northern Pacific SSTs lead to increased winter/ spring moisture over the NAM region. This increased moisture requires more time and solar energy to evaporate the moisture and heat up the land and set up the land-ocean gradient that drives the monsoon, thus delaying the monsoon and summer streamflow. This hypothesis was previously tested and validated with an analysis of monsoon precipitation (Grantz et al. 2006). The southern region monsoon streamflow showed a much closer association with this hypothesis relative to the northern region streamflow. The results for the northern region streamflow are mainly due to the effect of spring snowmelt extending into the summer months in the northern region.

The role of antecedent land and ocean conditions in modulating the following summer monsoon streamflow appears to be quite significant. This enhances the prospects for long-lead forecasts of monsoon streamflow timing and amount over the southwestern U.S., which could have significant implications for water resources planning and management in this water-scarce region.

CHAPTER 4

STREAMFLOW FORECAST

Introduction

Farmers in the desert southwest rely heavily on North American Monsoon (NAM) rains, in conjunction with spring runoff water held in storage, to irrigate their crops. Water management in this region, however, typically neglects monsoon streamflows in seasonal planning and operational strategies. The extreme variability of the summer monsoon presents a unique challenge that water managers often regard as too much risk for operations. As a result, runoff from large monsoon events, which can amount to a significant portion of the annual streamflow in the semi-arid region, must sometimes be spilled or released, thus disallowing the use of that water. If these events could be predicted and the operations could be adapted accordingly, the additional water would significantly benefit water users in the basin.

This chapter develops a seasonal (spring/monsoon) streamflow forecasting model for the Pecos River in New Mexico. First an overview of the Pecos River water resources system is provided; this includes a brief description of the physical basin and the policies and operations on the system. This is followed by the forecasting requirements for the basin. Next, predictors for forecasting the seasonal streamflow are identified and subsequently, the forecasting model is developed and

the best set of predictors in the modeling framework is selected. Finally, the skill and utility of the forecast model is evaluated.

Pecos River Basin

Selection Criteria

For the forecasting and water management application of this research a streamflow basin that meets the following criteria was identified.

- Has a significant summer streamflow component

- Is affected by large-scale and/or local-scale climate features (this is important for forecasting)

- Has significant water management issues impacted by summertime streamflow (e.g., irrigation, municipal and industrial, hydropower, environmental needs)

- Has policies or operations that rely on or could benefit from knowledge of the summer hydroclimate

- Has natural flow data available, either from the HCDN data set or computed

- Ideally, has a decision support tool already built and in use

Given the above criteria, the Pecos River Basin in New Mexico was selected because the river and its tributaries exhibit a significant summer streamflow component and have various water management issues and operations that may benefit from improved knowledge of the NAM variability and predictability.

The Pecos River originates in the Sangre de Cristo Mountains near Santa Fe, New Mexico. It flows in a southerly direction across the plains of eastern New Mexico for approximately 500 miles until crossing into Texas south of Carlsbad, New Mexico. In Texas, the Pecos River flows another 400 miles to its confluence with the Rio Grande near Shumla, Texas. The total drainage area at its confluence with the Rio Grande is 33,000 square miles, 19,000 of which lie within New Mexico (Boroughs and Stockton 2005). Figure 23 shows the topography and location of the Pecos River watershed.
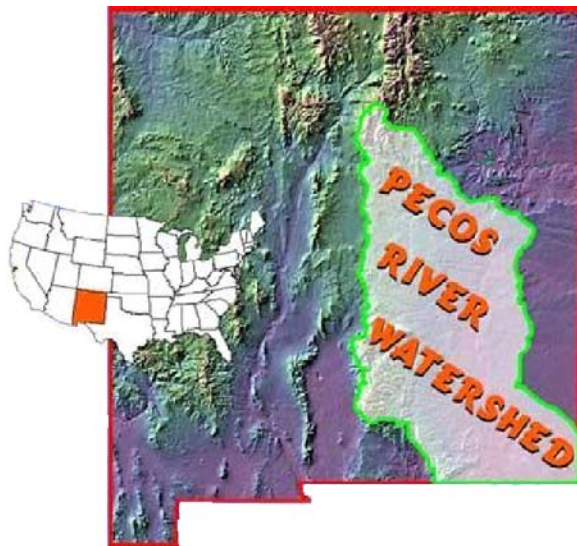
Figure 23. Pecos River Basin topography. Image courtesy of NMISC.

The Pecos River Basin occupies most of the eastern half of the state of New Mexico. The headwaters of the Pecos River lie at an elevation of over 12,000 feet and at the New Mexico-Texas state line the basin elevation is less than 2,000 feet. Average annual precipitation varies throughout the Pecos River Basin. In the northern mountainous regions, average annual precipitation is 16 to 17 inches per

year, much of it in the form of snow during the winter months. The eastern and northeastern plains receive an average of 13 inches per year, partly from snow and partly from rain. The lower elevation areas in the central and south basin receive an average of 11 inches per year, primarily from summer rainstorms. (NMOSE 2006)

Operations and Policies

Like most rivers in the western United States, the Pecos River has many competing demands for its limited water resources. These include agriculture, municipalities and industry, the environment, recreation, and inter-state delivery requirements. The U.S. Bureau of Reclamation (Reclamation), the U.S. Army Corps of Engineers (USACE), and the New Mexico Interstate Stream Commission (NMISC), among others, work together to manage the Pecos River to best meet the needs of these various interests.

The Pecos River in New Mexico is dammed at four major reservoirs, Santa Rosa, Sumner, Brantley, and Avalon, and supplies water to two major irrigation districts, the Fort Sumner Irrigation District (FSID) and the Carlsbad Irrigation District (CID) (Figure 24). Santa Rosa Dam, the north-most reservoir, is located north of the town Santa Rosa in Guadalupe County. Sumner Dam is approximately 50 miles downstream of Santa Rosa Dam near the town Ft. Sumner in De Baca County and Brantley Dam is upstream of Carlsbad in Eddy County. Avalon Dam is located 10 miles downstream of Brantley Dam. The three larger reservoirs, Santa Rosa, Sumner, and Brantley were built for flood control and to provide storage for CID, while Avalon Dam primarily provides elevation head for the main CID diversion. CID is located near the town of Carlsbad and diverts an annual average of

76,000 acre-feet to irrigate a potential 25,055 acres. The smaller FSID is located 14 miles below Sumner Dam near the town of Ft. Sumner and diverts an average of 38,200 acre-feet annually to irrigate 6,500 acres. River pumpers not formally organized as an irrigation or conservancy district also divert an annual average of 4,200 acre-feet between Sumner Dam and Brantley Dam.
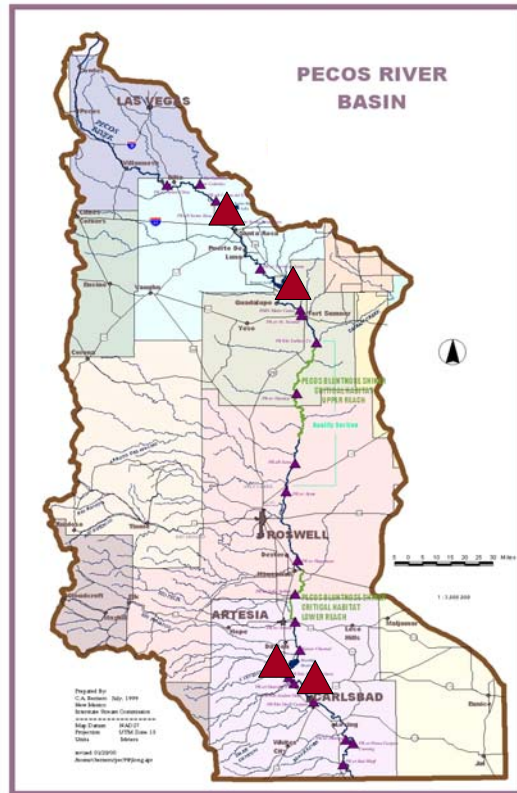
Figure 24. Pecos River Basin. Large triangles represent reservoirs. Image courtesy of Craig Boroughs.

The reservoirs of the Pecos River system are operated primarily to optimize water delivery to CID farmers. A main objective is to keep Pecos River water stored upstream in Santa Rosa and Sumner reservoirs for as long as possible, then release the water in block releases when addition water is needed in Brantley Reservoir. The purpose of the block releases is to limit evaporation and seepage in the middle

stretches of the river. Block releases are made only during the irrigation season, March 1st to October 31st, and are initiated and stopped based on storage triggers in Brantley Reservoir. Other releases include flood control releases, the evacuation of water above the conservation storage limit, and releases for FISD, which can divert up to 100 cfs of natural river flow during irrigation season. (Boroughs and Stockton 2005)

In addition to irrigation, Pecos River water must also be managed for environmental objectives as well as inter-state stream deliveries, among other objectives. In 1987, the Pecos bluntnose shiner (*Notropis simus pecosensis*) (shiner) was listed as federally threatened under the Endangered Species Act (ESA) of 1973. A biological opinion issued in 1991 concluded that pre-1991 operations would likely jeopardize the continued existence of the shiner and adversely modify the critical habitat of this species. Under the ensuing National Environmental Policy Act (NEPA) process, Reclamation developed a daily-timestep water operations computer model of the Pecos River and Reasonable and Prudent Alternatives (RPAs) to existing operations. These alternatives include limiting block releases to 15 consecutive days, requiring 14 days between block releases and eliminating block releases for a 6-week period around the beginning of August. (Boroughs and Stockton 2005)

Litigation between New Mexico and Texas over Pecos River water is a major component of the river's history. The 1949 Pecos River Compact divides the water of the Pecos River between the States, but, because of the river's irregular flow, does not specify a particular amount of water to be delivered by New Mexico to Texas

each year. Lawsuits, amended decrees, and settlements followed and today's agreement is the result of New Mexico paying Texas of a large sum of money, the purchasing and leasing water rights to deliver water to Texas, and conjunctive use with groundwater. Today CID still operates the reservoirs as efficiently as possible to yield the most water to their farmers to either irrigate or lease to the State.

Pecos River operations for CID make use of existing storage levels in the basin and do not utilize forecasts of incoming water. Annual irrigation allotments are established on March 1st based on the basin storage on that date. This allotment is increased throughout the irrigation season (on May 1st, June 1st, July 15th, and September 1st) if additional water enters the system. An advanced knowledge of the incoming spring and summer runoff could provide a better estimate of the irrigation season's allotment, thus allowing farmers to better plan types and sizes of crops. In a similar vein, block releases are based on storage in Brantley Reservoir and do not account for the possibility of inflows below Sumner from monsoon rainfall. Consequently, after a block release Brantley Reservoir is often unable to accommodate monsoon runoff and the system is forced to spill water to Texas. Given an advanced knowledge of monsoonal runoff, operators could better manage block releases, thus potentially reducing spills to Texas and increasing deliveries to CID.

Forecasting requirements

It is apparent from the previous section that improved management on the Pecos River Basin can potentially be achieved by using skillful forecasts of spring and summer runoff to adjust block release and allotment criteria and minimize spill to Texas. For the allotment criteria, a forecast is required at each allotment calculation

date: March 1st, May 1st, June 1st, July 15th, and September 1st.   At each of these dates, the total remaining irrigation season inflow volume to the entire basin must be predicted to determine how much additional water will be available for irrigation. For the adjustment of block releases, forecasts of basin inflows below Sumner Reservoir are required.   Because of the localized and erratic nature of monsoon thunderstorms, it is impractical to predict basin-wide monsoon precipitation on sub-seasonal timescales.   Hence, for the block releases seasonal streamflows were forecasted at the above listed five dates.   At each lead time the inflow volume for the remainder of the irrigation season is forecasted (e.g., on March 1st the March 1st to October 31st inflow volume is required, on May 1st the May 1st to October 31st inflow volume, and so on) in the upper and lower Pecos basin.

For each forecast lead time, potential predictors of the seasonal streamflow are identified from the land-ocean-atmosphere system.   The best predictor combination is obtained for a nonparametric forecasting model (Grantz et al., 2005; Prairie et al., 2006), thus producing the best forecast model.   Forecasts are issued in a cross-validated mode and their skills evaluated.   This process is described in the following sections.

Data

The following data sets for the period 1949 – 1999 were used for the forecast component of this research.

Streamflow

Monthly streamflow data for the Pecos River Basin were obtained from Craig Boroughs of the Hydrology/Water Operations Work Group for the Carlsbad Project

Water Operations and Water Supply Conservation NEPA process. This data set is the result of an extensive study of inflows to the Pecos River performed for the NEPA process. The study designated seven sub-basins in which inflows to the Pecos River were calculated. The seven sub-basins are: above Santa Rosa reservoir, Puerto de Luna, Acme, Lake Arthur, Artesia, Kaiser, and Dam Site 3. For the inflows to Santa Rosa reservoir, United States Geological Survey (USGS) gaged flow could be used. Due to damming and diversions, gaged flow in the remaining six subbasins does not accurately reflect natural river flow, thus calculations were required to establish a natural flow data set for these river reaches.

Annual hydrographs of the seven side inflows to the Pecos River are shown in Figure 25. It can be seen that the runoff in the first two subbasins and bottom five subbasins are climatologically similar. Of all the stations, the two northern stations (i.e., the upper basin) contain a significant amount of streamflow in the months before July. Conversely, the bottom five stations (i.e., lower basin) are monsoon streamflow (i.e., after July) dominated. Though Puerto de Luna could also be grouped with the lower stations, the requirements of the forecast locations make clustering the top two stations together a good option.

Grouping the stations, an index of upper-basin (above Santa Rosa and Puerto de Luna) streamflow was developed by adding the flow at these two locations for each season separately (March to June, May to June, June, July to October, and September to October). An index of the lower-basin below Sumner Reservoir (Acme, Lake Arthur, Artesia, Kaiser, and Dam Site 3) was similarly estimated. Henceforth, these two indices are referred to as upper and lower basin streamflow. As an
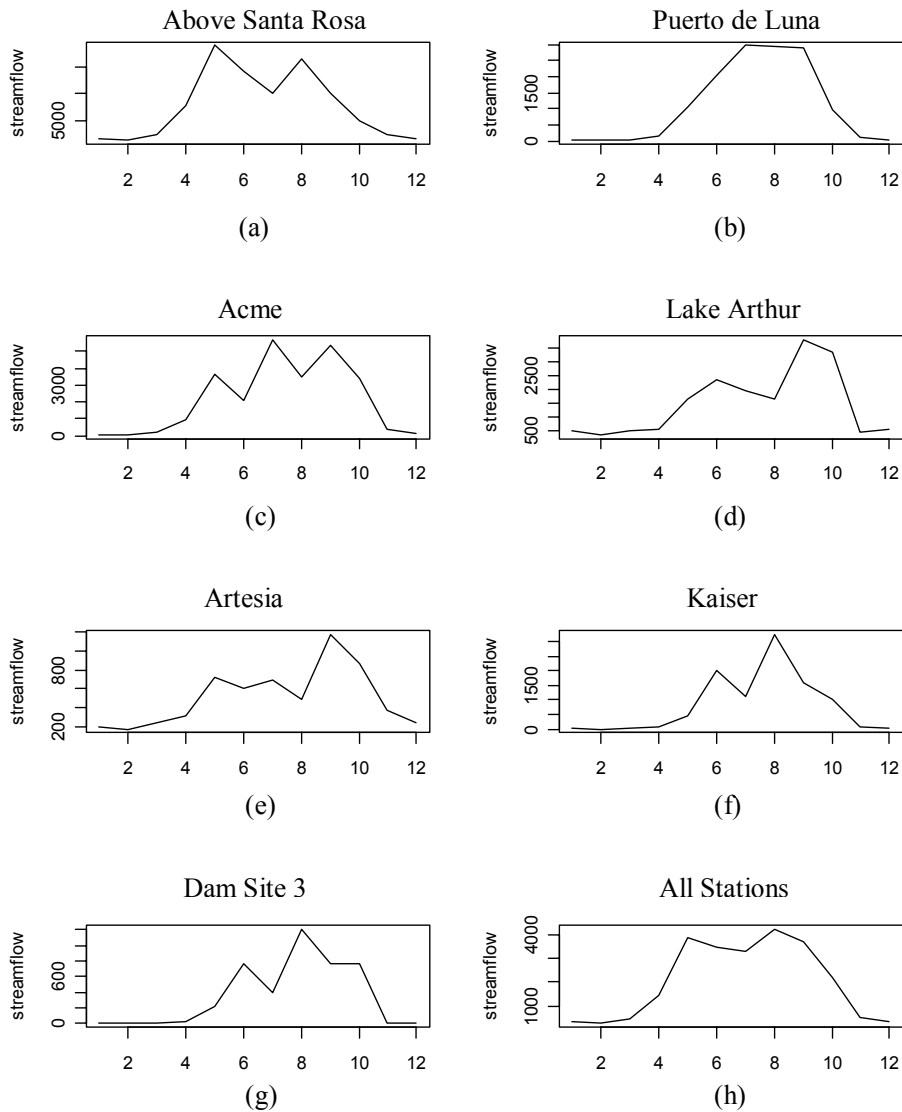
Figure 25. Pecos River side inflow hydrographs. Stations a to g are listed from north to south.

illustration, the upper and lower basin streamflow of the March to June season are shown in Figure 26. Operationally, lower basin streamflows are needed for adjustment of block releases. Both the upper and lower basin streamflows are used for the calculation of allotments.
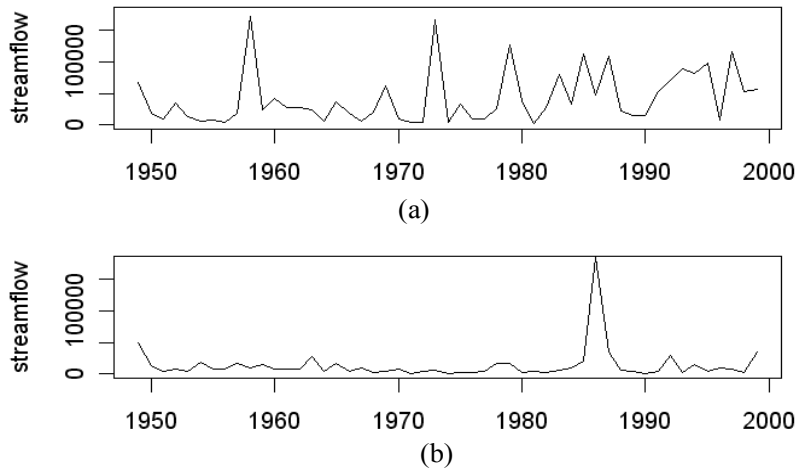
Figure 26. March to June streamflow in the upper (a) and lower (b) Pecos River.

Precipitation, PDSI, Temperature, and SWE

Monthly precipitation, Palmer Drought Severity Index (PDSI), a surrogate for soil moisture, and temperature data for climate divisions in the western U.S. were obtained from the U.S. climate division data set from the NOAA-CIRES Climate Diagnostics Center (CDC) website (www.cdc.noaa.gov). Monthly snow water equivalent (SWE) data were obtained from the Natural Resources Conservation Service (NRCS) National Water and Climate Center website (www.wcc.nrcs.usda.gov). The SWE data is gathered from snow course and snotel stations in upper Pecos Basin, however, due to paucity of locations (five in the basin) and incomplete data sets, only one station, Panchuela snow course site, could be used in this study. The Panchuela site is located near the headwaters of the Pecos River just north of the town of Pecos at an elevation of 8,400 feet.

Monthly values of large-scale ocean and atmospheric variables such as sea surface temperatures (SSTs), geopotential heights, precipitable water, air temperatures, sea level pressures, and zonal winds come from the NCEP/NCAR Re-analysis data set (Kalnay et al. 1996). These were obtained from the NOAA-CIRES CDC website (www.cdc.noaa.gov).

Identification of Predictors

The first step in the forecasting framework is to identify predictors of flows in the basin. From Chapters 2 and 3, it is known that winter, spring, and early summer large-scale land-ocean-atmosphere features are well related to spring and summer streamflows in the NAM region. Therfore, the upper and lower Pecos irrigation season streamflows developed earlier are correlated with the preceding season's large-scale land-ocean-atmosphere variables.

It is recognized that the signals that affect spring streamflow distinctly differ from those that affect monsoon streamflow (e.g., Figure 15 and Figure 19 in Chapter 3). In light of this, predictors for the spring component of the irrigation season (March to June) and the summer component (July to October) were investigated separately. Thus, predictors for 16 different seasonal streamflows on the upper and lower Pecos, at all five lead times were identified separately. The 16 forecasts are:

- March 1st: March-June upper Pecos, March-June lower Pecos, July-October upper Pecos, July-October lower Pecos

- May 1st: May-June upper Pecos, May-June lower Pecos, July-October upper Pecos, July-October lower Pecos

- June 1st: June upper Pecos, June lower Pecos,

                       July-October upper Pecos, July-October lower Pecos

- July 15th: July-October upper Pecos, July-October lower Pecos

- Sept 1st: Sept-October upper Pecos, Sept-October lower Pecos

The results presented in Chapters 2 and 3 suggest that irrigation season streamflows in the Pecos River Basin are likely modulated by large-scale land-ocean-atmosphere climate patterns potentially related to well known phenomena such as the El Niño-Southern Oscillation (ENSO) and the Pacific Decadal Oscillation (PDO). The standard indices of these phenomena, PDO, NINO3, NINO3.4, NINO4, NINO1.2, bivariate ENSO, North Atlantic Osciallation (NAO), Pacific/North American (PNA) pattern, Southern Osciallation Index (SOI), Tropical Northern Atlantic (TNA) index, and Trans-NINO Index (TNI) showed little or no statistically significanct correlation with the irrigation season streamflows in the basin. This is not surprising given that these teleconnection patterns, though dominant on a large scale, often fail to provide predictive skill in individual basins, particularly if the basin is outside the defined core teleconnection regions (e.g., McCabe and Dettinger, 2002). Moreover, relatively minor shifts in large-scale atmospheric patterns can result in large differences in the surface climate (e.g., Yarnal and Diaz, 1986), suggesting that predictive indices may need to be basin-specific. Thus, the seasonal streamflows were correlated with the land-ocean-atmosphere variables (e.g., 500mb geopotential height fields, SSTs, etc.) from preceding seasons to identify potential predictors in the Pecos River Basin. This method of predictor identification has been successfully used in the forecast of streamflows in western U.S. and rainfall forecast

over Thailand (e.g., Grantz et al. 2005; Regonda et al. 2006; Singhrattna et al. 2005)

Figure 27 presents the correlations between the winter (Dec-Feb) SSTs, 500mb geopotential heights (henceforth, referred to as Z500) and 200mb zonal winds in the Pacific Ocean with the upper Pecos spring (Mar-Jun) and summer (Jul-Oct) streamflow. The figure demonstrates that patterns related to spring streamflow differ dramatically from, and are almost opposite to, those for the summer streamflow. For the March to June streamflow, there are strong positive correlations (approximately 0.5) with SSTs in the equatorial Pacific and strong negative correlations

(a)   (b)
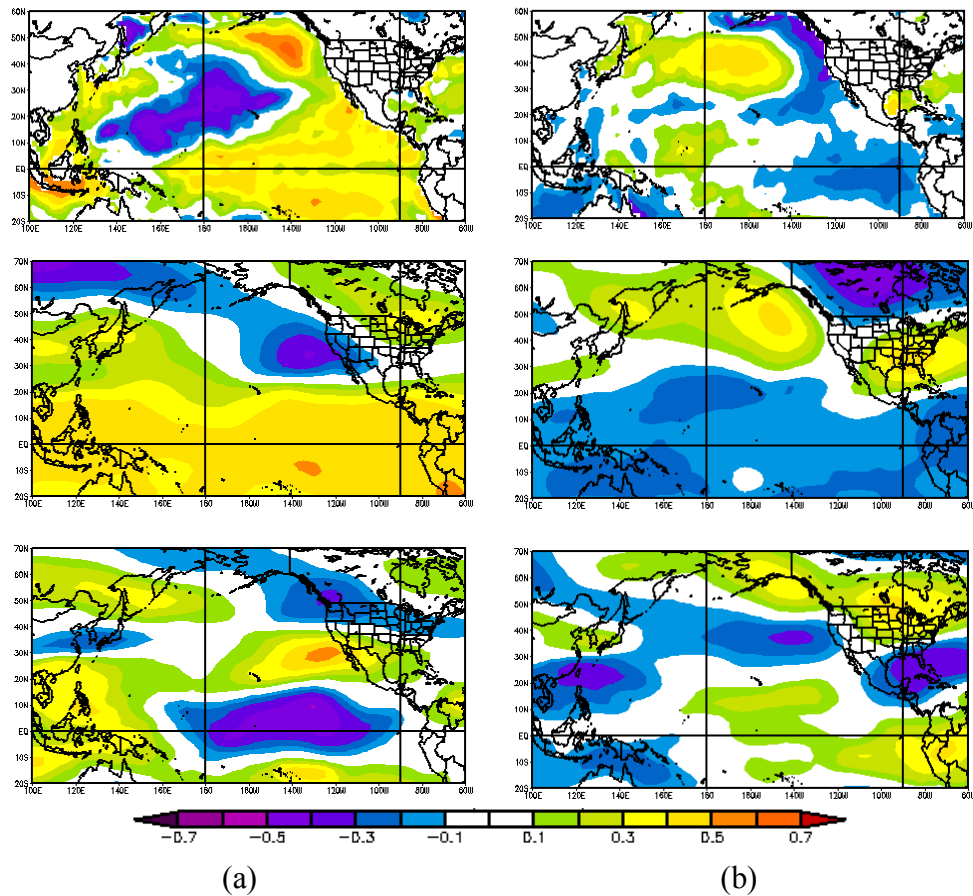
Figure 27. December to February Z500, SSTs, and 200mb zonal winds (top to bottom, respectively) correlated with upper Pecos March to June (a) streamflow and July to October (b) streamflow. Images provided by the NOAA-CIRES Climate Diagnostics Center, in Boulder, Colorado from their web site at www.cdc.noaa.gov.

(approximately -0.5) with SSTs in the northern Pacific. Above normal equatorial SSTs in winter (i.e., El Niño conditions) are known to be related to above average winter precipitation and streamflow in the southwestern U.S. (e.g., Cayan and Peterson 1989, Redmond and Koch 1991, Piechota et al. 1997, and the findings from this research in Chapters 2 and 3). Thus, the correlation pattern seen in this figure is consistent with prior findings.

Correlations between the Z500 and the March to June streamflow (Figure 27, a, middle) resemble the PNA pattern (e.g., Wallace and Gutzler 1981; Barnston and Livezey 1987; Leathers et al. 1991), though shifted slightly south. The negative correlation pattern off the coast of California indicates that when winter pressures in this region are below average, spring streamflow in the Pecos River Basin is above average. This is consistent, in that negative pressure anomalies in the northern hemisphere induce counter-clockwise winds around the pressure centers, in this case bringing southerly winds over the Pecos River Basin. Southerly winds tend to be warm and moist, thus increasing the chances of enhanced winter precipitation and, consequently, higher streamflows the following spring. Hence, the negative correlation pattern emerges.

The 200mb zonal winds (Figure 27, a, bottom) corroborate the correlation patterns seen in the Z500, showing positive correlations in the region below and to the right of the negative pressure center where the winds are strongest.

The correlation patterns for July to October monsoonal streamflow (Figure 27, b) are effectively opposite to those for the spring streamflow, though they are somewhat weaker. This inverse relationship is consistent with the results of Chapter

3 and the known inverse relationship between winter precipitation and subsequent summer precipitation in southwestern U.S. (e.g., Gutzler, 2000; Higgins and Shi, 2000; Lo and Clark, 2002). Large-scale climate patterns that increase winter precipitation, and hence spring streamflows, tend to decreased summer precipitation and streamflow by decreasing the land-ocean temperature contrast, a key driver of the summer monsoon. The comparably weaker correlation patterns are likely due to the fact that NAM precipitation is highly variable and relatively weakly modulated by antecedent large-scale climate features.

The correlations between the December to February SSTs, Z500 and 200mb zonal winds in the Pacific Ocean and the lower Pecos spring and summer streamflow are presented in Figure 28. The correlation patterns for the lower Pecos, though
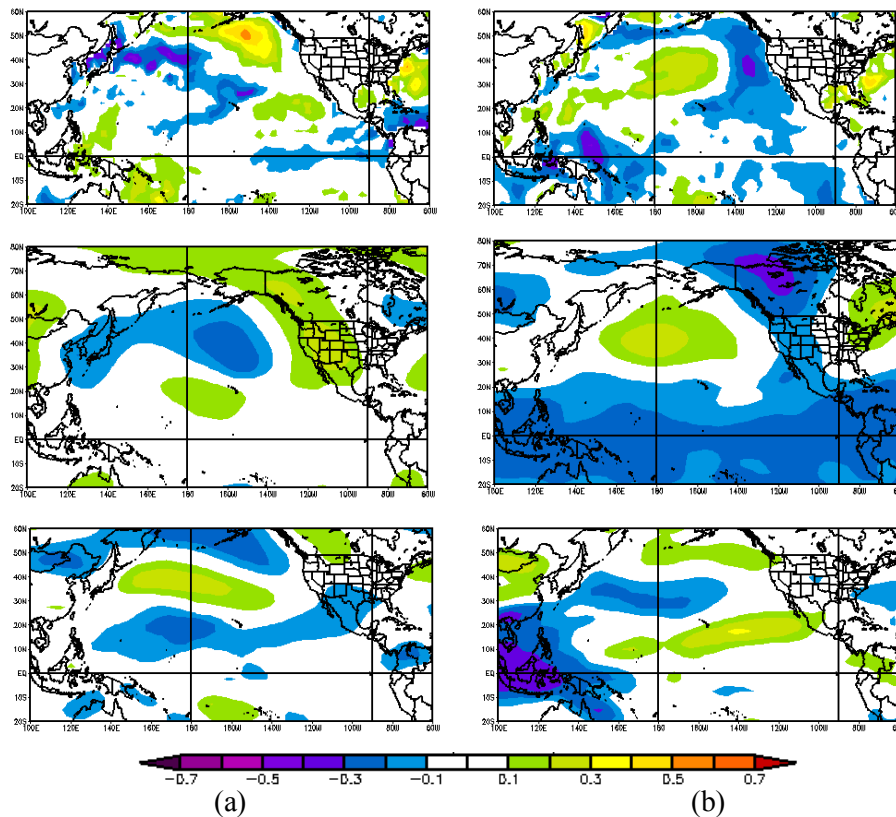
Figure 28. Same as Figure 27, except for the lower Pecos streamflow.

generally that same as those for the upper Pecos (Figure 27), are significantly weaker and less organized. This is particularly true for the March to June correlations when streamflow signal in the lower Pecos is considerably smaller than that for the upper Pecos (see Figure 25). In addition, the lower Pecos streamflow is a sum of the inflow at five locations that do not correlate well with each other, and thus may not exhibit as cohesive a signal as the upper two stations.

Correlations between the upper Pecos streamflow and the December to February PDSI and Precipitation across all U.S. climate divisions are presented in Figure 29. The correlations over the New Mexico region are positive for March to
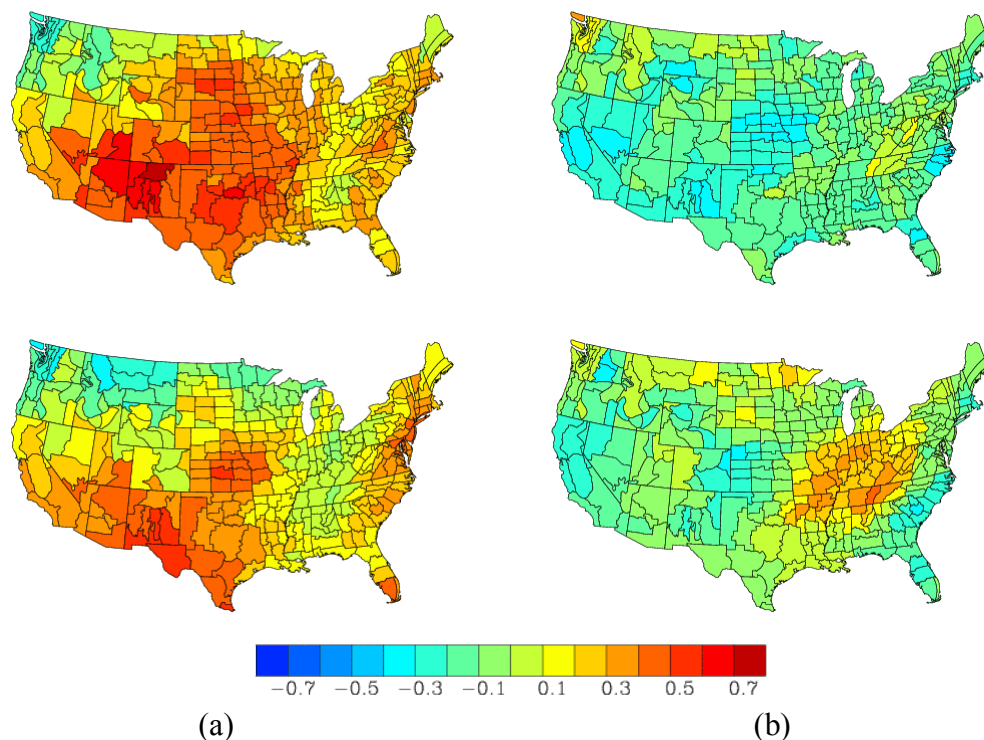
Figure 29. December to February PDSI (top) and Precipitation (bottom) correlated with upper Pecos March to June (a) streamflow and July to October (b) streamflow. Images provided by the NOAACIRES Climate Diagnostics Center, in Boulder, Colorado from their web site at www.cdc.noaa.gov.

June indicating that increased winter soil moisture and precipitation lead to increased spring streamflow in the Pecos. Conversely, the correlations over the New Mexico region are negative for the July to October streamflow, suggesting that wetter winters lead to drier summers, and vice versa. Correlations for the lower Pecos River are similar, though not as strong (figures not shown).

For the May 1st forecast, correlations between the December to April large-scale climate variables and May to June and July to October streamflow in the upper Pecos are investigated (Figure 30). It can be seen from this figure that the patterns are similar to the December to February correlations (Figure 27). Correlations with

(a)   (b)
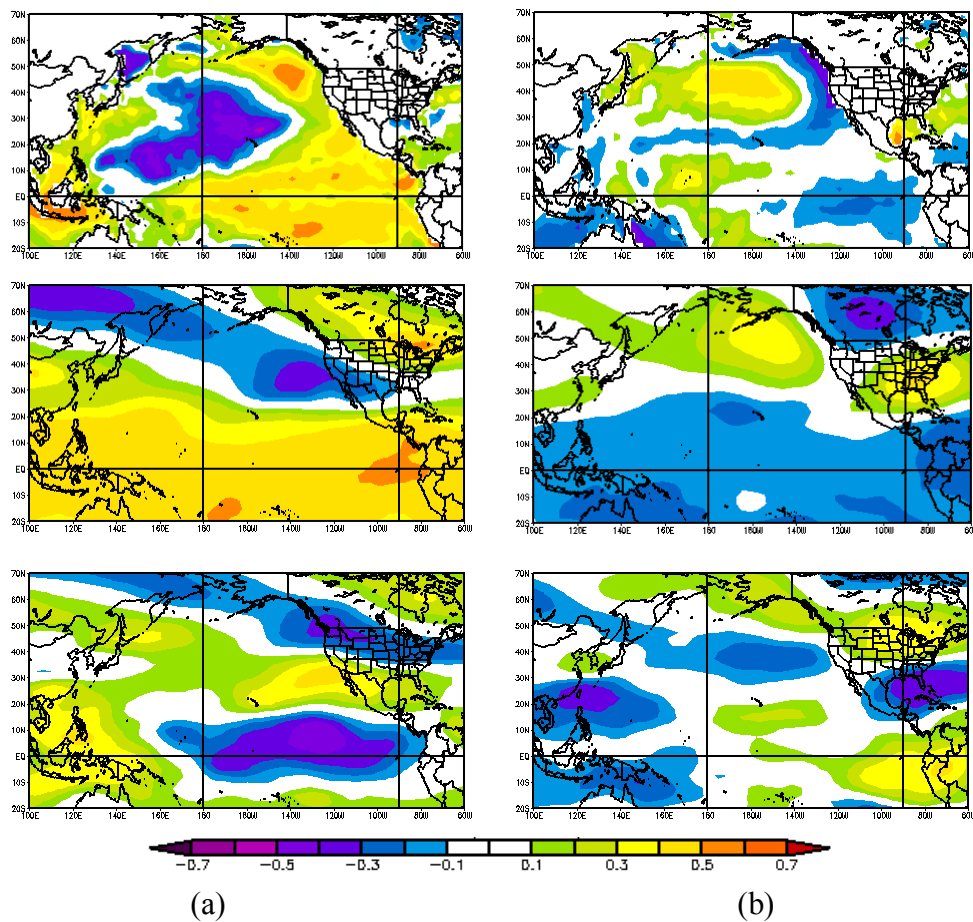
Figure 30. Same as Figure 27 except for December to April climate variables.

the antecedent PDSI and precipitation correlations (Figure 31) are also comparable with those of the December to February period (Figure 29). Correlations for the lower Pecos are similar, though weaker (figures not shown). This suggests that the large-scale climate patterns modulating the winter, and in particular spring, streamflows are persistent and well organized and, thus, can potentially help provide skillful seasonal streamflow forecasts.

(a)   (b)
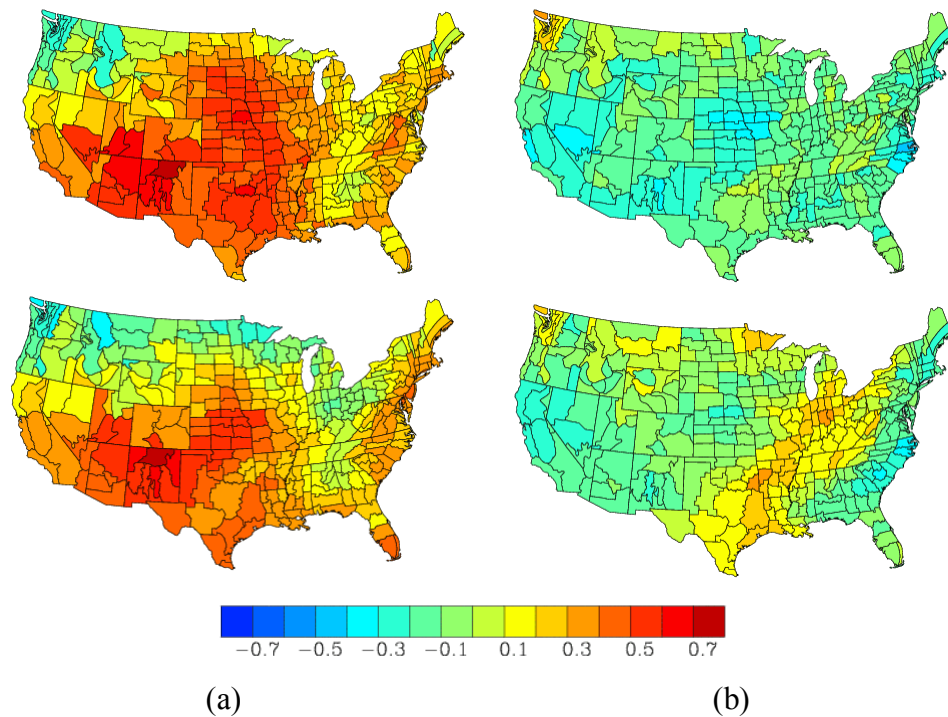
Figure 31.   Same as Figure 29 except for December to April PDSI and Precipitation

Predictors for the June 1st and July 15th forecast lead times present similar correlation patterns to those for the March 1st and May 1st lead times. This is because it is the winter large-scale climate that most affects monsoon streamflow and December to May variables are used as predictors for all lead times.

For the September 1st forecast lead time, correlations of the September to October streamflow with antecedent July to August large-scale climate and hydroclimate (i.e., PDSI and precipitation) variables are shown in Figure 32. The
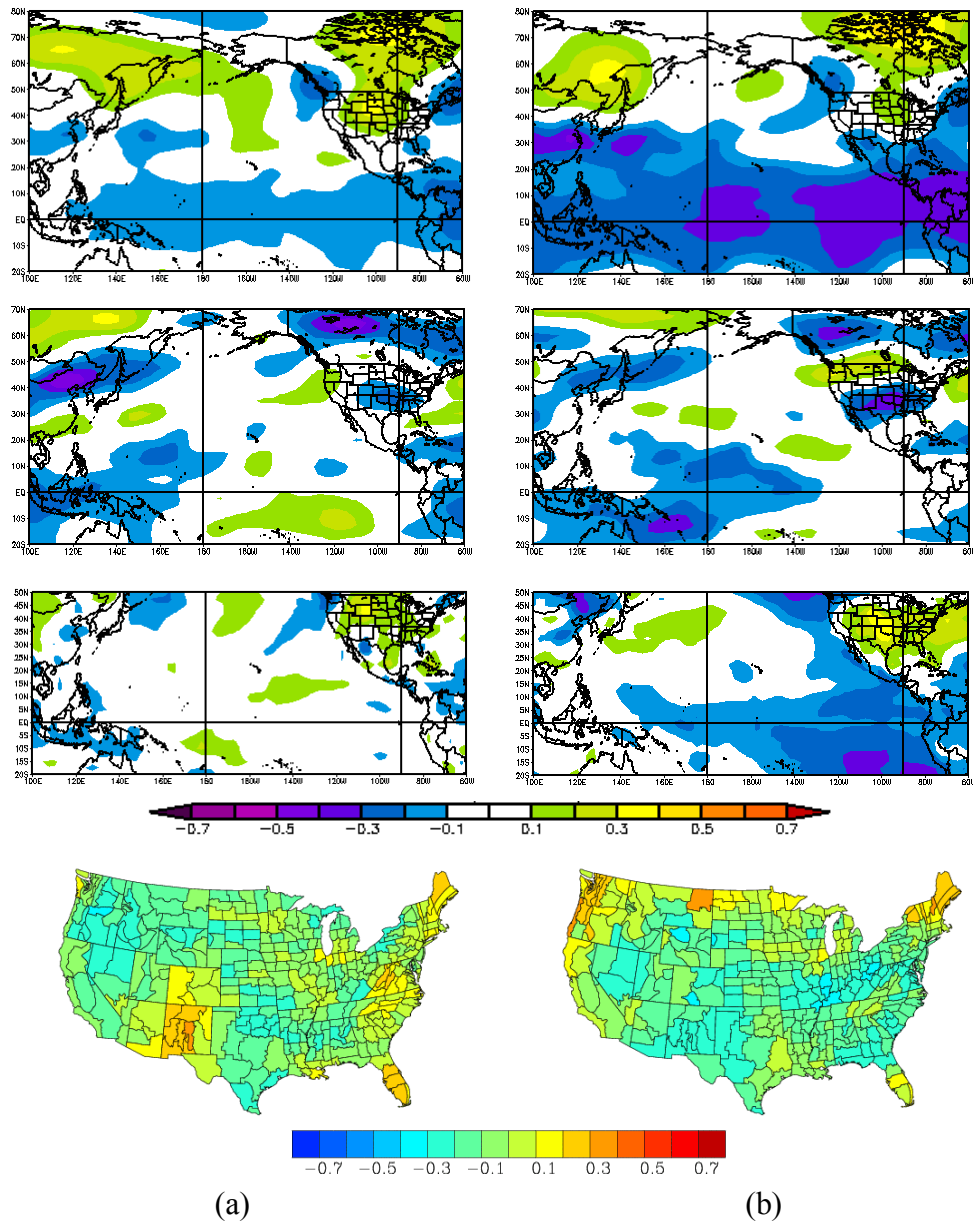
Figure 32. Predictors September to October streamflow in the upper Pecos (a) and lower Pecos (b). From top to bottom they are: Jul-Aug Z500 (a) and (b); Jul-Aug air temperature (a) and Dec-Jul air temperature (b); Jul-Aug 200mb zonal winds (a) and (b); Jul-Aug precipitation (a) and Dec-Jun PDSI (b). Images provided by the NOAACIRES Climate Diagnostics Center, in Boulder, Colorado from their web site at www.cdc.noaa.gov.

patterns are considerably weaker and less organized than those for the earlier forecast dates. It is also interesting to note that the patterns driving the lower Pecos River are stronger than those driving the upper Pecos River; this is the converse of the findings for the earlier forecast dates. This is consistent with the findings in Chapters 2 and 3 which demonstrated that the drivers of late-season monsoon precipitation and streamflow are not nearly as obvious as those for the early season monsoon.

A good portion of the irrigation season streamflow in the Pecos River comes in spring largely due to snowmelt runoff. Thus, SWE could also be a potential predictor of the seasonal streamflow. Figure 33 shows the scatterplots of the March 1st and April 1st SWE with the May to June streamflow in the upper and lower Pecos. Figure 34 shows the same for the June streamflow. As expected, SWE is positively
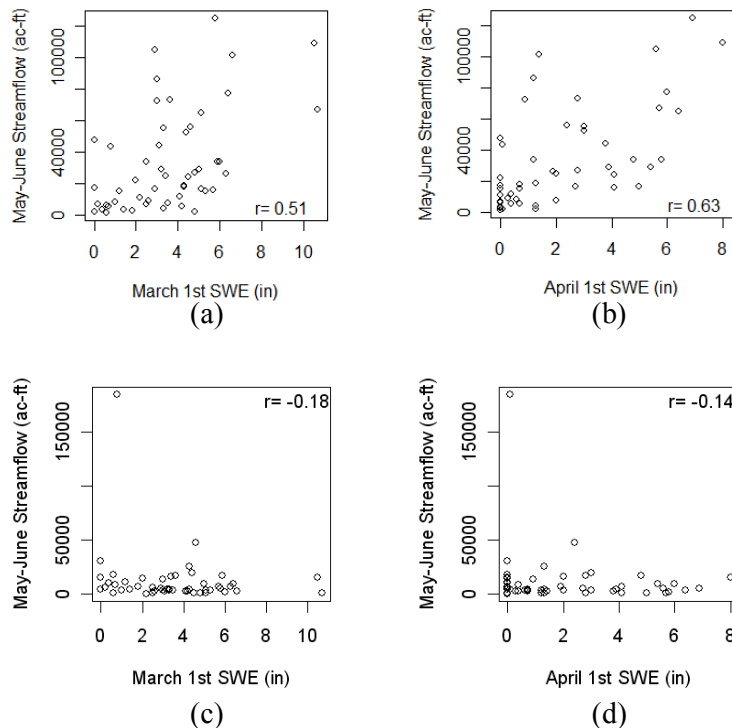
Figure 33. May to June streamflow with March 1st SWE (a, c) and April 1st SWE (b, d) in the upper (a,b) and lower (c,d) Pecos River.

correlated with spring streamflow. For the upper Pecos, the April 1st SWE is a better indicator of spring runoff than the March 1st SWE. This relationship is typical of basins across the western U.S. because the April 1st SWE usually provides a more accurate representation of total winter snowpack in a basin. It is interesting to note that for most years in the Pecos River Basin, the April 1st SWE is actually lower than the March 1st SWE, implying that the winter snowpack begins to melt sometime in March. The SWE—spring streamflow relationship, however, is not as strong as is typical in several other Western U.S. basins; for example, the Truckee-Carson Basin (Grantz et al. 2005) and the Gunnison Basin (Regonda et al. 2006). This could be due to the fact that only one snow course site was available for this study. Because of anomalies and errors in snow course data, more measurements and locations provide
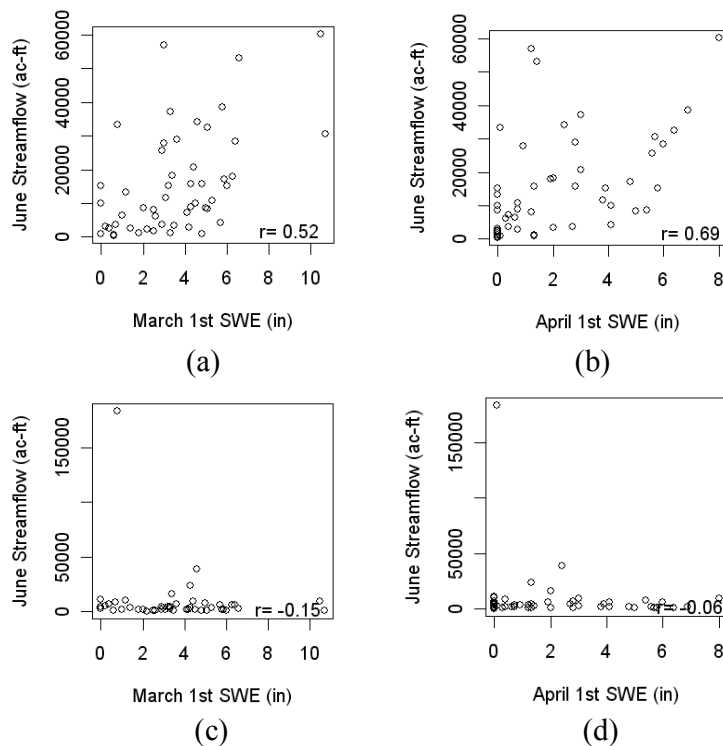
Figure 34. June streamflow with March 1st SWE (a, c) and April 1st SWE (b, d) in the upper (a, b) and lower (c,d) Pecos River.

a better indication of total snowpack, and hence runoff, in a basin. Also, in 1986, the lower Pecos River experienced a very wet June though the SWE in that year was below average. It is believed that the June runoff in that year was due to early monsoon rainfall, rather than snowmelt. This outlier significantly affects the Pearson's R values reported here.

Correlations between SWE and the summer (Jul-Oct) Pecos streamflow (Figure 35) demonstrate the well-documented negative relationship between monsoonal streamflow and the preceding winter's snowfall (Gutzler 2000; Higgins and Shi 2000; Lo and Clark 2002; Zhu et al. 2005).
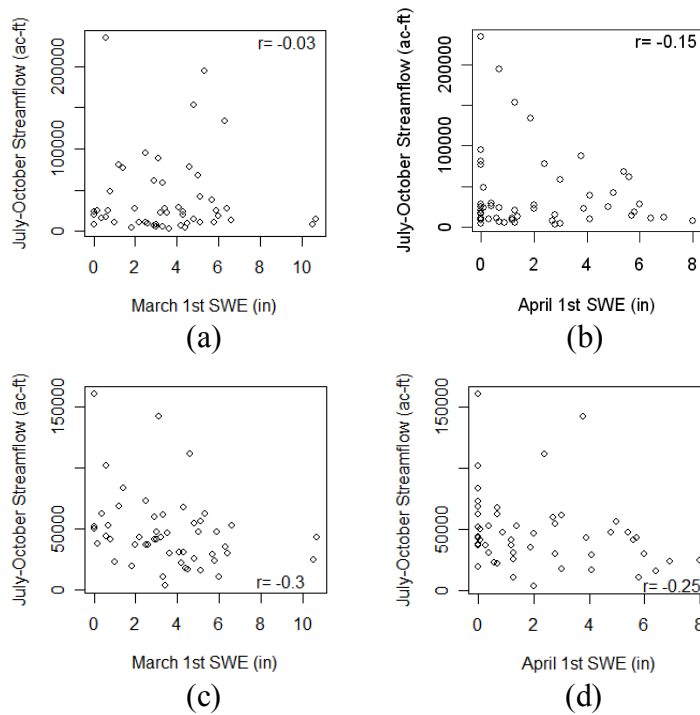
Figure 35. SWE with July to October streamflow: upper Pecos and March 1st (a) and April 1st SWE (b), lower Pecos and March 1st (c) and April 1st SWE (d).

Streamflows are generally autocorrelated; thus to garner potential predictors from this phenomenon, seasonal streamflows were correlated with the preceding

seasonal or monthly streamflows (Figure 36). Strong autocorrelations are evident especially with the May to June streamflows and the preceding April flows in the upper Pecos. Also, the June streamflows demonstrate substantial correlation with the preceding May flows. Weak autocorrelations in the spring streamflows were observed in the lower Pecos streamflows.

| (a) | (b) | (c) |
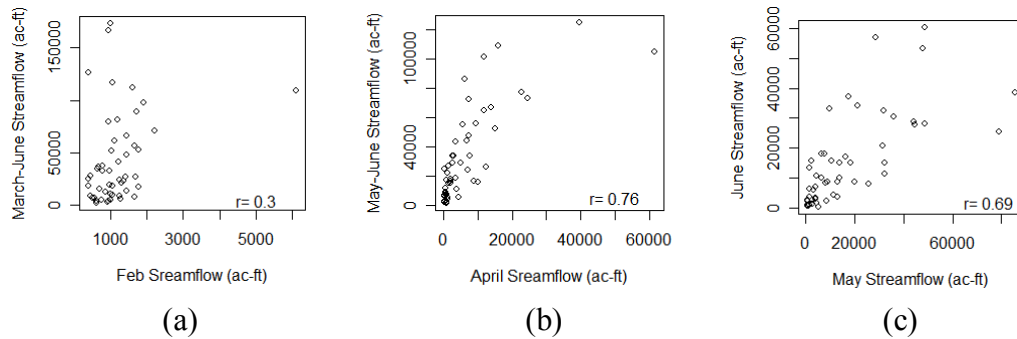
Figure 36. Lag-1 streamflow correlations for the upper Pecos River.

Based on all the correlation maps and scatterplots developed (some of which are presented above), predictors to each seasonal streamflow are compiled. Using the correlation maps, regions of high correlation (positive or negative) are identified and the variable is averaged over the region for each year, thus resulting in a predictor timeseries. In cases when there are regions with significant positive and negative correlation, the timeseries are computed separately for each region and then one timeseries is subtracted from the other to result in a single predictor time series. Thus, for each forecast lead time all the potential predictors are identified and timeseries are computed. These are compiled in Table 6.

Table 6. Potential predictors.

	Upper Basin Spring	Upper Basin Summer	Lower Basin Spring	Lower Basin Summer
Mar 1st	Dec-Feb: Z500 (pos-neg) SSTs (pos-neg) Z Winds (pos-neg) SWE (Mar 1) PDSI Precip Feb streamflow	Dec-Feb: Z500 (pos-neg) SSTs (pos-neg) Z Winds ((pos-neg) SWE (Mar 1) PDSI Air Temp	Dec-Feb: Z500 (pos-neg) SSTs (pos-neg) SWE (Mar 1) PDSI Precip	Dec-Feb: Z500 (pos-neg) SSTs (pos-neg) Z Winds SWE (Mar 1) PDSI Precip
May 1st	Dec-Apr: Z500 (pos-neg) SSTs (pos-neg) Z Winds (pos-neg) SWE (Mar 1st) SWE (Apr 1st) PDSI Air Temp Apr streamflow	Dec-Apr: Z500 (pos-neg) SSTs (pos-neg) Z Winds (pos-neg) SWE (Mar 1st) SWE (Apr 1st) PDSI Air Temp SSTs (gulf)	Dec-Apr: Z500 SSTs (pos-neg) SWE (Mar 1st) SWE (Apr 1st) PDSI Air Temp	Dec-Apr: Z500 SSTs (pos-neg) SWE (Mar 1st) SWE (Apr 1st) Precip
Jun 1st	Dec-May: Z500 (pos-neg) SSTs (pos-neg) Z Winds (pos-neg) SWE (Mar 1st) SWE (Apr 1st) PDSI Precip Air Temp May streamflow	Dec-May: Z500 (pos-neg) SSTs Z Winds (pos-neg) SWE (Mar 1st) SWE (Apr 1st) PDSI Precip Air Temp	Dec-May: Z500 SSTs (pos-neg) Z Winds(pos-neg) SWE (Mar 1st) SWE (Apr 1st) PDSI Air Temp	Dec-May: Z500 SSTs (pos-neg) Z Winds (pos-neg) SWE (Mar 1st) SWE (Apr 1st) PDSI Precip Air Temp
Jul 15th		Dec-May: Z500 (pos-neg) SSTs (pos-neg) Z Winds (pos-neg) SWE (Mar 1st) SWE (Apr 1st) PDSI Air Temp		Dec-May: Z500 SSTs Z Winds SWE (Mar 1st) SWE (Apr 1st) PDSI Precip
Sep 1st		Jul-Aug: Z500 SSTs (Dec-May) Z Winds Z Winds (Dec-May) SWE (Mar 1st) SWE (Apr 1st) Precip Air Temp Jul-Aug streamflow		Jul-Aug: Z500 Z500 (Dec-Jul) Z Winds Z Winds (Dec-Jul) SWE (Mar 1st) SWE (Apr 1st) PDSI (Dec-Jun) Air Temp (Dec-Jul)

Forecast Model

Many of the predictors selected for forecasting the seasonal streamflows in the Pecoso River Basin are highly correlated (e.g., SWE and precipitation or the Z500 and 200mb zonal winds) and are likely responses to the same physical mechanism. Including all the correlated predictors in a forecasting model can lead to over-fitting and poor skill in prediction; this is known as multicollinearity. Thus, the best subset of predictors needs to be identified. This section presents the forecast modeling framework first, followed by the method for selecting the best subset of predictors.

Forecast Model Framework

Statistical forecast models can be generally represented as:

$$Y = f(x_1, x_2, x_3, \ldots x_p) + e$$

where f is a function fitted to the predictor variables $(x_1, x_2, \ldots, x_p)$, Y is the dependent variable (in this case the spring or monsoon streamflows) and e is the errors, typically assumed to be normally (or Gaussian) distributed with a mean of 0 and variance σ.

Traditional (also known as parametric) models assume that the underlying function relating the predictor and the dependent variable is linear and fit a linear equation by minimizing the errors. This is also known as linear regression (Helsel and Hirsch 1995) and is of the form:

$$Y = a_1 x_1 + a_2 x_2 + \ldots + a_p x_p + b + e$$

where the dependent variable Y is linearly fit to the predictor variables $(x_1, x_2, \ldots, x_p)$, $a_1, a_2, \ldots, a_p$ are the regression coefficients, b is the intercept, and e is the errors assumed to be normally distributed with a mean of 0 and variance σ. The fitted linear

model is tested for adequacy. The theory behind linear regression has been well developed and several software packages exist for ease of implementation.

However, linear regression has several shortcomings, including the following. (i) The assumption that the underlying function is linear can be restrictive. (ii) The data have to be normally distributed for testing model adequacy. If the data are not normally distributed they have to be transformed. This task can be quite difficult to achieve on real data. (iii) The least squares method of model parameter estimation is very sensitive to outliers. (iv) Higher order models (quadratic, cubic, etc.) require a larger number of model parameters to be estimated, thus increasing model uncertainty. The main limiting feature of the traditional linear model is that a single model of the form of the equation above is fitted to the entire dataset and as a result local nonlinearities cannot be adequately captured.

Nonparametric methods, which are data driven, address the drawbacks of the traditional models. In this, the form of the underlying function, f, is not assumed for the entire dataset, but rather it is estimated "locally" at each point of interest. This local estimation is the key difference from the traditional approach and one that provides the capability to capture any arbitrary feature (linear or nonlinear) that might be present in the data. There are several nonparametric methods for functional estimation. These include kernel-based techniques (Bowman and Azzalini 1997), splines, K-nearest neighbor (K-NN) local polynomials (Owosina 1992; Rajagopalan and Lall 1999), local weighted polynomials (Loader 1999), etc. Owosina (1992) performed an extensive comparison of a number of traditional parametric and nonparametric regression methods on a variety of synthetic and real data sets. He

found that the nonparametric methods out-performed the parametric alternatives in all the cases.

The local weighted polynomials approach (henceforth, LOCFIT) developed by Loader (1999) is simple, robust and easy to implement. Furthermore, it has been extensively applied to forecasting streamflow and precipitation (e.g., Grantz et al. 2005; Singhrattna et al. 2005; Regonda et al. 2006) with good success.

Briefly, the LOCFIT method obtains the value of the function f at any point 'x*' by fitting a polynomial to a small set (K) of nearest neighbors to 'x*'. Once the K-nearest neighbors are identified, there are two main options:

(i)   The neighbors can be resampled with a weight function that gives more weight to the nearest neighbors and less to the farthest, thus generating an ensemble (e.g., Lall and Sharma 1996; Rajagopalan and Lall 1999; Yates et al. 2003; Souza and Lall 2003)

(ii)   A polynomial of order p can be fit to the neighbors using weighted least squares (where the nearest neighbor is given most weight and the farthest neighbor the least). The polynomial is then used to estimate the dependent variable (Loader 1999).

Thus, the parameters to be estimated are the size of the neighborhood (K) and the order of the polynomial (p). These are obtained using the objective score function Generalized Cross Validation (GCV), which is given as:

$$GCV(K,p) = \frac{\sum_{i=1}^{N} \dfrac{e_i^2}{N}}{\left(1 - \dfrac{q}{N}\right)^2}$$

where e_i is the model residual, N is the number of data points, and q is the fitted degrees of freedom (related to the number of model parameters) of the forecasting model (Loader 1999). The GCV score is calculated on several combinations of K and p and the combination producing the minimum GCV is selected as the best. GCV has been shown to be a good approximation of the predictive capability of the model (Craven and Whaba 1979). This is unlike other measures such as mean squared error or R^2 which capture how well the model fits the data.

Also, it should be noted that if K is equal to N (all the data points), if all the neighbors are given equal weight, and if a linear polynomial is fit, then the model collapses to traditional linear regression. Thus, the local polynomial approach is a general framework which includes the linear regression as a special case.

The LOCFIT method also provides the error variance, σ, of the estimate at x*. This, in conjunction with an assumption of normally distributed errors, can provide the confidence interval. Also, random deviates from a normal distribution with mean 0 and variance σ can be added to the estimate from the local polynomial to generate ensembles. This method was used for ensemble forecasting of streamflows (Regonda et al. 2006) and monsoon rainfall in Thailand (Singhrattna et al. 2005). To better capture the local error distribution around x*, Prairie et al. (2005, 2006) proposed a residual resampling approach. This approach was also used in Grantz et al. (2005) to provide ensemble forecasts of spring seasonal streamflows in the Truckee-Carson

River Basin. A brief description of the residual resampling methodology abstracted from Grantz et al. (2005) is given below:

(i) For a given data set, the best choice of neighborhood size (K) and the order of polynomial (p) are obtained using objective criteria such as Generalized Cross Validation (GCV) or likelihood.

(ii) At each observed data point, x_j, K nearest neighbors are identified and a local polynomial of order p is fitted. This fit is then used to estimate the value of the dependent variable (i.e., the conditional mean) and consequently, the residual, e_j.

(iii) For a new data point, x_{new}, at which an estimate is required, the conditional mean value, Y_{new}, is obtained using the step ii, above.

(iv) Next, one of the K nearest neighbors of $x_{new,}$ say x_i, is selected and its corresponding residual, e_i is then added to the mean forecast ($Y_{new} + e_i$) thus obtaining one of the ensemble members. The selection of one of the neighbors is done using a weight function of the form:

$$W(j) = \frac{1}{j \sum_{i=1}^{k} \frac{1}{i}}$$

This weight function gives more weight to the nearest neighbor and less to the farthest neighbors. The number of neighbors to be used to resample the residuals need not be same as the number of neighbors used to perform the local polynomial in step 1. In practice, square root of (n-1) is used to resample the residuals.

(v)   Step iv is repeated to provide ensembles.

The residual resampling approach can be better visualized in Figure 37. The figure shows the scatter plot of the December to February PDSI and the March to June streamflow in the upper Pecos River. The solid line is the LOCFIT estimates through the scatter. The bootstrapping of the residuals for the ensemble forecast is depicted in the dashed box.
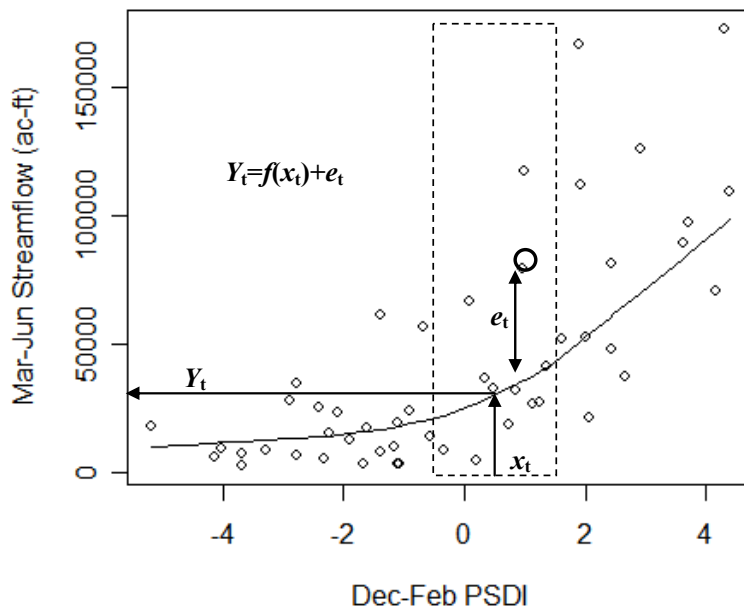
Figure 37. Residual resampling

Predictor Selection

As mentioned earlier, the predictors obtained for the streamflow forecast in the Pecos River Basin can be highly correlated with eachother. Thus, the best subset of predictors must be selected for use in the forecasting model described above. Typically this is done using stepwise regression (e.g., Rao and Toutenburg 1999; Walpole et al. 2002) wherein an objective function such as Mallow's C_p statistic, the

adjusted R^2, Akaike's Information Criteria (AIC), or an F-test is calculated from the fitted model to several predictor combinations. The best subset is then selected based on the combination that gives the optimal value for the chosen objective function.

In this study the best set of predictors for each forecast lead time is obtained by minimizing the objective function GCV described earlier. The GCV score can be used to obtain the best subset of predictors along with the parameters K and p of the LOCFIT. This was proposed by Regonda et al. (2005) and subsequently used effectively in Grantz et al. (2005) and Regonda et al. (2006). Because the GCV rewards for parsimony, typically only one of several related predictors is selected.

In the Pecos River Basin, a wet forecast is particularly useful to water management as policy can be best modified in wet years. If the forecast predicts a wet monsoon allotments can be increased and block releases can be limited. In normal and dry years, the allotment calculation and block release criteria will remain largely the same. Therefore, the GCV score is computed for the wet years using all combinations of predictors and LOCFIT parameters. The predictor combination that produced the minimum GCV score is selected for use in the forecasting model. Wet years are defined as those with historical streamflows above the 66th percentile.

The best predictor combinations for the upper and lower Pecos River streamflow forecasts at all lead times are shown in Table 7.

Table 7. Selected predictors.

	Upper Basin Spring	Upper Basin Summer	Lower Basin Spring	Lower Basin Summer
Mar1st	Dec-Feb: SSTs (hi-lo) Z Winds (hi-lo) PDSI	Dec-Feb: Z500 (hi-lo) PDSI	Dec-Feb: Z500 (hi-lo) PDSI	Dec-Feb: Z500 (hi-lo) Z Winds PDSI
May 1st	Dec-Apr: SWE (Apr 1st) Apr streamflow	Dec-Apr: SWE (Mar 1st) SSTs (gulf)	Dec-Apr: SSTs (hi-lo) SWE (Mar 1st)	Dec-Apr: Z500 SWE (Apr 1st)
Jun 1st	Dec-May: Z500 (hi-lo) SWE (Mar 1st) May streamflow	Dec-May: SSTs SWE (Mar 1st) Air Temp	Dec-May: SSTs (hi-lo) SWE (Mar 1st)	Dec-May: Z500 Air Temp
Jul 15th		Dec-May: SWE (Mar 1st) Air Temp		Dec-May: Z500 SSTs
Sep 1st		Jul-Aug: SSTs (Dec-May) Z Winds (Dec-May) Air Temp Jul-Aug streamflow		Jul-Aug: Z500 Z500 (Dec-Jul)

Another approach to picking the best subset of predictors is to include several models in the final forecasting model. This is also known as the multi-model approach and recent studies show that multi-model ensemble forecasts can perform much better than a single model forecast (Krishnamurti et al. 1999, 2000; Rajagopalan et al. 2002; Hagedorn et al. 2005). Because real data sets are noisy, several predictor and parameter combinations produce GCV values that are close to the minimum GCV. As a result, it is hard to select the combination with the least GCV and ignore the others (Regonda et al., 2006). The best approach to address this is to produce a multi-model ensemble combination wherein ensembles are generated from all candidate models and optimally combined (e.g., Krishnamurti et al. 1999, 2000; Rajagopalan et al. 2002; Hagedorn et al. 2005; Regonda et al. 2006)

Forecast Model Evaluation

Ensemble forecasts of seasonal streamflows are generated for each year at each of the five lead times using the best subset of predictors in the forecast modeling framework described above. The ensemble forecasts are generated in a cross-validated mode. In this, for each year's forecast, that year's streamflow is dropped out of the model and the model is built on the rest of the data. This is repeated for each year in the 1949-1999 period. The ensembles provide a forecast of the probability density function (PDF) and, hence, probabilistic skill measures are required for forecast evaluation.

One common probabilistic skill measure is the Ranked Probability Skill Scores (RPSS) (Wilks 1995). The RPSS is typically used by climatologists and meteorologists to evaluate a model's skill in capturing categorical probabilities relative to climatology. Here, the tercile boundaries, i.e., 33rd percentile and 66th percentile are used to obtain three equal categories. Values above the 66th percentile are in the above normal category, below the 33rd percentile are in the below normal category, and the remainder fall in the normal category. The categorical probability forecast is obtained as the proportion of ensemble members falling in each category. The climatology forecast is the proportion of historical observations in each category – in this case, it is $^{1}/_{3}$.

For a categorical probabilistic forecast in a given year, $P = (P_1, P_2, \ldots P_k)$ (where k is the number of mutually exclusive and collectively exhaustive categories; here it is 3) the rank probability score (RPS) is defined as:

$$RPS = \sum_{i=1}^{k} \left[\left(\sum_{j=1}^{i} p_j - \sum_{j=1}^{i} d_j \right)^2 \right]$$

The vector d (d_1, d_2, ... d_k) represents the observations, such that d_k equals one if the observaion falls in the kth category and zero otherwise. The RPSS is then calculated as:

$$RPSS = 1 - \frac{RPS(\text{forecast})}{RPS(\text{climatology})}$$

The RPSS ranges from positive 1 (perfect forecast) to negative infinity. Negative RPSS values indicate that the forecast has less accuracy than climatology. The RPSS essentially measures how often an ensemble member falls into the category of the observed value and compares that to the climatological forecast. In this application the RPSS is calculated for each year and the median value is reported.

Another traditional skill measure, Pearson's correlation coefficient R, is used to measure the correlation between the median of the ensemble forecast and the observed seasonal streamflow.

Results

Spring Forecast

Figure 38 shows the results for the March 1st forecast for the upper Pecos March to June streamflow. This model uses the December to February SST (high minus low), 200mb zonal wind, and PDSI indices in the forecast (see Table 7). The solid line in the plots represents the historical flow values. The boxplots at each year illustrate the ensemble forecast in that year. Larger boxplots indicate greater forecast uncertainty, or a wider range of possible streamflow values in the ensemble. The

dashed horizontal lines, which represent the quantiles (5th, 25th, 50th, 75th, and 95th percentile) of the historical data, help the viewer ascertain the relative streamflow in each year.   Though the forecasting model does not cleanly predict the observed streamflow in every year, every observed value is within the 5th and 95th percentiles of the ensemble forecast for that year, indicating that the observed flow was not out of the range of forecasted possibilities. More importantly, the model does a good job of predicting whether the streamflow will be above average or below average. It is also interesting to point out that the median of the ensemble is not in the center of the box, thus illustrating skew in the ensemble forecast, a feature that linear techniques cannot produce. Representing skew in the ensemble is important in determining exceedance probabilities.
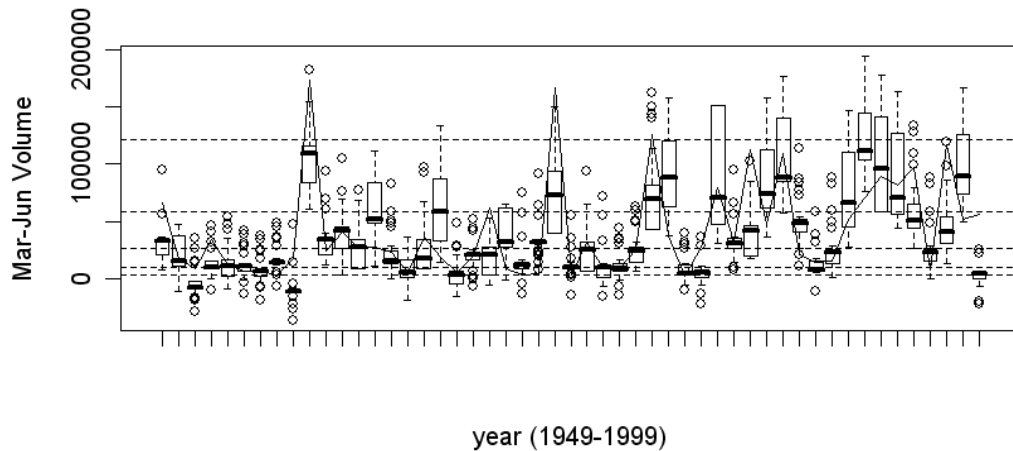
Figure 38. Timeseries of March to June upper Pecos streamflow with ensemble forecasts for each year (1949-1999). The solid line represents the historical timeseries. The boxplots represent the ensemble forecast issued from March 1st in each year. The dashed horizontal lines represent the quantiles of the historical data (5th, 25th, 50th, 75th, and 95th percentiles).

The corresponding skill scores for the March 1st forecast are displayed in Figure 39.   Figure 39(a) illustrates the relationship between the median (most

probable value) of the ensemble forecast and the observed value in all years. The correlation coefficient of 0.69 denotes that the model is good at predicting the observed value. Boxplots of the RPSS values for all years, wet years and dry years are presented in Figure 39(b-d). The wet and dry years are defined as years with streamflows above the 66th percentile and below the 33rd percentile, respectively. The median RPSS values are listed below the boxplots. It can be seen that the model performs quite well overall, doing particularly well in wet years, with decreased skill in dry years.

| (a) | (b) | (c) | (d) |
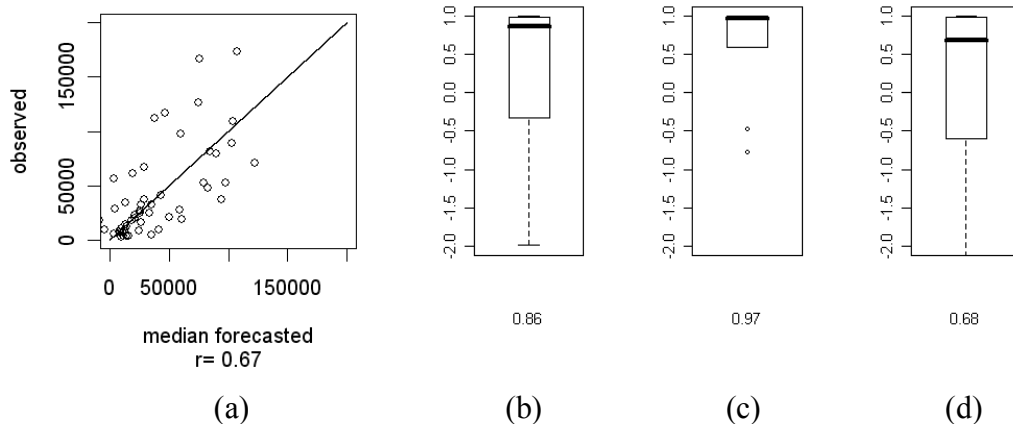
Figure 39. Skill scores for the March 1st forecast of March to June upper Pecos streamflow. Median of the ensemble forecast vs. observed streamflow (a), and RPSS for all years (b), wet years (c) and dry years (d). Median RPSS values are listed below the boxplots.

The corresponding results for the spring flow forecast from May 1st are shown in Figure 40 and Figure 41. Here too, the ensemble forecasts are quite skillful, particularly in the wet years. The R value for the median of the forecast is 0.82 and the RPSS median values are 0.83, 0.97, and 0.71 for all years, wet years, and dry years, respectively. The boxplots of the ensembles are tighter than those for the March 1st forecast signifying decreased uncertainty. Also, the May 1st forecast has

higher skill. This skill improvement is due to the predictors for the May 1st streamflow, April 1st SWE and April streamflow, both of which are very good indicators of streamflow.
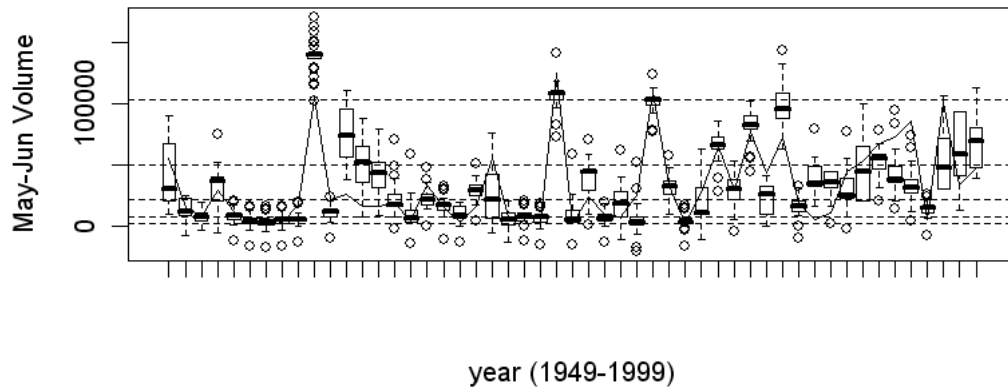
Figure 40. Same as Figure 38, except for the May 1st forecast of May to June streamflow.

(a)	(b)	(c)	(d)
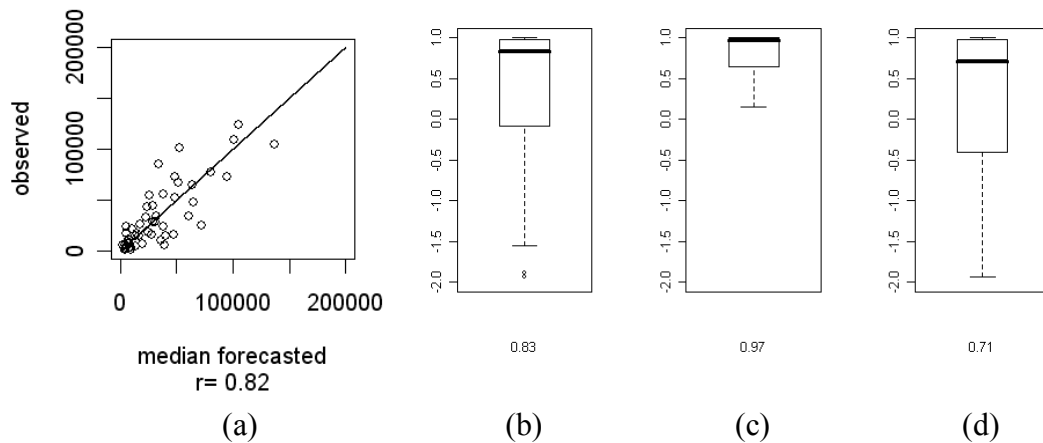
Figure 41. Same as Figure 39, except for the May 1st forecast of May to June streamflow.

Results for the lower Pecos River streamflows are less skillful than those for the upper Pecos streamflows (figures not shown). For example, the March 1st forecast of March to June lower Pecos streamflow exhibits a positive RPSS (0.46) only in the wet years and Pearson's R value of 0.42. Results improve for the May 1st

forecast with RPSS values of 0.30, 0.50, and 0.23 for all years, wet years, and dry years, respectively. The decreased forecast skill for the lower Pecos streamflow is consistent with the previous section's finding that the predictor correlation patterns are weaker and less organized that those for the upper Pecos flows. Also, the lower Pecos River does not receive very much streamflow in the spring and, thus, does not exhibit a strong response to the climate.

Summer Forecast

Results for the May 1st forecast of the summer monsoon streamflows in the upper Pecos River are shown in Figure 42 and Figure 43. As with the previous forecast, the RPSS values are highest for wet years (0.63) with decreased values in all years (0.57) and dry years (0.54) and the Pearson's R is 0.55. The July to October forecast for the upper Pecos will be used in the calculation of allotments. In years with a wet forecast, the allotment will be increased, thus the wet years forecast skill is most important.
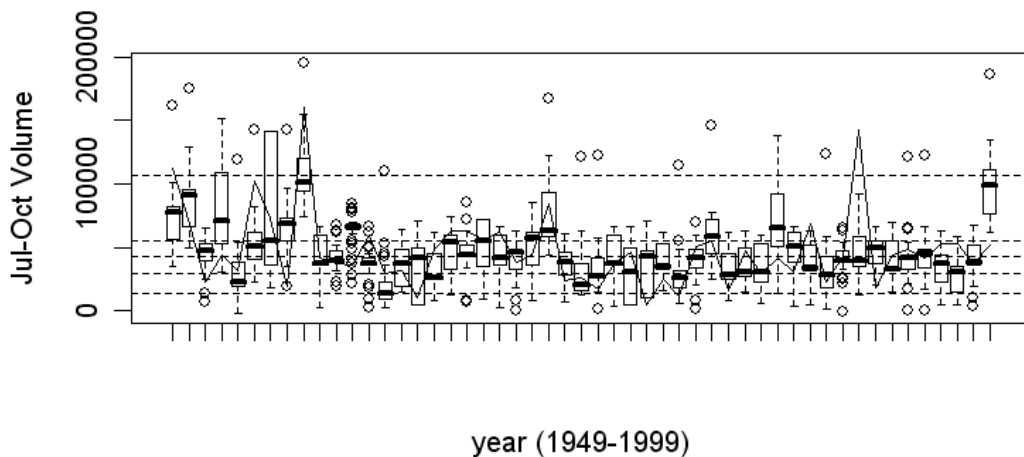
Figure 42. Same as Figure 38, except for the May 1st forecast of July to October streamflow.

(a)   (b)   (c)   (d)
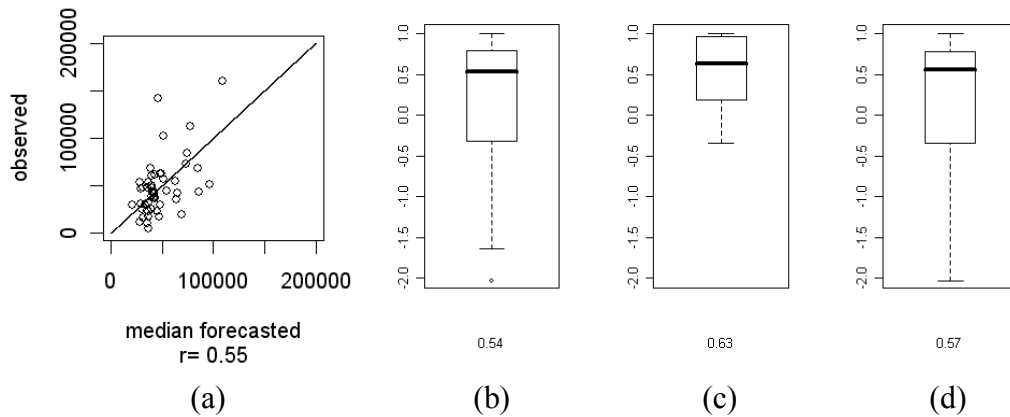
Figure 43. Same as Figure 39, except for the May 1st forecast of July to October streamflow.

The June 1st forecast of summer monsoon streamflows in the upper Pecos River (Figure 44 and Figure 45) improves on the May 1st forecasts. This indicates that the monsoon season streamflow forecast depends more on variables known immediately prior to the monsoon start (e.g., December to May variables, rather than December to April variables). RPSS values for the June 1st forecast are 0.12, 0.73, and 0.22 in all years, wet years, and dry years, respectively and the Pearson's R is
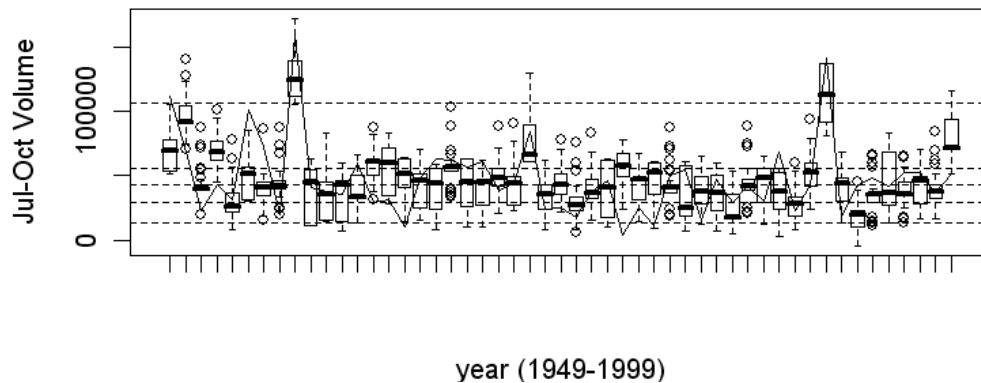
Figure 44. Same as Figure 38 except for the June 1st forecast of July to October streamflow.
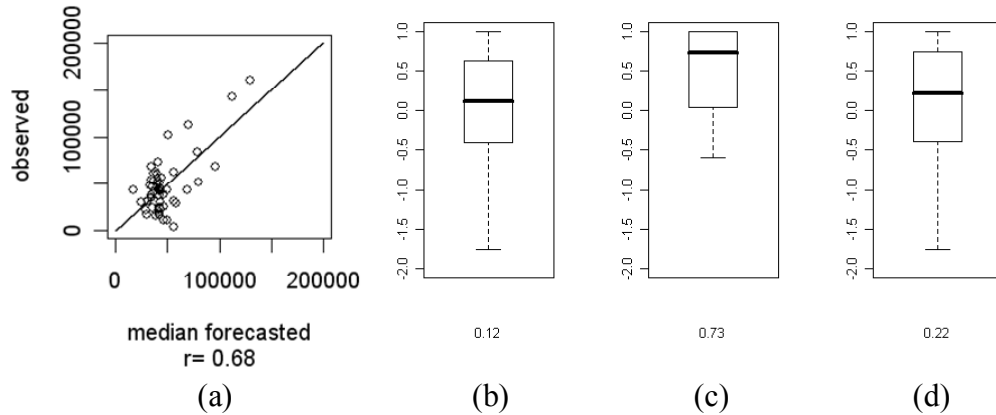
Figure 45. Same as Figure 39, except for the June 1st forecast of July to October streamflow.

0.68. It is interesting to point out that the RPSS values for all years and dry years are actually lower than those for the May 1st forecast. This is not contradictory given that model selection was based on performance in wet years.

The July 15th forecast is actually issued on July 1st, since all predictors use monthly data. The results for the July 1st forecast of the July to October streamflow on the lower Pecos are shown in Figure 46 and Figure 47. RPSS values for this forecast are 0.12, 0.89, and 0.17 in all years, wet years, and dry years, respectively. Pearson's R is 0.46.
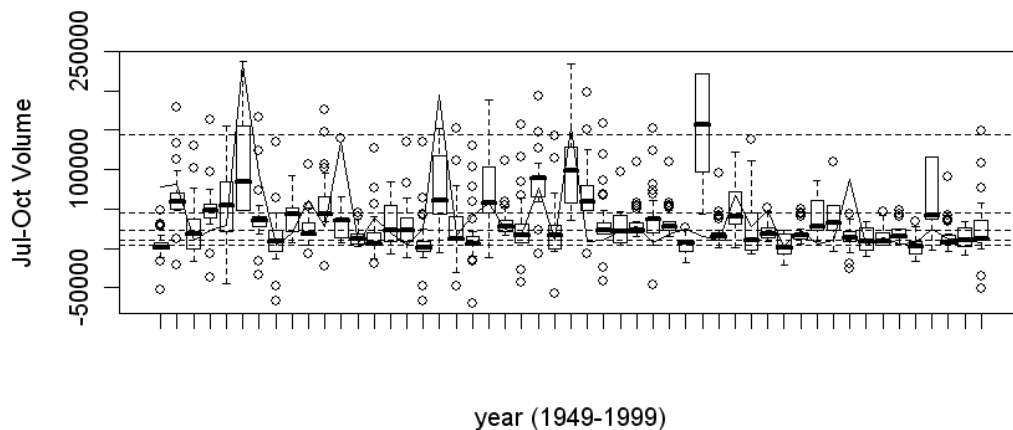
Figure 46. Same as Figure 38, except for the July 1st forecast of July to October streamflow on the lower Pecos.
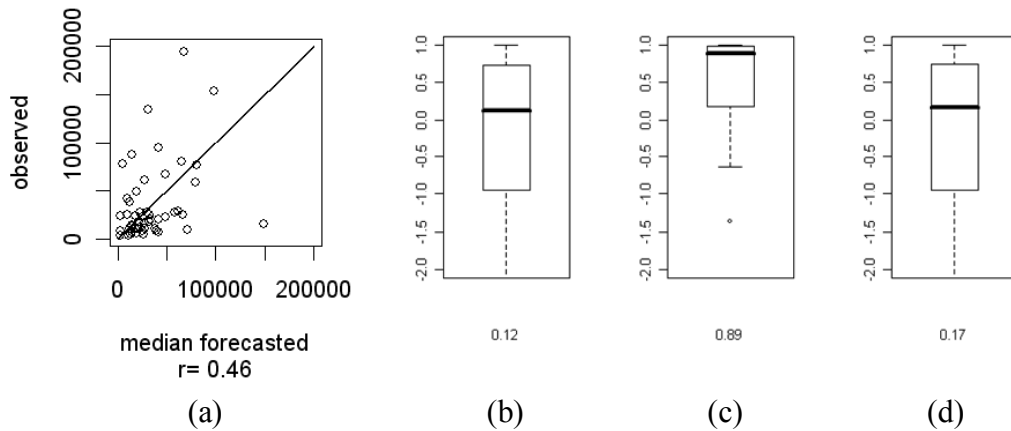
Figure 47. Same as Figure 39, except for the July 1ˢᵗ forecast of July to October streamflow on the lower Pecos.

The RPSS and correlation results for all the seasonal streamflow forecasts of the lower and upper Pecos River Basin at all five lead times are shown in Table 8.

Table 8. Skill scores for all forecasts

		RPSS			Correlation
		All Years	**Wet Years**	**Dry Years**	
Mar 1ˢᵗ	*Upper Mar-Jun*	.86	.97	.68	.67
	Upper Jul-Oct	.17	.46	.26	.47
	Lower Mar-Jun	-.32	.46	-.44	.42
	Lower Jul-Oct	.05	.55	.29	.17
May 1ˢᵗ	*Upper May-Jun*	.83	.97	.71	.82
	Upper Jul-Oct	.54	.63	.57	.55
	Lower May-Jun	.30	.50	.23	.09
	Lower Jul-Oct	-.09	.46	-.06	.23
Jun 1ˢᵗ	*Upper Jun*	.45	1.00	.44	.76
	Upper Jul-Oct	.12	.73	.22	.68
	Lower Jun	-.07	.46	-.27	.30
	Lower Jul-Oct	-.17	.49	.21	.15
Jul 15ᵗʰ	*Upper Jul-Oct*	.22	.56	.24	.38
	Lower Jul-Oct	.12	.89	.17	.46
Sep 1ˢᵗ	*Upper Sep-Oct*	-.07	.33	.01	.23
	Lower Sep-Oct	.14	.80	.23	.87

Summary and Discussion

A modeling framework to provide ensemble forecasts of irrigation season streamflows in the Pecos River Basin was developed and demonstrated. Predictors were identified from the large-scale land-ocean-atmosphere system in preceding seasons. A robust nonparametric method based on local weighted polynomials was used to select the best subset of predictors and, consequently, the ensemble forecasts of seasonal streamflows were issued. Based on current operating criteria, irrigation season ensemble forecasts were generated at five lead times, March 1st, May 1st, June 1st, July 15th, and September 1st, in the upper and lower Pecos River Basin.

The forecast framework exhibited significant skill overall, but more so during wet years. Furthermore, the upper Pecos had higher skill than the lower Pecos. Operations and management on the Pecos, specifically the calculation of irrigation allotments and block releases, may be improved through skillful forecasts of spring and summer streamflows. To this end, improved skills in wet years are important as this is when policy can be best modified to take advantage of skillful spring and summer forecasts.

The ensemble forecasts will next be used to calculate threshold exceedance probabilities for modifying existing policy and operations in a water operations model of the Pecos River. Because existing policy and operations use reservoir storage values (i.e., volumes at single nodes in the river) it was acceptable to sum the inflows from the two and five sub-basins in the upper and lower basins, respectively. If operations required actual inflows at nodes throughout the river the ensemble forecast of the upper and lower basins would need to be disaggregated (e.g., Prairie et al. 2006) to flows at the desired locations.

CHAPTER 5

WATER MANAGEMENT APPLICATION

Introduction

Decision support systems (DSSs) are used to make operational and planning decisions as well as to formulate strategies to satisfy the ever-changing legal requirements and multiple objectives of a river basin. With the highly variable flows, complex operations and changing policies of the Pecos River system, water managers and policy makers have much to balance in the basin. The Pecos River DSS provides the ability to model various flow and policy scenarios to help water managers with operational decision making.

This chapter describes the coupling of streamflow forecasts developed in Chapter 4 with the Pecos River Basin DSS for the improvement of water management. The chapter is organized as follows: First a description of the Pecos River DSS and the implemented policies and operations is presented. Next the coupling of streamflow forecasts with the DSS is described. This is followed by the results and analysis of the model runs. A summary and discussion concludes the chapter.

Pecos River Decision Support System

Background

The Pecos River DSS was developed in response to a National Environmental Policy Act (NEPA) directive after the Pecos bluntnose shiner (shiner) was listed as

endangered in 1987. The development of a DSS was deemed necessary to evaluate various management strategies and policy change scenarios on the Pecos River. After an extensive data collection effort, a daily-timestep water operations computer model of the river was developed using the general-purpose river and reservoir modeling software RiverWare (Zagona et al. 1998 and 2001). Development of the Pecos RiverWare model was a collaborative effort with contributions from the U.S. Bureau of Reclamation (Reclamation), the New Mexico Interstate Stream Commission (NMISC), the New Mexico Office of the State Engineer (NMOSE), Carlsbad Irrigation District (CID), the U.S. Fish and Wildlife Service (Service), the U.S. Army Corps of Engineers (Corps), the New Mexico Department of Game and Fish, Pecos Valley Artesian Conservancy District (PVACD), and the Center for Advanced Decision Support for Water and Environmental Systems (CADSWES). After its completion, the model underwent an extensive evaluation and review process by stakeholders and representatives from different federal, state, and local agencies. The Pecos River DSS models the policies and operations of the Pecos River as well as all of the physical processes associated with the river. The Pecos RiverWare model is shown in Figure 48.

Simulation of Physical Processes

The Pecos RiverWare model simulates the physical movement of water through the system using standard hydrologic and hydraulic principles. The model developers selected from a suite of different algorithms to simulate these processes based on the data they had available and the level of detail that was desired. For
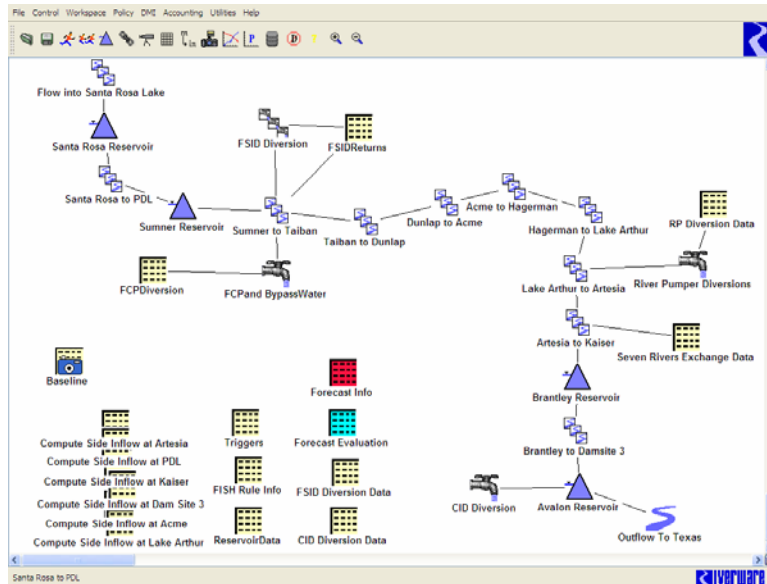
Figure 48. Pecos RiverWare model

example, routing through a reach can be simulated using time-lag, impulse response, Muskingum, Muskingum-Cunge, kinematic wave or storage routing routines. Due to the morphology of the Pecos River and shape of typical inflow hydrographs, flood waves during the summer monsoon season significantly attenuate as these waves propagate down the river. It was thus important to implement a routing methodology that would appropriately represent flood wave travel times (translation) and reduction in peak discharge (attenuation) of flood waves. The Muskingum-Cunge routing method was selected for this reason. Other selectable physical process algorithms include tailwater calculation, evaporation and streambank storage and returns. By modeling the hydrologic and hydraulic mechanisms in the system, the Pecos RiverWare model aims to accurately simulate the total amount of water moving through the system at any place and any time during the simulation run.

The policies and operations of the Pecos River are implemented with rules. These rules, based on user-defined, prioritized logic, govern simulations of reservoir releases and diversions throughout the river system. The rules dictate how much water to release from each reservoir and to divert at each diversion site. By using different rules to move water through the system, it is possible to simulate flow patterns using different policies. These rules are written in the form of prioritized logic to govern the movement of the inflows throughout the system. Flood control algorithms, flow requirements for fish and allotments and diversions for agriculture are examples of rules implemented in the Pecos RiverWare model. Because the policies and laws are expressed as dynamic data (rather than compiled in the model code), water managers and policy makers can easily turn different rules on or off to test the outcome of different policy scenarios. In this way, water managers and policy makers can determine the potential impacts of pending laws and policies to help in planning and decision making.

Pecos River Operations and Policies

The Pecos River (Figure 49) has multiple competing demands for its limited water resources. These include agriculture, municipalities and industry, the environment, recreation, and inter-state delivery requirements. The reservoirs of the Pecos River system are operated primarily to optimize water delivery to CID farmers. In addition to irrigation, Pecos River water must also be managed for protection of the shiner and its habitat as well as inter-state flow deliveries to Texas, among other objectives. A general overview of Pecos River operations and policies was presented

in Chapter 4. Here, a more detailed description of two major operating criteria, block releases and CID irrigation allotments, is provided. Block releases and irrigation allotments are the two operations that this study examines to incorporate spring and summer streamflow forecasts and improve water management. For a complete discussion of these and other river operations, see Boroughs and Stockton (2005).
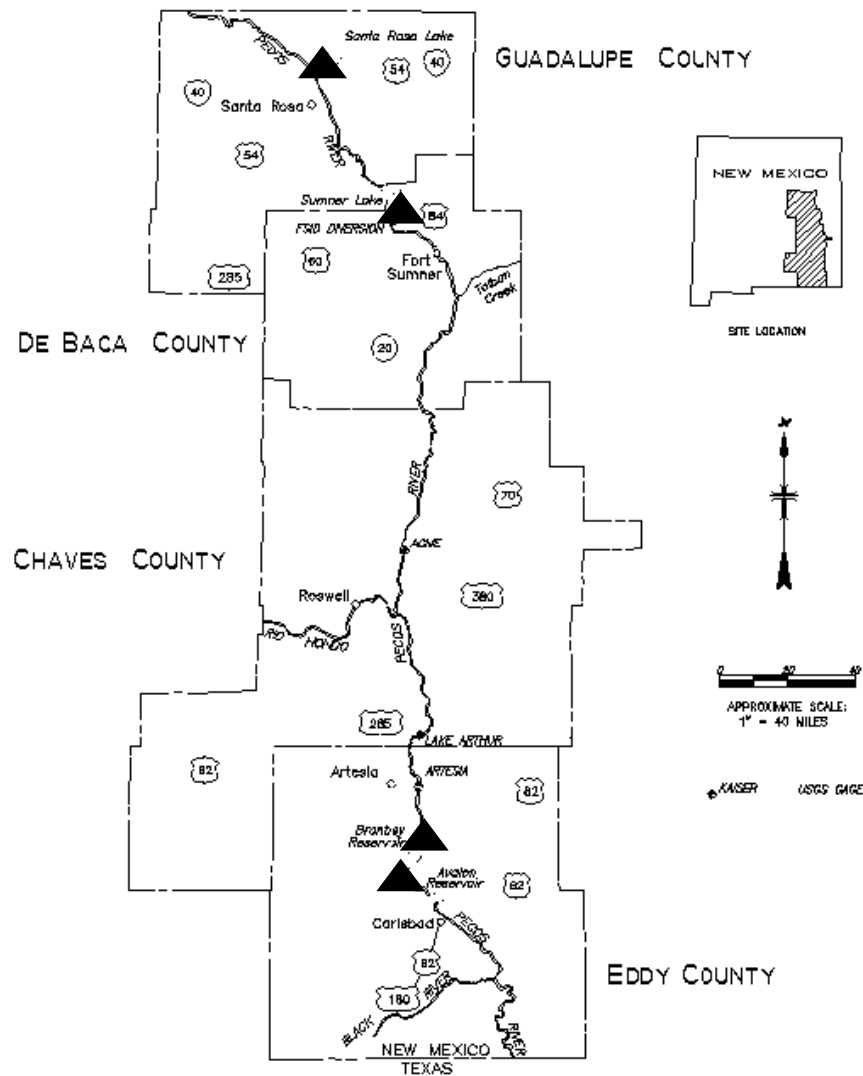
Figure 49. Pecos River study area modeled with RiverWare. Reservoirs are represented as triangles. Image courtesy of Craig Boroughs.

Carlsbad Irrigation District Allotments and Diversions

CID allotments and diversions are principally a function of storage levels in the four basin reservoirs. Reservoir storage levels are referenced to calculate the allotment and then a diversion schedule is developed based on this allotment. The allotment is the quantity of water assured to irrigators; diversions represent the actual water delivered.

The annual allotment is set by CID on March 1st based on the water in storage at that date. This spring allotment is considered partial and can be increased throughout the irrigation season as more water becomes available in the basin. Five trigger dates, March 1st, May 1st, June 1st, July 15th, and September 1st, are used to review storage conditions and determine whether the allotment can be increased. These dates are based on the Pecos Basin's irrigation season trends. The March 1st allotment is used for the first big diversion of the season that begins mid-March for the first irrigation of alfalfa and the pre-planting of cotton. Irrigation may increase in mid-May for the second planting of alfalfa. In June there may be another increase for the first irrigation of cotton and hay. Diversions are then typically continuous throughout July and August. September brings the watering of new hay and then diversions typically decrease until October 31st.

The allotment is calculated as:

$$Allotment = \frac{IrrigableAcres\left[MAX\left[MIN\left(\frac{\left(\begin{array}{c}Ba\sin Storage + DiversionsToDate\\ -StorageTo\operatorname{Re}tain\end{array}\right)}{IrrigableAcres},\ MaxAllotment\right),\ LastCalculatedAllotment\right]\right]}{DeliveryEfficiency}$$

where *Basin Storage* is the current CID storage in the four basin reservoirs, *Max Allotment* is 3.7 acre-ft/acre, *Delivery Efficiency* is the efficiency for delivery of water from the CID diversion gate to the farms (74.2%), *Irrigable Acres* is 25,055 acres, and *Storage to Retain* is the water to be retained for the next irrigation season (1,000 acre-ft). This formula ensures that the allotment will either stay constant or increase through any given year's irrigation season, but will not exceed the maximum allotment allowed by law.

Diversion schedules are established using the allotment calculated from current basin conditions. In RiverWare the diversion schedules are set based on the historical diversion-allotment relationship. Irrigation season schedules are available for 1.0, 1.5, 2.0 … 3.5 acre-ft/acre allotments. Once determined, the diversion schedule for the season is set as input at Avalon Reservoir. Daily diversion rates at the Avalon diversion gate range from 100 cfs to 375 cfs. Annual diversions to CID average 76,500 acre-ft and are limited to 125,200 acre-ft. Because the Pecos RiverWare DSS models Santa Rosa to Avalon, return flows from CID are neglected in the model; a separate accounting model is used to calculate inter-state water deliveries to Texas. The total allowable system storage (i.e., in all four reservoirs) for CID is 176,500 acre-ft; anything above this value must be released downstream to Texas.

Block Releases

Block releases are made from Santa Rosa and Sumner reservoirs to meet CID irrigation demands. The premise of block releases is to store Pecos River water upstream for as long as possible, then release it in blocks to limit evaporation and

seepage in the middle stretches of the river. Block releases are initiated and stopped based on storage triggers in Brantley Reservoir. Most of the water moved downstream is then stored in Brantley Reservoir; Avalon Reservoir provides elevation head at the main CID diversion gate. Block releases typically last 15 days and are usually made one to two times per irrigation season. In some years there are zero or three block releases.

The main criteria for block releases as implemented in the Pecos RiverWare model are outlined below:

- Block releases only during irrigation season (Mar 1st to Oct 31st)

- Santa Rosa releases 1,150 cfs; Sumner releases 1,250 cfs

- Block releases initiated when Brantley drops below 8,000 acre-ft and there is water available in Santa Rosa or Sumner.

- Early season provision: in March and April, block releases initiated when Brantley drops below 17,000 acre-ft. (This is to move more water down to Brantley early in the season to improve the water quality at Brantley.)

- No block releases are started from Santa Rosa if Sumner storage is above 33,000 acre-ft.

- No block releases are started from Santa Rosa if Santa Rosa storage is less than 2,400 ac-ft.

- Balance storages between Santa Rosa and Sumner regardless of the demand at Brantley: if Santa Rosa to Sumner storage ratio

is 7:1 or greater OR if Sumner is below 6,000 acre-ft and Santa Rosa is above 2,400 acre-ft, release 1,050 cfs from Santa Rosa until storage ratio is 5:1

- Stop block releases when Brantley is above 24,500 acre-ft (for Santa Rosa) and 26,000 acre-ft (for Sumner).

- Stop thresholds are lower after Sept 1st: when Brantley exceeds 6,000 acre-ft plus the remaining CID diversion for the irrigation season.

- Stop block releases in Santa Rosa if Santa Rosa storage drops below 6000 acre-ft; stop releases from Sumner if Sumner drops below 5480 acre-ft.

There are several inherent assumptions associated with block releases. The start triggers take into account the travel time between the upper reservoirs and Brantley Reservoir (approximately five days). The stop triggers consider the block release water still traveling down the river. Finally, the block release volumes are based on the assumption of additional water entering the river from Fort Sumner Irrigation District (FSID) returns and base inflows between Acme and Artesia.

NEPA policy alternatives for the protection of the shiner and its habitat are also included in the model. These alternatives include limiting block releases to 15 consecutive days, requiring 14 days between block releases and eliminating block releases for a 6-week period around the beginning of August. Like the other block release criteria, the NEPA policy alternatives are written into the RiverWare rules

and, thus, can easily be turned on or off. The NEPA policy alternatives were simulated in this study.

Implementation of Forecasts in Pecos RiverWare Model

Background

Water management of the Pecos River does not utilize seasonal streamflow forecasts in reservoir operations. The extreme variability of both spring and summer streamflow in this basin presents a unique challenge that is regarded as too much risk for operations. As a result, water managers are never left empty handed after operating and planning for water that may not come. The flip side of this, however, is that water managers and water users in the basin also never benefit from the advance planning made possible by streamflow forecasts.

Annual allotments are estimated based on March 1st reservoir storage levels; typically well before the end of the spring runoff. Current operations increase the allotment incrementally as water becomes available in the basin. However, forecasts of the entire irrigation season runoff would allow for a better estimate of the annual allotment, thus providing farmers with better information to plan for the coming irrigation season. The benefits of this might include providing farmers with better information for planning types and sizes of crops as well as a larger initial allotment and, thus, initial crop output.

Block Releases are made assuming inflows only from FSID returns and base inflows between Acme and Artesia. Runoff from monsoon events, which can amount to a significant portion of the basin annual streamflow, is not accounted for in the determination of block releases. These extra inflows must sometimes be spilled or

107

released, thus disallowing the use of that water. Forecasts of these inflows would allow operators to limit block releases, keep that water stored upstream for later use and, instead, utilize the monsoon runoff that might otherwise have been spilled.

Overview of Approach

The approach taken in this study is to capitalize on wet forecasts. It is presumed that in normal or dry years operations will not change. In effect, the current operations plan for the dry scenario on the Pecos River and a normal or dry forecast would make no difference in management strategies. In wet years, however, an increase in the initial allotment and a decrease in block releases could increase deliveries to CID and decrease spills to Texas. The approach of this research is to take advantage of wet forecasts while introducing minimum risk to the system.

Because the policies implemented in the Pecos RiverWare ruleset do not incorporate streamflow forecasts, the rules were modified for this study. The rules and functions associated with block releases and allotment calculations were adapted to incorporate streamflow forecasts. Two new rulesets were created: one that includes block release modifications and one that integrates changes to the allotment calculations. A baseline ruleset was maintained for comparison purposes. In addition, all necessary forecast data was imported to the model.

Modifications for CID Allotments

The formula used to calculate CID allotments was modified to include the forecasted seasonal inflows as water available to CID. The goal is to add the

forecasted inflows to the current basin storage value to improve the annual allotment estimate. The calculation of allotments, as modified for this study is given as:

$$Allotment = \frac{IrrigableAcres\left[MAX\left[MIN\left(\frac{\left(\begin{array}{c}Ba\sin Storage + ForecastedAdditionalStorage\\ + DiversionsToDate - StorageToRetain\end{array}\right)}{IrrigableAcres}, MaxAllotment\right), LastCalculatedAllotment\right]\right]}{DeliveryEfficiency}$$

where *Forecasted Additional Storage* is the inflow forecast for the entire Pecos River Basin. Because allotments cannot be decreased after the initial allotment on March 1st, a conservative inflow forecast was used in this study. The idea is to avoid the risk of assigning too large of an allotment on the March 1st date and running out of water before the end of the irrigation season. A conservative inflow forecast will add very little to the allotment in a dry or normal year, but will increase the allotment in a wet year.

The 5th, 10th, 25th, and 50th percentile forecasts of basin inflows were evaluated for use as the "conservative" *Forecasted Additional Storage* in this study. These percentile forecasts were calculated from the ensemble forecasts generated in Chapter 4. Daily timeseries of the four percentile forecasts were created to hold the five forecasts dates for each year from 1949 to 1999. These timeseries contained mostly NANs with values only on each of the five forecast dates in each of the years. These four timeseries were imported into the Pecos RiverWare model to be accessed by the rules.

The function for calculating the CID allotment was changed to use the equation provided above in conjunction with the most recent *Forecasted Additional*

Storage value (i.e., conservative inflow forecast). All rules that set the CID allotments and diversions call to the Estimate CID Allotment function, thus only one allotment function required modification.

Modifications for Block Releases

The stop triggers for block releases were adjusted based on the forecasts for inflows to the lower Pecos basin. The general premise is that if the forecasted inflows for a given year are above some wet threshold, the threshold stop trigger (i.e., the reference storage level in Brantley Reservoir) is decreased. It was decided that the stop triggers should be adjusted, rather than the start triggers (or both), to avoid undue risk of under-delivery to CID. For example, block releases are initiated when Brantley Reservoir requires additional water for irrigation deliveries. Given a wet forecast, block releases could be deferred assuming that the water would enter the system via runoff below Sumner Reservoir. However, because the forecasts are seasonal, even a perfect forecast would provide no guarantee that the water would come in time to meet CIDs demands. Adjusting the stop triggers, in contrast, allows Brantley Reservoir to receive water via block releases when storage levels are low, but only fill partway, thus leaving storage space to capture monsoon runoff below Sumner Reservoir. If the runoff does not come, another block release can be initiated when the storage in Brantley Reservoir drops below the start threshold and, thus, CID is unlikely to be shorted.

The forecasted probability of being wet was calculated from the ensemble streamflow forecasts for the lower Pecos basin. In this study three definitions for "wet" were evaluated: flows above the 66th, 75th, and 90th percentile of historical

data. The probability of exceeding the 66th, 75th, and 90th percentile was calculated for each year at each of the five forecast lead times. In addition, because the first three forecast dates each include two forecasts (e.g., the March 1st forecast consists of a forecast of the March to June streamflow and a forecast of the July to October flow) exceedance probabilities were calculated for the 'near term' forecast and for the 'full season' forecast. The near term forecast is the forecast for the time period immediately following the forecast date. The full season forecast is the sum of the spring and the summer forecasts. For example, the near term forecast for one year would consist of forecasts for March to June (issued on March 1st), May to June (issued on May 1st), June (issued on June 1st), July to October (issued on July 1st), and September to October (issued on September 1st). The full season forecast for one year would comprise the following forecasts: March to October, May to October, June to October, July to October, and September to October. Both the near term and the full season forecasts were examined in this study to determine which provided better information for the adjustment of block releases. Daily timeseries of the threshold exceedance probabilities were created to hold the five forecasts for each year from 1949 to 1999. These timeseries, like the percentile forecasts for the allotment calculations, were mostly NANs, containing exceedance probabilities only on each of the five forecast dates in each of the years. Timeseries of exceedance probabilities were created for the 66th, 75th and 90th percentile definitions of 'wet' for both the near term and full season forecasts. The six timeseries were imported into the Pecos RiverWare model to be accessed by the rules.

The amount by which to reduce the storage thresholds was explored through trial and error. The baseline Brantley Reservoir storage threshold levels of 24,500 acre-ft and 26,000 acre-ft for Santa Rosa and Sumner reservoirs, respectively, were systematically reduced in increments of 2,000 acre-ft to 10,500 acre-ft and 12,000 acre-ft, respectively, to evaluate improvements to water management.

The rules for stopping a block releases were changed to first check the forecasted probability of exceeding the wet threshold. If the forecast exceeded the wet threshold, the decreased Brantley Reservoir storage threshold levels (i.e., adjusted stop triggers) were used. If the forecast did not exceed the wet threshold, the baseline storage threshold levels for Brantley Reservoir were used. Since the forecasts are only issued at five dates during the irrigation season, the block release rules checked the most recent forecast date's wet threshold exceedance probability. Because block release rules are written separately for Santa Rosa Reservoir and Sumner Reservoir, the rules associated with each reservoir were modified. The logic of all rules and functions modified or created for this study is provided in Appendix A.

One risk associated with the adjustment of stop triggers is that block releases may be stopped early in anticipation of monsoon runoff. If the monsoon runoff does not come, it is possible that due to NEPA restrictions an additional release may not be allowed during the timeframe required for the water to reach Brantley Reservoir and meet CID demands. This could happen during the 6 week period in August or when a second block release is needed before the end of the 15 day wait period between block releases. The risk of this scenario depends on the timing of the original block release, but may be reduced by limiting the decrease in the stop triggers. Any

reduction in this risk is likely associated with a reduction in the benefits of changing the block releases.

Skill Evaluation

The utility of incorporating forecasts into water management in the Pecos River Basin is evaluated based on two key variables: deliveries to CID and spill from Avalon reservoir. An increase in deliveries to CID and a decrease in spill from Avalon are considered improvements to existing operating procedures. A single end-of-run value is obtained for each of the variables by converting daily flow values to volumes and summing up all days of the model run. Though the Pecos RiverWare model simulates daily operations from 1940 to 1999, data limitations restricted the forecasts to begin in 1949. Thus, skill is evaluated on the 1949 to 1999 period. The results from each of the two policy modification scenarios (i.e., block releases and allotments) are examined separately and independently.

Results

Scenario 1: Adjustment of Allotment Criteria

Simulations of the adjustment of allotment criteria scenario were run using the 5th, 10th, 25th, and 50th percentiles of the inflow forecasts to entire Pecos River Basin. Of these, the 10th percentile forecast produced the best results and these are presented here. The higher percentile forecasts overall delivered more water to CID, however, in a few years when the forecast was significantly greater than the observed value, Brantley Reservoir continued to try to meet the diversion schedule (based on the allotment) and ran out of water and the model run aborted. A more thorough

sensitivity analysis would provide a better understanding of which forecasts are best utilized for the change of allotments. The model was also run with the baseline scenario (i.e., no changes in the allotment calculation) for comparison purposes.

When compared with the baseline scenario, the forecast scenario produced an increase in CID deliveries of approximately 540,000 acre-ft, or 14%, over the 51 year period. Total spills from Avalon reservoir decreased by 240,000 acre-ft, or 18%. These results demonstrate that the incorporation of spring and summer streamflow forecasts into operations on the Pecos River significantly improves water management in the basin.

Figure 50 shows the allotments for the model run using the baseline scenario (represented in black) and the model run using the forecast scenario (represented in blue). Each "spike" in the plot represents the five allotments for one year. In this and all subsequent timeseries plots, the baseline scenario and the forecast scenario produce the same results for the first 10 years of the model run. This is because no forecast was available until 1949, thus the policy was only modified for simulations

Baseline   Modified
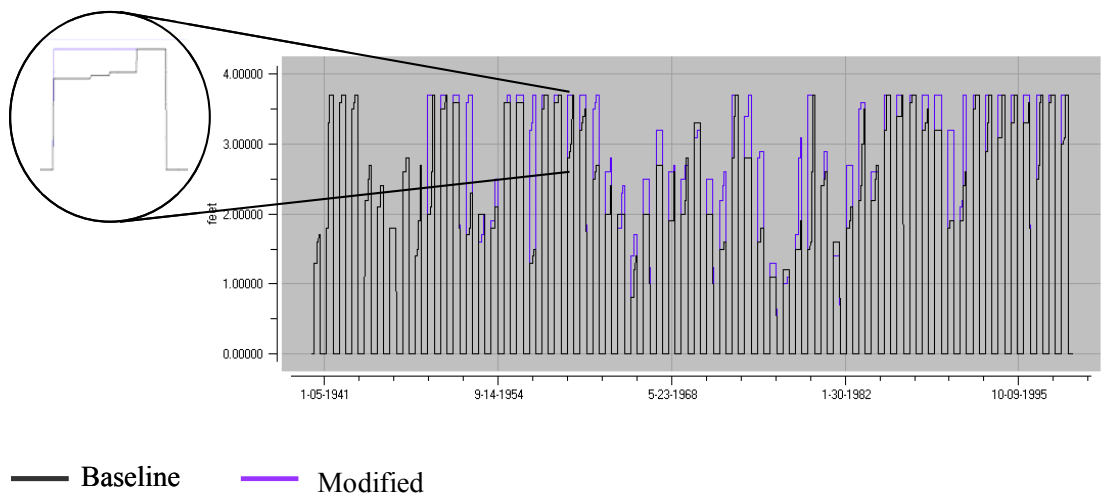
Figure 50. CID allotments.

after this date. Comparisons are only made for the 1949 to 1999 time period. Figure 50 shows that the allotments are larger when the streamflow forecast is used in the allotment calculation. In many years the baseline allotment starts out low and then increases throughout the season to eventually match, or come close to, that of the forecast scenario, thus demonstrating that streamflow forecasts help produce a better calculation of the annual irrigation allotment. In some years the forecast scenario increases throughout the irrigation season. This demonstrates that updated forecasts throughout the season (including the challenging late season monsoon forecast) help provide a better allotment calculations.

The PDFs of the annual allotments for March 1st, May 1st, June 1st, and July 15th are shown in Figure 51(a-d, respectively). The allotments from the forecast
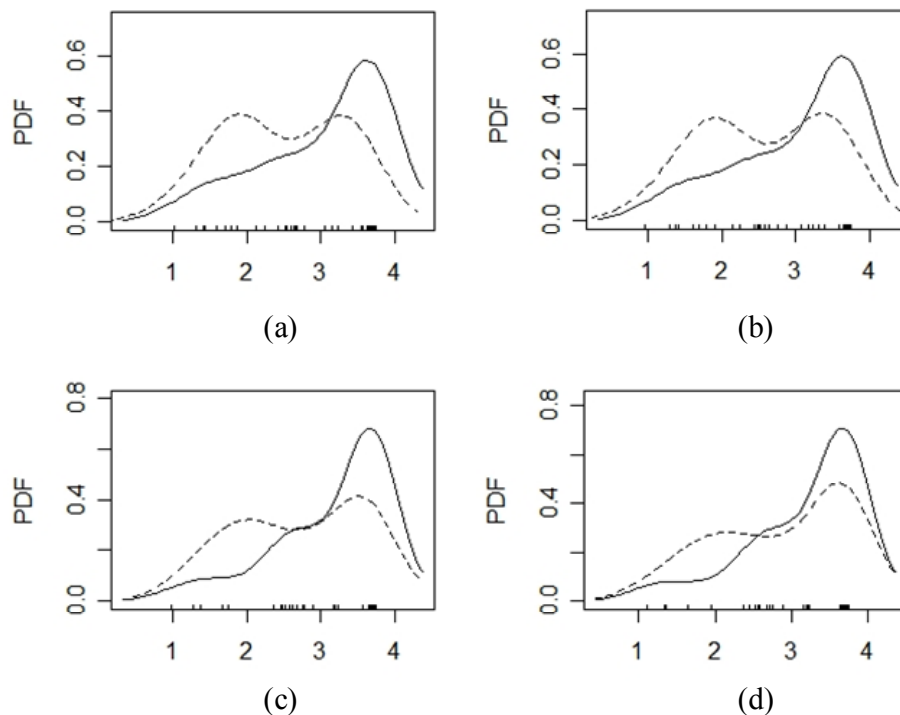
Figure 51. PDFs of allotments (acre-ft/acre) for March 1st (a), May 1st (b), June 1st (c) and July 15th (d). The solid and dashed lines represent the forecast and baseline scenarios, respectively.

scenario (solid line) are consistently larger than the baseline scenario allotments (dashed line) at all of the allotment calculation times. The PDFs show how the allotments of the baseline scenario start out relatively low in the early season (Figure 51 a,b) and then increase throughout the season (Figure 51 c,d) to eventually come much closer to those of the forecast scenario.

The increase in deliveries to CID is shown in Figure 52. Because diversion schedules are determined based on allotments, these diversions closely match the results of the allotments shown in Figure 50. The PDFs of the deliveries during each of the five subseasons (March 1st to April 31st, May 1st to May 31st, June 1st to July 14th, July 15th to August 31st, and September 1st to October 31st) are shown in Figure 53. Like the allotments (Figure 51), the baseline scenario deliveries are relatively low in the early irrigation season and then increase throughout the irrigation season. By comparison, the forecast scenario deliveries are consistently larger (or equal to, at the end of the irrigation season) the baseline scenario deliveries, thus demonstrating that using a forecast in the irrigation allotment calculations results in increased water delivery to CID.
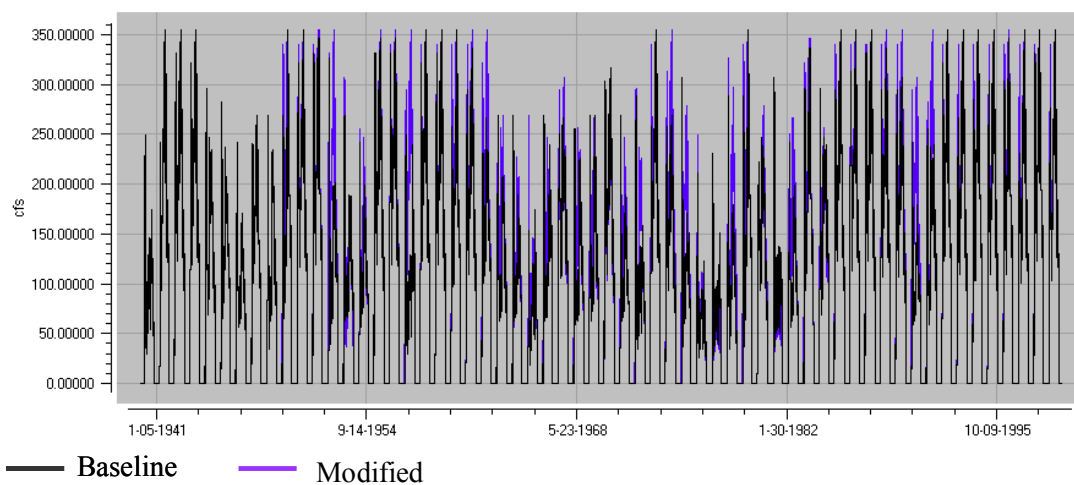
Figure 52. Deliveries to CID.
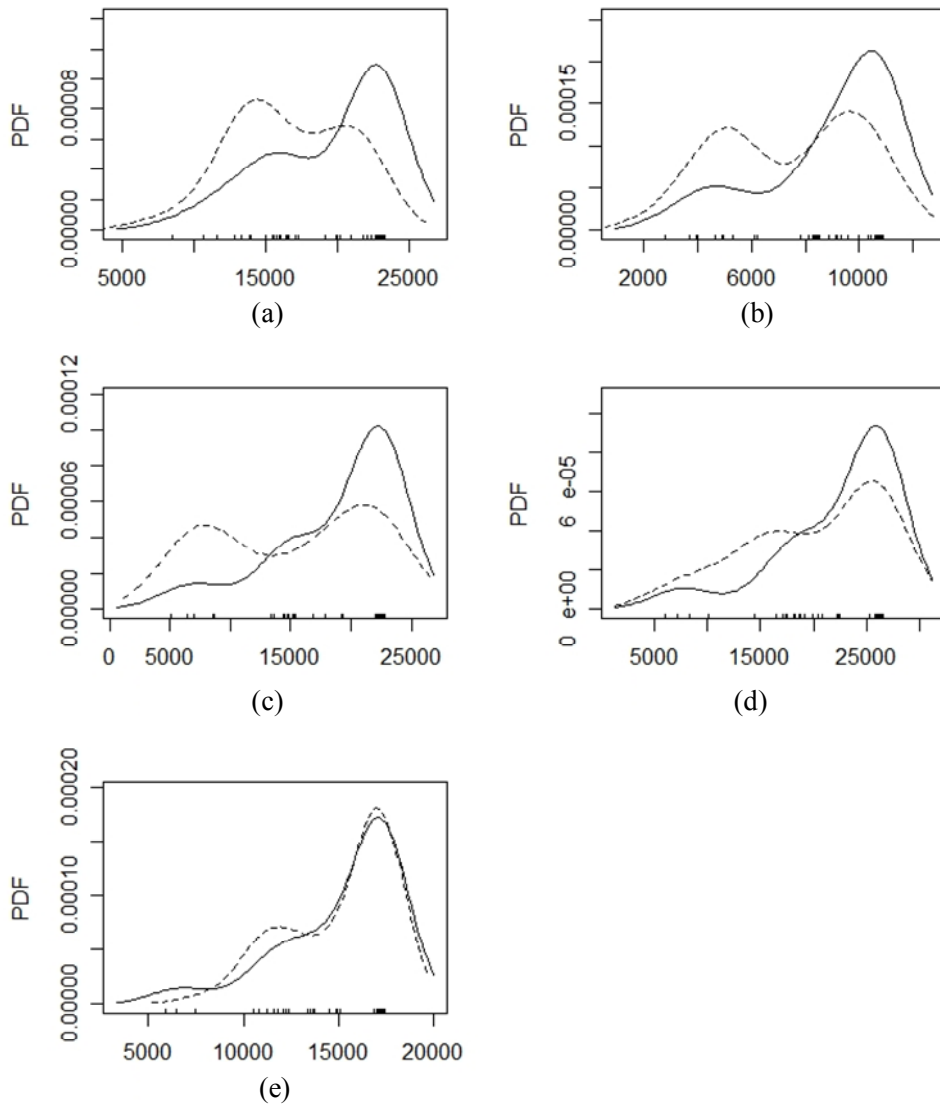
Figure 53. PDFs of annual deliveries to CID (acre-ft) during the March 1st to April 31st (a), May 1st to May 31st (b), June 1st to July 14th (c), July 15th to August 31st (d), and September 1st to October 31st (e) seasons.   The solid and dashed lines represent the forecast and baseline scenarios, respectively.

The decrease in spill between the forecast and baseline scenarios is shown in Figure 54. Because more basin water is utilized through the increased allotments, less water is spilled at Avalon Reservoir.

117
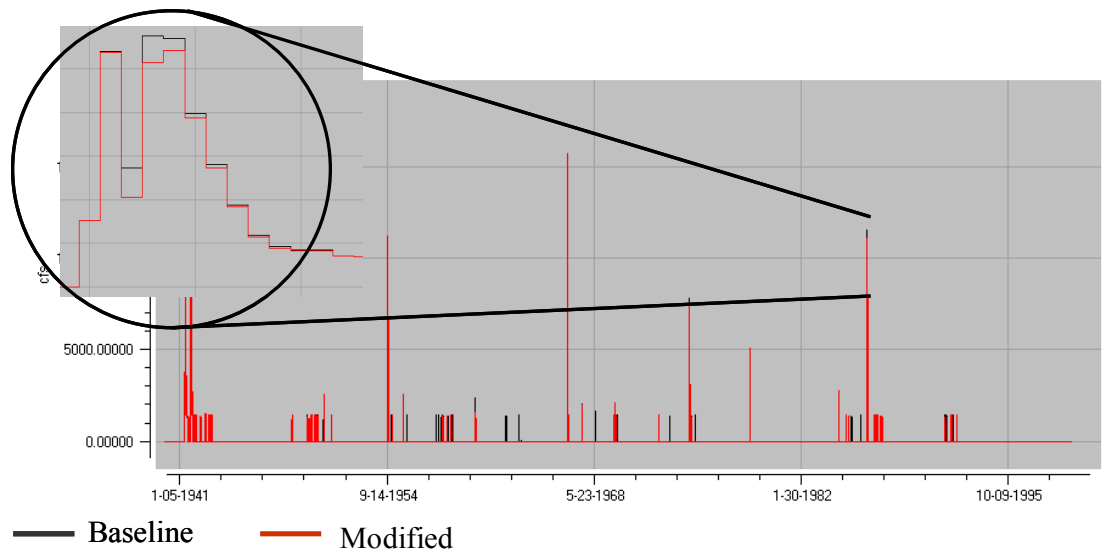
Figure 54. Spills from Avalon Reservoir.

The differences in deliveries to CID between the modified and baseline scenarios in each of the five subseasons are shown in Table 9. The largest improvements to the baseline scenario are made during the mid-irrigation season (i.e., June 1st to July 14th) with the smallest improvements coming at the end of the irrigation season (i.e., September 1st to October 31st). Figure 55 shows the typical stages of crop development for cotton, hay, and alfalfa—the main CID crops. For all these crops, water requirements are low in the early vegetative period, approximately 10 percent of the total water requirements. They are high during the flowering period when leaf area is at its maximum, approximately 50 to 60 percent of total and then later in the growing period, the water requirements decline (Food and Agriculture Organization 2006). Based on the natural water requirements for CID crops, the large increase in water deliveries during the mid-irrigation season could directly improve overall crop production.

118

Table 9. Difference in deliveries to CID between modified scenario and baseline scenario is the five subseasons.

Season	Total difference in deliveries (modified scenario – baseline scenario)
March 1st to April 31st	145,000 acre-ft
May 1st to May 31st	80,000 acre-ft
June 1st to July 14th	190,000 acre-ft
July 15th to August 31st	115,000 acre-ft
September 1st to October 31st	5,000 acre-ft
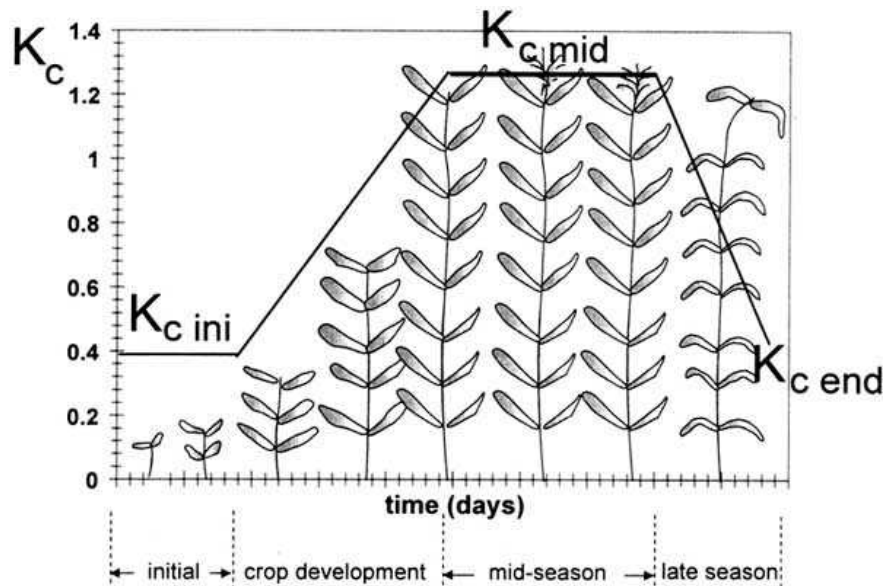
Figure 55. Crop stages of cotton, alfalfa and hay. Image courtesy of the Food and Agriculture Organization of the United Nations.

Assigning a dollar value to the benefit of increased irrigation water is somewhat arbitrary without having a predetermined use for the water. However, one cost estimate for pumping to augment irrigation water in the Pecos basin is $100/ acre-ft water (NMOSE 2006). Using this estimate and the increase of 540,000 acre-ft of CID deliveries, the benefit of using a forecast is $540 million over the 51 year period, or approximately $10.6 million per year. CID farmers could potentially use the increased deliveries instead of relying on pumped water or if they could lease the

119

water to the State of New Mexico for deliveries to Texas. Alternatively, CID farmers could use the increased mid-season deliveries for increased crop production and lease the extra water to the State during the early- and late- irrigation season. Regardless of the use, the increase in water available for irrigation would be of significant value to CID farmers.

Scenario 2: Adjustment of Block Releases

For the adjustment of block releases multiple simulations were run using combinations of near term and full season forecasts, the three definitions for wet (66th 75th, and 90th percentile), various changes to Brantley Reservoir storage threshold levels, and the wet threshold exceedance value. For determining the best combination of variables, both observed flow values and forecasted values were used. Interestingly, between the near term and full season forecasts, one did not consistently produce better results than the other. Also, sequential decreases in storage threshold levels for Brantley Reservoir did not produce sequential changes in total spill. Similarly, there appeared to be no trend among the 66th, 75th and 90th percentile results. Furthermore, many of the simulations actually produced an increase in total spill. This was seen using both forecasted and observed inflow values with the modified block releases. After an extensive analysis, only a 1% reduction in spill was obtained using the observed flow values. No combinations used in this study produced measurable improvements using the forecast. The results of the observed flows are presented here with an analysis of the problem. It is emphasized that the values for these variables reported in this study cannot be deemed the optimal values

for operations. Additionally, other policy adjustments to block releases (e.g., start triggers, block release flow rates, etc.) were not explored.

Using the 75th percentile of lower basin 'near term' streamflow and decreasing the stop threshold levels to 16,500 and 18,000 for Santa Rosa and Sumner reservoirs, respectively produced the best results with the observed data in this study. The improvement was a less than 1% reduction in the spills from Avalon Reservoir and less than 1% increase in deliveries to CID. Figure 56 shows how the block releases
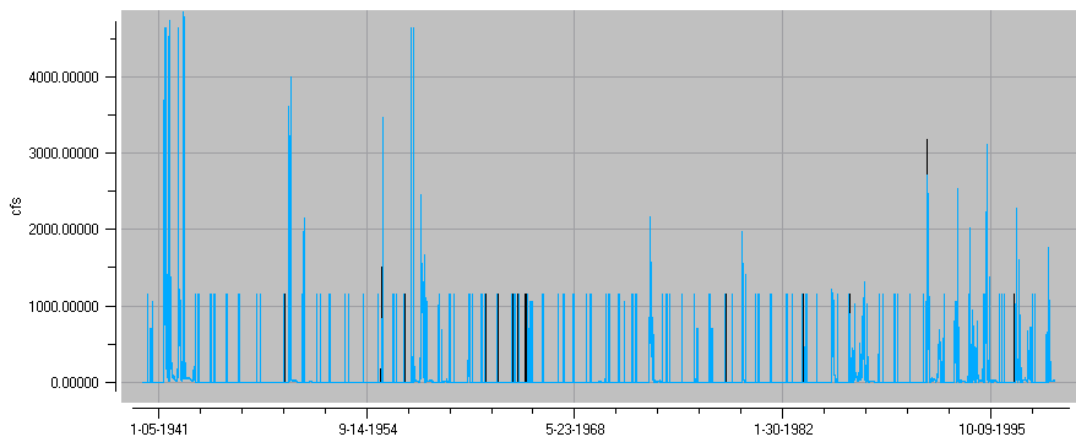
(a)
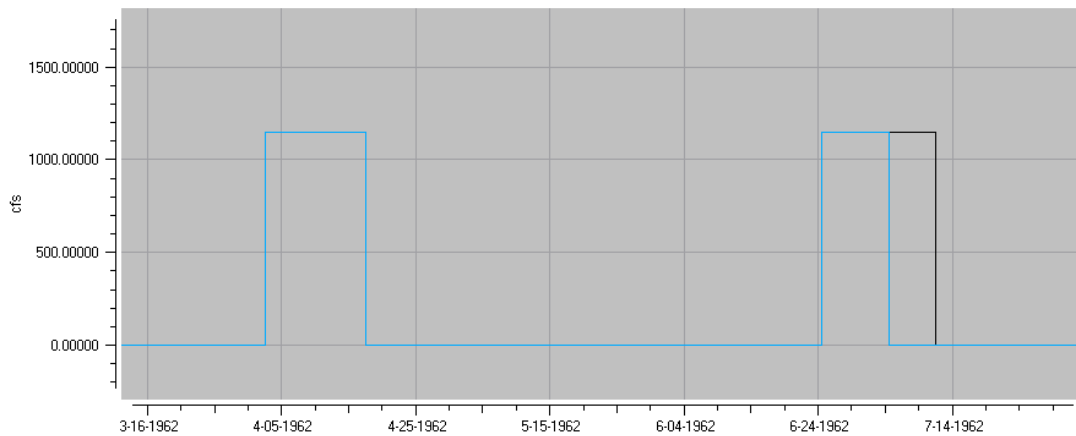
(b)

—— Baseline   —— Modified

Figure 56. Outflow from Santa Rosa Reservoir over the entire time range (a) and in 1962 (b).

are altered by the change in policy. The block releases are the outflow values at 1150 cfs. For the most part, the baseline and modified policy scenarios produce the same block releases. However, as shown in Figure 56(b), in some instances (i.e., in years with a wet forecast), the modified policy scenario shuts off the block release earlier than the baseline scenario.

Figure 57 shows the spill comparison between the baseline scenario and the scenario that uses observed flows to modify block releases. It can be seen that the spills are largely the same for the baseline scenario and the reduced block release scenario. For only one of the large storms, did the change in block releases reduce the resulting spill; and even this reduction was relatively small. For several other additional small events, the change in block releases created space in Brantley Reservoir to hold the incoming event.
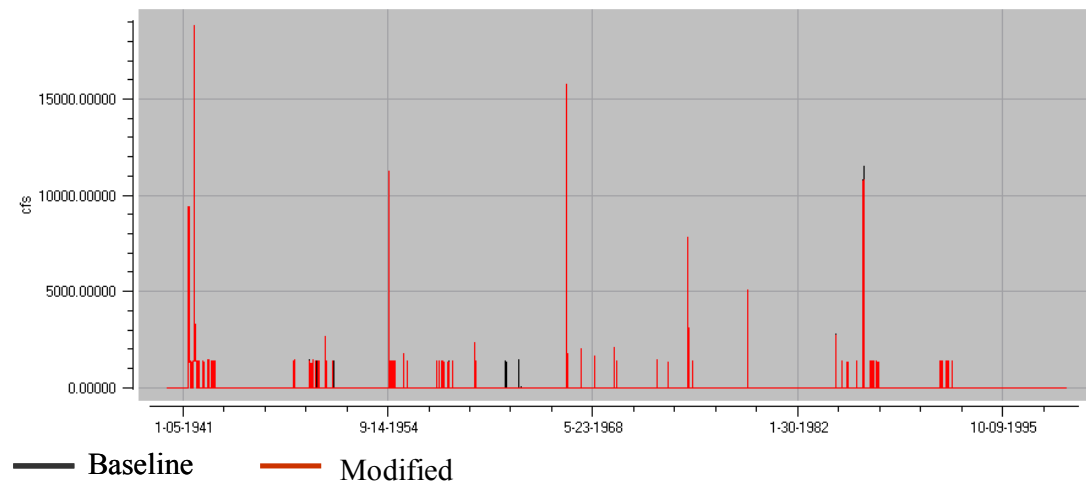
Figure 57. Spill from Avalon Reservoir.

So why is the reduction in block releases not creating space in Brantley Reservoir to capture the large monsoon events? Figure 58 shows the inflows to Brantley Reservoir during two different years. Figure 58 (a) shows how the block

release flood wave spreads out by the time it reaches Brantley Reservoir. Figure 58 (b) shows a block release arriving at Brantley, followed by the largest monsoon event in the time period. The block release volume is very small in comparison to the volume of water from monsoon runoff, thus leaving any reduction in the block release insignificant.
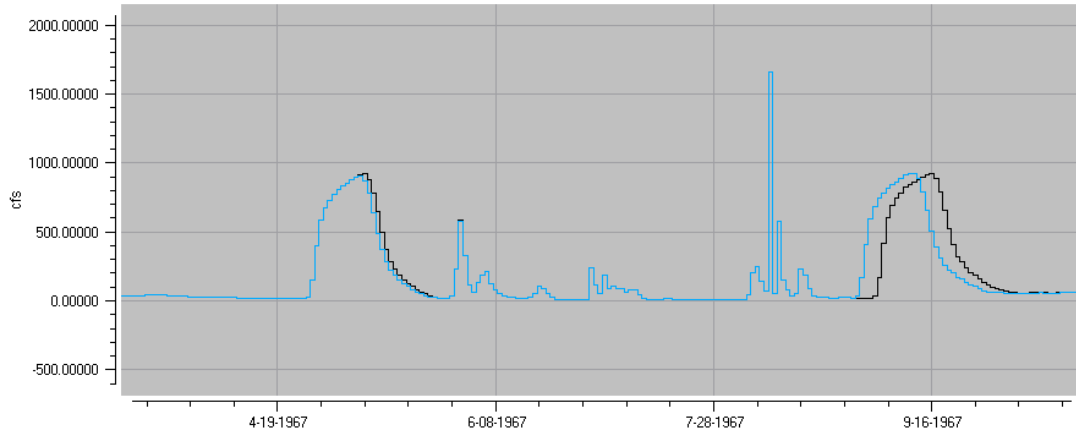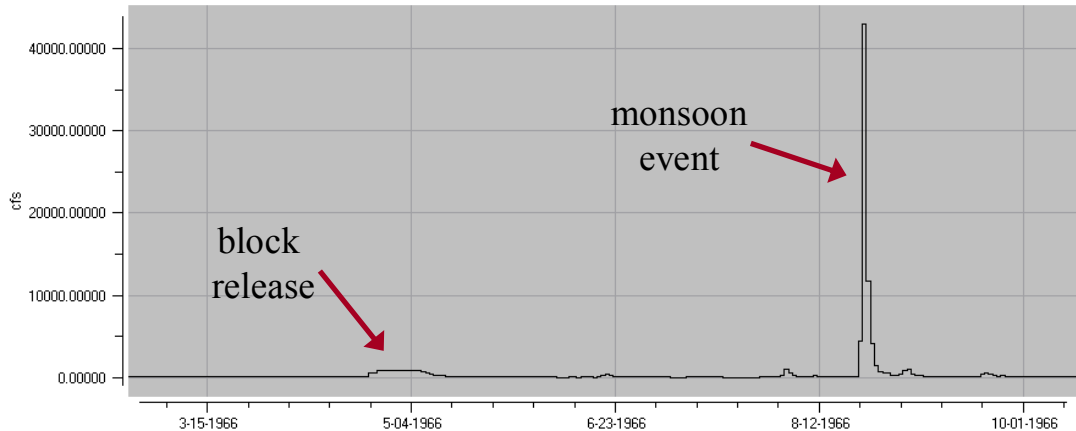
Figure 58. Inflows to Brantley Reservoir in 1967 (a) and 1966 (b).

The goal of holding back on block releases to create space for large monsoon events is not very practical in this application. Due to the relative sizes of block releases and large monsoon runoff events, even a perfect forecast could not

significantly alter operations. Improvements could potentially be greater if more risk was taken and in forecasted wet years block releases were not initiated at all. However, any further reduction of spill might also adversely affect deliveries to CID if water was not available in Brantley Reservoir in time for diversions.

Summary and Conclusions

Irrigation season streamflow forecasts on the Pecos River were used to drive a DSS to demonstrate potential improvements to water management in the basin. Policies and operations in the Pecos RiverWare water operations model were modified to implement seasonal streamflow forecasts. Two scenarios were tested: (i) the inclusion of streamflow forecasts in the calculation of irrigation allotments to provide a better estimate of the season's available water and, thus, deliver more water to irrigators, and (ii) the reduction of block releases in forecasted wet years to better capture monsoon runoff in the lower Pecos basin and, thus, reduce spill to Texas. The results of these two scenarios were compared with exiting operations. Results for the allotment scenario show a 14% increase in irrigation deliveries. Results for the adjustment of block releases show insignificant improvements due to relative size of block releases in comparison with large monsoon events. The coupling of streamflow forecasts with a decision tool in the Pecos River Basin demonstrates that using large-scale climate information to predict NAM streamflow can have significant positive impacts on water management in the region.

Discussion

The results presented here demonstrate the utility of incorporating streamflow forecasts of the spring runoff and summer monsoon into water management on the

124

Pecos River Basin. These results by no means represent the optimal adjustments to policy or combination of forecasts, but rather are used to demonstrate potential benefits. A more in-depth study, including a sensitivity analysis, is necessary before the optimal scenario can be established.

The issue of inter-state stream deliveries to Texas was not directly addressed in this study. This complex issue is an important component of management in the Pecos River Basin. The reduction of spill, or outflow, from Avalon Reservoir was a primary objective of the water management application of this research. This objective translates to increased water for CID, but also to decreased deliveries to Texas. The reduction of spills to Texas is legal given the existing laws of the basin, as long as the total CID storage in the basin never exceeds 176,500 acre-ft (with 42,000 of that at Brantley Reservoir). However, if the spills to Texas were significantly decreased for sustained periods of time, this could potentially cause problems for the State of New Mexico. Though CID would be operating legally, the State would be required to make up for any deficits in deliveries to Texas. Currently the State does this by purchasing and leasing water rights from CID and other farmers in the basin. CID operates the reservoirs as efficiently as possible to avoid spills and yield the most water to their farmers to irrigation or, now, to lease to the State.

Another item of discussion is that the July 15th forecast is actually issued on July 1st, since the forecast predictors are based on monthly data. Operationally, however, the forecast is used on July 15th. This means that any streamflow that comes in the first two weeks of July will not be accounted for in the adjustment of block releases and allotment criteria. Generally speaking, this should not have a

significant negative impact on water management. However, in situations when a very large monsoon even occurs in the first weeks of July, the system may not operate to total efficiently. In this situation, if the July 1st forecast predicts wet, block releases may be reduced on July 15th to allow for inflows below Sumner Reservoir. However, because the monsoon event already happened, the inflows will not come, thus triggering a second block release sooner than may have otherwise occurred.

CHAPTER 6

CONCLUSIONS AND RECOMMENDATIONS

This chapter summarizes and concludes this thesis. The motivation of this research is reviewed, the final results and conclusions are summarized, and the main contributions of this research are highlighted. Lastly, recommendations for future work that will improve and extend this study are provided.

Summary and Conclusions

The North American Monsoon (NAM) delivers roughly half of annual precipitation in the southwestern U.S. However, this important moisture source is highly variable and predicting the space-time variability of monsoonal precipitation and streamflow is key to efficient water resources management in the region.

This study developed a framework for diagnosing NAM hydroclimate variability, forecasting this variability and then applying the forecasts to improve water management in the region. The results of this study demonstrate the utility of incorporating large-scale climate information in forecasts of monsoon streamflow to improve water management in the NAM region. Though this study focused on the Pecos River Basin, the framework presented here is general and could be applied to any basin in the NAM region.

Precipitation Analysis

The first component of this study examined the variability of precipitation in New Mexico and Arizona. The results showed a significant delay in the monsoon rainfall cycle over the past 50 years. This was manifested as a decrease in July rainfall, a corresponding increase in August and September rainfall, and a delay in the Julian day when the 10th, 25th, 50th, 75th, and 90th percentile of seasonal precipitation had accumulated. Relating these attributes to antecedent winter/spring land and ocean conditions inspired the following hypothesis: warmer tropical Pacific sea surface temperatures (SSTs) and cooler northern Pacific SSTs in the antecedent winter/spring leads to wetter than normal conditions in the southwestern U.S.. This enhanced antecedent wetness delays the seasonal heating of the North American continent that is necessary to establish the monsoonal land-ocean temperature gradient and, in turn, delays the initiation and strength of the ensuing monsoon. Through this relationship, it was proposed that increased ENSO activity in recent decades has lead to the evident delay in the seasonal cycle of NAM precipitation.

The result that the monsoon cycle has been delayed by an average of two weeks over the past 50 years is interesting and is not known to have been reported in the literature. This shift in the monsoon cycle has significant implications for water management in the region. Furthermore, the hypothesis presented here is unique in its linking monsoon variability (and the recent delay) to large-scale climate via interaction with the land. While similar hypothesis exist, none have included both large-scale climate and the land, nor have they related the linkages to the timing of the monsoon.

The streamflow analysis component of this study was performed on winter, spring and summer streamflows in New Mexico and Arizona. Streamflow stations were grouped into north (snowmelt dominated), central (early snowmelt and rain dominated), or south (summer rainfall dominated) regions based on streamflow climatology and peak flow month. The winter/spring streamflow exhibited a significant increasing trend, likely driven by enhanced ENSO activity in recent decades. Both the magnitude and timing of early summer streamflows showed a significant relationship with antecedent winter/spring precipitation in the NAM region, with increased precipitation favoring a weaker and later streamflow cycle, and vice-versa. Because summer streamflows in the northern region are significantly impacted by the antecedent spring runoff, a simple approach was applied to remove this influence. The hypothesis proposed in the precipitation chapter was tested and validated with streamflow variability. Results for the southern region monsoon streamflow supported the hypothesis more than the northern region streamflow. The results for the northern regions streamflow are mainly due to the effect of spring snowmelt extending into the summer months in the northern region.

While NAM precipitation has been widely analyzed, only one known study has been conducted on the NAM streamflow. This research is unique in that it analyzed streamflow using observational data (rather than models) and it focused on the more variable region of New Mexico and Arizona (rather than Mexico). In addition, the technique of grouping stations based on peak flow month provided important insight to the relative importance of monsoon runoff in each region. This

grouping technique could be useful in other streamflow studies (monsoon or otherwise) in the region. That the streamflow results corroborate those of the precipitation analysis strengthens the conclusions of both analyses.

Seasonal Streamflow Forecast

A modeling framework to provide ensemble forecasts of streamflows during the irrigation season on the Pecos River Basin was developed and demonstrated. Predictors were identified from the large-scale land-ocean-atmosphere system from the preceding seasons. Based on current operating criteria, irrigation season forecast ensembles were generated at five lead times, March 1st, May 1st, June 1st, July 15th, and September 1st, in the upper and lower Pecos River Basin. A robust nonparametric method based on local weighted polynomials was used to select the best subset of predictors and consequently generate the ensemble forecasts. The forecast framework exhibited significant skill overall, but more so during wet years.

No known study has attempted to forecast the interannual variability of the NAM. This research succeeded in the difficult task of forecasting this highly variable phenomenon and the skill was remarkably high, particularly in the wet years. Because water management in the region operates under the dry monsoon assumption, the high forecast skill in wet years has important implications for capitalizing on this "extra" water.

Irrigation season streamflow forecasts on the Pecos River were coupled with the Pecos River Basin water operations model to demonstrate potential improvements to water management in the basin. Because current operations do not utilize forecasts of spring or monsoon streamflow, existing policies and operations in the DSS were modified to make use of the forecasts. Two scenarios were tested: (i) the inclusion of streamflow forecasts in the calculation of irrigation allotments to provide a better estimate of the season's available water and, thus, deliver more water to irrigators, and (ii) the reduction of block releases in forecasted wet years to better capture monsoon runoff in the lower Pecos Basin and, thus, reduce spill to Texas. The results of these two scenarios were compared with exiting operations. Results for the allotment scenario showed a 14% increase in irrigation deliveries. Results for the adjustment of block releases showed insignificant improvements due to relative size of block releases in comparison with large monsoon events.

Though many studies acknowledge the NAM's importance to water and agriculture management in the region, the process of using monsoon streamflow forecasts in a water operations model to improve planning and management is new. The coupling of streamflow forecasts with a water management tool in the Pecos River Basin demonstrates that using large-scale and local-scale climate information to predict the NAM can have significant positive impacts on water management in the region.

Recommendations for Future Work

Many areas of this research warrant further research and analysis. Several issues that should be addressed to complete this study as well as possibilities for extending the techniques of this research to new realms are addressed here.

1. This study put forth a hypothesis that links sea surface temperatures (SSTs) in the Pacific Ocean to the modulation of monsoon variability via the land. This hypothesis was supported through statistical analysis of observational data. More rigorous testing is necessary before this theory can be confirmed. Additional studies should include physical models. One analysis might simulate heating in the areas of the Pacific Ocean identified in this research to determine the effects on monsoon precipitation and streamflow. Another study might investigate the link between the land and the monsoon directly. For example, if pre-monsoon moisture is increased via model simulation, do the model results show a delay in the ensuing monsoon precipitation and streamflow?

2. The streamflow analysis in this study used a very simple method to remove the baseflow from northern stations and thus isolate monsoon streamflow. Because the north has many more streamflow stations, relative to the central and south regions, this region presents a wealth of data that would be helpful to produce more statistically robust results. It would be beneficial to use a more sophisticated method to isolate monsoon streamflow in the region and potentially strengthen the streamflow results of this study.

3. The water management application of this research modified existing policy in the Pecos River Basin to demonstrate the utility of incorporating

streamflow forecasts of the spring and summer monsoon into water management. The results of this study by no means represent the optimal adjustments to policy or combination of forecasts, but rather are used to demonstrate potential benefits. A more in-depth study, including a sensitivity analysis, is necessary before the optimal scenario can be established and operations can be adequately adjusted. One approach might be to use optimization to maximize irrigation water deliveries and minimize spill to Texas by changing the variables of reservoir thresholds, forecast percentiles and exceedance probability thresholds, etc.

4. This research applied a framework of monsoon diagnostics and forecasting to water management in the Pecos River Basin. Using this framework in other NAM basins would be helpful to further the understanding of how NAM variability affects water management in the region.

5. The improvements to water management in this study were monetarily quantified using only one dollar value estimate for water in the Pecos River Basin. A comprehensive economic analysis of the improvement to water management would provide a more tangible understanding of the value of including forecasts in water management in the Pecos River Basin.

6. This study did not address the implications of increased CID efficiency relative to inter-state deliveries to Texas. Before any policies or operations could be modified in the basin, a comprehensive analysis should be undertaken to determine the impact on this important legal requirement. It is important to point out that CID's gain does not translate linearly into Texas'

loss. A more efficient management of the system may actually result in decreased evaporation and seepage, rather than simply a reduction in spill. The relative changes in each of these variables should be evaluated.

7. The modification of block releases, a bi-weekly timescale operation, was based on season streamflow forecasts. It is possible that shorter timescale forecasts (e.g., two weeks) might show a larger improvement to block release policy modifications.

8. The public health and safety implications of utilizing a monsoon forecast could be explored. For example, does the potential for mosquito born viruses and/or flash floods increase in wet monsoon years? And if so, could a forecast of the monsoon benefit local public health and safety agencies in planning operations.

REFERENCES

Allan, R., J. Lindesay, and D. Parker, 1996: El Niño Southern Oscillation & Climatic Variability, National Library of Cataloguing-in-Publication, Collingwood.

Anderson, B., and H. Kanamaru, 2005: The diurnal cycle of the summertime hydrologic atmospheric cycle over the southwestern U.S.. *Journal of Hydrometeorology*, **6**, 219–228.

Adams, D.K., and A.C. Comrie, 1997: The North American Monsoon. *Bull Bulletin of the American Meteorological Society,* **78**, 2197-2213.

Barlow, M.,S. Nigam, and E.H. Berbery, 1998: Evolution of the North American monsoon system. *Journal of Climate,* **11**, 2238-2257.

Barnston, A.G., and R.E. Livezey, 1987: Classification, seasonality, and persistence of low-frequency atmospheric circulation patterns. *Monthly Weather Review*, **109**, 1542-1566.

Berbery, E.H., 2001: Mesoscale moisture analysis of the North American monsoon. *Journal of Climate,* **14**, 121–137.

Boroughs, C. and T. Stockton, 2005: Pecos RiverWare Model DRAFT Report: Volume II in a series of model documents. Prepared on behalf of the Hydrology/Water Operations Work Group for the Carlsbad Project Water Operations and Water Supply Conservation NEPA Process.

Bowman, A. and A. Azzalini, 1997: Applied smoothing techniques for data analysis. Oxford, UK.

Brenner, I.S., 1974: A surge of maritime tropical air—Gulf of California to the southwestern United States. *Monthly Weather Review*, **102,** 375–389.

Bryson, R.A., and W.P. Lowry, 1955: Synoptic climatology of the Arizona summer precipitation singularity. *Bulletin of the American Meteorological Society,* **36**, 329–339.

Carleton, A.M., 1986: Synoptic-dynamic character of "bursts" and "breaks" in the southwest U.S. summer precipitation singularity. *Journal of Climate,* **6**, 605–623.

Carleton, A.M., 1987: Summer circulation climate of the American Southwest: 1945–1984. *Ann. Assoc. Amer. Geogr.,* **77**, 619–634.

Carleton, A.M., D.A. Carpenter, and P. J. Weser, 1990: Mechanisms of interannual variability of southwest United States summer precipitation maximum. *Journal of Climate,* **3**, 999-1015.

Castro, C.L., T.B. McKee, and R.A. Pilke, 2001: The relationship of the North American Monsoon to tropical and North Pacific surface temperatures as revealed by observational analysis. *Journal of Climate,* **14**, 4449-4473.

Cayan, D.R., and D.H. Peterson, 1989: The influence of North Pacific atmospheric circulation on streamflow in the west, in Aspects of Climate Variability in the Pacific and the Western Americas. *Geophys. Monogr. Ser.,* **55**, 365-374.

Cayan, D.R., and R.H. Webb, 1992: El Niño/Southern Oscillation and streamflow in the western United States, in El Niño: Historical and Paleoclimate Aspects of the Southern Oscillation. Diaz, H.F. and Markgraf, V., eds., Cambridge University Press, 29-86.

Cayan, D.R., K.T. Redmond, and L.G. Riddle, 1999: ENSO and hydrologic extremes in the western United States. *Journal of Climate,* **12**, 2881-2893.

Cayan, D.R., S.A. Kammerdiener, M.D. Dettinger, J.M. Caprio, and D.H. Peterson, 2001: Changes in the Onset of Spring in the Western United States. *Bulletin of the American Meteorological Society,* **82**, 399-415.

Chow, V.T., D.R. Maidment, and L.W. Mays, 1988: Applied Hydrology. McGraw Hill, Inc. New York.

Clark, M.P., M.C. Serreze and G.J. McCabe, 2001: Historical effects of El Nino and La Nino events on the seasonal evolution of the montane snowpack in the Columbia and Colorado River Basins. *Water Resources Research,* **37**, 741-757.

Comrie, A.C., and E.C. Glenn, 1998: Principal components-based regionalization of precipitation regimes across the southwest United States and northern Mexico, with an application to monsoon precipitation variability. *Climate Research,* **10**, 201-215.

Craven, P., and G. Whaba, 1979: Optimal smoothing of noisy data with spline functions, *Numerische Mathematik,* **31**, 377-403.

Dai, A., F. Giorgi, and K.E. Trenberth, 1999: Observed and model-simulated diurnal cycles of precipitation over the contiguous United States. *Journal of Geophysical Research,* **104**, 6377-6402.

Dettinger, M.D., and D.R. Cayan, 1995: Large-scale atmospheric forcing of recent trends toward early snowmelt runoff in California. *Journal of Climate,* **8,** 606–623.

Douglas, M.W., R.A. Maddox, K. Howard, and S. Reyes, 1993: The Mexican monsoon. *Journal of Climate,* **6**, 1665-1677.

Dracup, J. S. and E. Kahya, 1994: The relationships between U.S. streamflow and La Nina events. *Water Resources Research,* **30**, 2133-2141.

Ellis, A.W., and T.W. Hawkins, 2001: An apparent atmospheric teleconnection between snow cover and the North American monsoon. *Geophysical Research Letters,* **28**, 2653-2656.

Ellis A.W., E.M. Saffell, and T.W. Hawkins, 2004: A method for defining monsoon onset and demise in the southwestern USA. *International Journal of Climatology,* **24**, 247-265.

Food and Agriculture Organization of the United Nations, Crop Water Management, Retrieved November 10, 2006, from their website at www.fao.org/ag/agl/aglw/cropwater.

Gochis, D.J., J.W. Shuttleworth, and Z. Yang, 2003: Hydrometeorological response of the modeled North American Monsoon to convective parameterization. *Journal of Hydrometeorology,* **4**, 235–250.

Grantz, K., B. Rajagopalan, M. Clark, and E. Zagona, 2005: A technique for incorporating large-scale climate information in basin-scale ensemble streamflow forecasts. *Water Resources Research,* **41**, W10410.

Grantz, K., B. Rajagopalan, M. Clark and E. Zagona, 2005: Seasonal Shifts in the North American Monsoon. *Journal of Climate* (in press).

Gutlzer, D.S., 2000: Covariability of spring snowpack and summer rainfall across the southwest United States. *Journal of Climate*, **13**, 4018-4027.

Guttman, N.B., J.R. Wallis, and J.R. M. Hosking, 1992: Spatial Comparability of the Palmer Drought Severity Index, *Water Resources Bulletin*, **28**, 1111- 1119.

Hagedorn, R., F. J. Doblas-Reyes and T. N. Palmer, 2005: The rationale behind the success of multi-model ensembles in seasonal forecasting. Part I: Basic concept. *Tellus A*, **57**, 219-233.

Hales, J.E., 1972: Surges of maritime tropical air northward over the Gulf of California. *Monthly Weather Review*, **100**, 298–306.

Hales, J.E., 1974: The southwestern United States summer monsoon source—Gulf of Mexico or Pacific Ocean. *Journal of Applied Meteorology,* **13**, 331–342.

Hamlet, A.F., and D.P. Lettenmaier, 1999: Columbia River streamflow forecasting based on ENSO and PDO climate signals. *Journal of Water Resources Planning and Management*, **125**, 333–341.

Hamlet, A.F., D. Huppert, and D.P. Lettenmaier, 2002: Economic Value of Long-Lead Streamflow Forecasts for Columbia River Hydropower. *Journal of Water Resources Planning and Management*, **128**, 91-101.

Hawkins, T.W., A.W. Ellis, J.A. Skindlov, and D. Reigle, 2002: Intra-annual analysis of the North American snow cover—monsoon teleconnection: seasonal forecasting utility. *Journal of Climate,* **15**, 1743-1753.

Helsel, D.R., and R.M. Hirsch, 1995: Statistical Methods in Water Resources. Elsevier Science Publishers, 522 pp.

Higgins, R.W., Y. Yao, and X.L. Wang, 1997: Influence of the North American monsoon system on the U.S. summer precipitation regime. *Journal of Climate,* **10**, 2600-2622.

Higgins, R.W., K.C. Mo, and Y. Yao, 1998: Interannual variability of the U.S. summer precipitation regime with emphasis on the southwestern monsoon. *Journal of Climate,* **11**, 2582-2606.

Higgins, R.W., Y. Chen, and A.V. Douglas, 1999: Interannual variability of the North American warm season precipitation regime. *Journal of Climate,* **12**, 653-680.

Higgins, R.W., and W. Shi, 2000: Dominant factors responsible for interannual variability of the summer monsoon in the southwestern United States. *Journal of Climate,* **13**, 759-776.

Hoerling, M.P., A. Kumar, and M. Zhong, 1997: El Niño, La Niña, and the Nonlinearity of their Teleconnections. *Journal of Climate*, **10**, 1769-1786.

Houghton, J.G., 1979: A model for orographic precipitation in the north-central Great Basin. *Monthly Weather Review*, **107**, 1462–1475.

Jain, S., and U. Lall, 2000: Magnitude and timing of annual maximum floods: Trends and large-scale climatic associations for the Blacksmith Fork River, Utah. *Water Resources Research,* **36**, 3641-3651.

Jain, S., U. Lall, 2001: Floods in a changing climate: Does the past represent the future?. *Water Resources Research,* **37**, 3193-3206, 10.1029/2001WR000495.

Kahya, E., and J.A. Dracup, 1993a: U.S. streamflow patterns in relation to the El Niño/Southern Oscillation. *Water Resources Research*, **29**, 2491– 2503.

Kahya, E., and J.A. Dracup, 1993b: The relationships between ENSO events and California streamflows, in <u>The World at Risk: Natural Hazards and Climate Change.</u> pp. 86– 95, Am. Inst. of Phys., Melville, N. Y.

Kahya, E., and J.A. Dracup, 1994a: The influences of type 1 El Niño and La Niña events on streamflows in the Pacific southwest of the United States. *Journal of Climate.*, **7**, 965– 976.

Kahya, E., and J.A. Dracup, 1994b: The relationships between U.S. streamflow and La Niña events. *Water Resources Research,* **30**, 2133– 2141.

Kalnay, E., M. Kanamitsu, R. Kistler, W. Collins, D. Deaven, L. Gandin, M. Iredell, S. Saha, G. White, J. Woollen, Y. Zhu, M. Chelliah, W. Ebisuzaki, W. Higgins, J. Janowiak, K. C. Mo, C. Ropelewski, J. Wang, A. Leetmaa, R. Reynolds, R. Jenne, and D. Joseph, 1996: The NCEP/NCAR reanalysis 40-year project. *Bulletin of the American Meteorological Society,* **77**, 437-471.

Kim, J., J. Kim, J.D. Farrara, and J.O. Roads, 2005: The Effects of the Gulf of California SSTs on Warm-Season Rainfall in the Southwestern United States and Northwestern Mexico: A Regional Model Study. *Journal of Climate*, **18**, 4970– 4992.

Krishnamurti, T.N., C.M. Kishtawal, T.E. LaRow, D.R. Bachiochi, Z. Zhang, C.E. Williford, S. Gadgil, and S. Surendran, 1999: Improved weather and seasonal climate forecasts from multi-model superensemble. *Science,* **285**, 1548–1550.

Krishnamurti, T.N., C.M. Kishtawal, Z. Zhang, T.E. LaRow, D.R. Bachiochi, C.E. Williford, S. Gadgil, and S. Surendran, 2000: Multi-model ensemble forecasts for weather and seasonal climate. *Journal of Climate*, **13,** 4196–4216.

Lall, U. and A. Sharma, 1996: A Nearest Neighbor Bootstrap for Resampling Hydrologic Time Series. *Water Resources Research*, **32**, 679-693.

Leathers, D.J., and B. Yarnal, and M.A. Palecki, 1991: The Pacific/North American teleconnection pattern and United States climate, Part I: Regional temperature and precipitation associations. *Journal of Climate*, **4**, 517-527.

Lins, H.F., 1997: Regional streamflow regimes and hydroclimatology of the United States. *Water Resources Research*, **33**, 1655-1668, 10.1029/97WR00615.

Livezey, R.E. and W.Y. Chen, 1983: Statistical field significance and its determination by Monte Carlo techniques. *Monthly Weather Review*, **111**, 46-59.

Lo, F., and M.P. Clark, 2002: Relationships between spring snow mass and summer precipitation in the southwestern United States associated with the North American monsoon system. *Journal of Climate,* **15**, 1378-1385.

Loader, C., 1999: Statistics and Computing: Local Regression and Likelihood. Springer, New York.

Mann, M. E., J. Park, and R. S. Bradley, 1995: Global interdecadal and century-scale oscillations during the past five centuries. *Nature*, **378**, 266-270.

Mantua, N.J., S.R. Hare, J.M. Wallace, and R.C. Francis, 1997: A Pacific interdecadal climate oscillation with impacts on salmon production. *Bulletin of the American Meteorological Society,* **78**, 1069-1079.

Mantua, N.J., and S.R. Hare, 2002: The Pacific Decadal Oscillation. *Journal of Oceanography,* **59**, 35– 44.

Matsui, T., V. Lakshmi, and E. Small, 2003: Links between snow cover, surface skin temperature, and rainfall variability in the North American Monsoon System. *Journal of Climate*, **16**, 1821–1829.

McCabe, G.J. and M.D. Dettinger, 2002: Primary Modes and Predictability of Year-to-Year Snowpack Variation in the Western United States from Teleconnections with Pacific Ocean Climate. *Journal of Hydrometeorology*, **3**, 13-25.

Mitchell, D.L., D. Ivanova, R. Rabin, T.J. Brown, and K. Redmond, 2002: Gulf of California sea surface temperature and the North American monsoon: mechanistic implication from observation. *Journal of Climate,* **15**, 2261-2281.

Mo, K.C., and J.N. Paegle, 2000: Influence of sea surface temperature anomalies on the precipitation regimes over the southwest United States. *Journal of Climate,* **13**, 3588-3598.

Mote, P.W., 2003: Trends in snow water equivalent in the Pacific Northwest and their climatic causes. *Geophysical Research Letters,* **30,** 1601–1604.

Mullen, S.L., and J.T. Schmitz, 1998: Intraseasonal Variability of the Summer Monsoon over Southeast Arizona. *Monthly Weather Review,* **126**, 3016-3035.

Newman, M., G.P. Compo, M.A. Alexander, 2003: ENSO-forced variability of the Pacific Decadal Oscillation. *Journal of Climate*, **16**, 3853-3857.

New Mexico Office of the State Engineer (NMOSE), Pecos River Basin, Retrieved Oct 11, 2006, from their website at www.ose.state.nm.us/isc_pecos.html.

Owosina, A., Methods for assessing the space and time variability of groundwater data, M.S. Thesis, Utah State University, Logan, Utah, 1992.

Piechota, T.C. and Dracup, J.A., 1996: Drought and Regional hydrologic Variation in the United States: Associations with El Nino/Southern Oscillation. *Water Resources Research,* **32**, 1359-1373.

Piechota, T.C., Dracup, J.A., and Fovell, R.G., 1997: Western US Streamflow and Atmospheric Circulation Patterns During El Nino-Southern Oscillation. *Journal of Hydrology,* **201**, 249-271.

Pizarro, G., and U. Lall, 2002: El Nino-induced flooding in the U.S. west: What can we expect?. *EOS Transactions, AGU*, **83**, 349-352.

Prairie, J., B. Rajagopalan, T. Fulp and E. Zagona, 2005: Statistical nonparametric model for natural salt estimation. *ASCE Journal of Environmental Engineering*, **131**, 130-138.

Prairie, J., B. Rajagopalan, U. Lall and T. Fulp, 2006: A Stochastic Nonparametric Technique for Space-Time Disaggregation of Streamflows. *Water Resources Research*, (in press).

Rajagopalan, B., U. Lall, and M. A. Cane, 1997: Anomalous ENSO occurrences: an alternate view. *Journal of Climate*, **10**, 2351-2357.

Rajagopalan, B. and U. Lall, 1999: A Nearest Neighbor Bootstrap Resampling Scheme for Resampling Daily Precipitation and other Weather Variables, *Water Resources Research*, **35**, 10, 3089-3101.

Rajagopalan, B., U. Lall, and S. Zebiak, 2002: Optimal Categorical Climate Forecasts through Multiple GCM Ensemble Combination and Regularization. *Monthly Weather Review*, **130**, 1792-1811.

Rao, C.R., and H. Toutenburg, 1999: Linear models: least squares and alternatives. Springer, New York.

Rasmusson, E.M., 1967: Atmospheric water vapor transport and the water balance of North America: Part 1. Characteristics of the water vapor flux field. *Monthly Weather Review*, **95**, 403–427.

Ray, A.J., G.M. Garfin, M. Wilder, M. Vasquez-Leon, M. Lenart and A.C. Comrie, 2006: Applications of monsoon research: Opportunities to inform decision making and reduce regional vulnerability. *Journal of Climate, special issue on NAME,* (in review).

Redmond, K.T., and R.W. Koch, 1991: Surface climate and streamflow variability in the western United States and their relationship to large-scale circulation indices. *Water Resources Research*, **27**, 2381-2399.

Regonda, S., B. Rajagopalan, M. Clark, and J. Pitlick, 2005: Seasonal cycle shifts in hydroclimatology over the Western U.S. *Journal of Climate*, **18**, 372-384.

Regonda, S., B. Rajagopalan, M. Clark and E. Zagona, 2006: Multi-model Ensemble Forecast of Spring Seasonal Flows in the Gunnison River Basin. *Water Resources Research* (in review).

Reitan, C.H., 1957: The role of precipitable water vapor in Arizona's summer rains. Tech. Rep. on the Meteorology and Climatology of Arid Regions 2, The Institute of Atmospheric Physics, The University of Arizona, Tucson, 19 pp.

Reiter, E.R., and M. Tang, 1984: Plateau effects on diurnal circulation patterns. *Monthly Weather Review,* **112**, 638–651.

Ropelweski, C.F., and M.S. Halpert, 1986: North American precipitation and temperature patterns associated with El Niño-Southern Oscillation (ENSO). *Monthly Weather Review,* **114**, 2352-2362.

Sheppard, P.R., A.C. Comrie, G.D. Packin, K. Angersbach, and M.K. Hughes, 2002: The climate of the U.S. Southwest. *Climate Research,* **21**, 219-238.

Sims, A.P., S.N. Dev Dutta, and S. Raman, 2002: Adopting drought indices for estimating soil moisture: A North Carolina case study. *Geophysical Research Letters*, **29**.

Singhrattna, N., B. Rajagopalan, M. Clark, and K. Krishna Kumar, 2005: Forecasting Thailand summer monsoon rainfall. *International Journal of Climatology,* **25**, 649–664.

Slack, J.R., A.M. Lumb, and J.M. Landwehr, 1993: Hydroclimatic data network (HCDN): A U.S. Geological Survey streamflow data set for the United States for the study of climate variation, 1874-1988. *Water Resour. Invest. Rep.*, 93-4076.

Souza F. A., and U. Lall, 2003: Seasonal to Interannual Ensemble Streamflow Forecasts for Ceara, Brazil: Applications of a Mutlivariate, Semi-Parametric Algorithm. *Water Resources Research*, **39**, 1307-1320.

Stewart, I.T., D.R. Cayan, and M.D. Dettinger, 2004: Changes in snowmelt runoff timing in western North America under a "business as usual" climate change scenario. *Climate Change,* **62,** 217–232.

Tang, M., and E.R. Reiter, 1984: Plateau monsoons of the Northern Hemisphere: A comparison between North America and Tibet. *Monthly Weather Review,* **112**, 617–637.

Tootle, G.A., T.C. Piechota, and A. Singh, 2005: Coupled oceanic-atmospheric variability and U.S. streamflow. *Water Resources Research,* **41**, W12408, doi:10.1029/2005WR004381.

Trenberth K.E., and T.J. Hoar, 1996: The 1990–1995 El Niño–Sourthern Oscillation event: Longest on record. *Geophysical Research Letters,* **23**, 57–60.

Trenberth, K. E., 1997: The definition of El Niño. *Bulletin of the American Meteorological Society,* **78**, 2271– 2777.

Trenberth K.E., A.G. Da, R.M. Rasmussen, and D.P. Parsons, 2003: The changing character of precipitation. *Bulletin of the American Meteorological Society,* **84**, 1205-1217.

von Storch, H., and F.W. Zwiers, 1999: Statistical Analysis in Climate Research, Cambridge University Press, 484 pp.

Wallace, J.M. and D.S. Gutzler, 1981: Teleconnections in the geopotential height field during the Northern Hemisphere Winter. *Monthly Weather Review,* **109**, 784-812.

Walpole, R.E., R.H. Myers, S.L. Myers, K. Ye, and K. Yee, 2002: Probability and Statistics for Engineers and Scientist, Prentice Hall, Upper Saddle River, N.J.

Wilks, D., 1995: Statistical Methods in the Atmospheric Sciences, Academic Press.

Yarnal B., and H.F. Diaz, 1986: Relationships between extremes of the Southern Oscillation and the winter climate of the Anglo-American Pacific coast. *Journal of Climatology*, **6**, 197-219.

Yates, D.S., Gangopadhyay, S., Rajagopalan, B., and Strzepek, K., 2003: A technique for generating regional climate scenarios using a nearest neighbor bootstrap. *Water Resources Research,* **39**, 1199.

Zagona, E.A., T.J. Fulp, H.M. Goranflo, and R. Shane,1998: RiverWare: A general river and reservoir modeling environment. Proceedings of the First Federal Interagency Hydrologic Modeling Conference. Las Vegas, NV. April 19-23. 5:113-120.

Zagona, E.A., T.J. Fulp, R. Shane, T. Magee, and H.M.Goranflo, 2001: RiverWare: A generalized tool for complex reservoir system modeling. *Journal of the American Water Resources Association*. **37**, 913-929.

Zhu, C., D. Lettenmaier, and T. Cavazos, 2005: Role of antecedent land surface condtions on North American Monsoon Rainfall variability. *Journal of Climate,* **18**, 3104-3121.

APPENDIX A

POLICY CHANGES TO PECOS RIVERWARE MODEL

Rules and Functions for Block Release Modifications

RULE: Continue Santa Rosa Block Release – WET Forecast

```
Santa Rosa Reservoir.Outflow []
  = IF ( # Forecast time range                                                    THEN
       ( @"Current Timestep"
         >= @"24:00:00 January 1, 1949" )
        AND # Wet forecast
            ( Forecast Info.LowerNearTermForecastProbabilityWET [ MostRecentForecastDate ( )]
              >= Forecast Info.WET threshold probability [] )
        # Lower Block Release threshold
        IF ( ( # SR stop threshold                                               THEN
             ( PreviousStorage ( % "Brantley Reservoir" )
               < StorageTriggerWETforecast ( % "Brantley Reservoir" ,
                                             4.00000000 ) )
            AND NOT SumnerBlockReleaseAt15Days ( )
            AND NOT TotalBlockReleaseDaysReached65 ( )
            OR # balance w/ Sumner
                ( PreviousStorage ( % "Sumner Reservoir" )
                  < StorageTriggerWETforecast ( % "Sumner Reservoir" ,
                                                3.00000000 ) )
            AND NOT MonthIsSeptOrOct ( ) )
          OR ( ( PreviousStorage ( % "Brantley Reservoir" )
                 < ( StorageTriggerWETforecast ( % "Brantley Reservoir" ,
                                                 3.00000000 )
                   + SumRemainingCIDDiversion ( ) )
               AND NOT SumnerBlockReleaseAt15Days ( )
               AND NOT TotalBlockReleaseDaysReached65 ( )
               OR PreviousStorage ( % "Sumner Reservoir" )
                   < StorageTriggerWETforecast ( % "Sumner Reservoir" ,
                                                 2.00000000 )
               AND MonthIsSeptOrOct ( ) )
          AND PreviousStorage ( % "Santa Rosa Reservoir" )
              > StorageTriggerWETforecast ( % "Santa Rosa Reservoir" ,
                                            1.00000000 )
         BlockRelease ( % "Santa Rosa Reservoir" )
```

```
        ELSE
            IF ⎧ PreviousStorage ( % "Brantley Reservoir" )                                    ⎫ THEN
               ⎪ < StorageTriggerWETforecast ⎛ % "Brantley Reservoir" , ⎞                     ⎪
               ⎪                             ⎝         0.00000000       ⎠                     ⎪
               ⎪ AND PreviousStorage ( % "Sumner Reservoir" )                                ⎪
               ⎨       < StorageTriggerWETforecast ⎛ % "Sumner Reservoir" , ⎞                 ⎬
               ⎪                                   ⎝        4.00000000      ⎠                 ⎪
               ⎪ AND PreviousStorage ( % "Santa Rosa Reservoir" )                            ⎪
               ⎩       > StorageTriggerWETforecast ⎛ % "Santa Rosa Reservoir" , ⎞            ⎭
                                                   ⎝         0.00000000        ⎠
                BlockRelease ( % "Santa Rosa Reservoir" )
            ENDIF
        ENDIF
    ELSE
        # Original threshold
        IF ⎧⎧⎧ PreviousStorage ( % "Brantley Reservoir" )                 ⎫⎫ THEN
           ⎪⎪⎪ < StorageTrigger ⎛ % "Brantley Reservoir" , ⎞             ⎪⎪
           ⎪⎪⎪                  ⎝        4.00000000         ⎠             ⎪⎪
           ⎪⎪⎨ AND NOT SumnerBlockReleaseAt15Days ( )                    ⎬⎪
           ⎪⎪⎩ AND NOT TotalBlockReleaseDaysReached65 ( )                ⎭⎪
           ⎪⎪ OR PreviousStorage ( % "Sumner Reservoir" )                ⎪
           ⎪⎨    < StorageTrigger ⎛ % "Sumner Reservoir" , ⎞            ⎬
           ⎪⎪                     ⎝       3.00000000        ⎠            ⎪
           ⎪⎩ AND NOT MonthIsSeptOrOct ( )                              ⎭
           ⎪ OR ⎧⎧ PreviousStorage ( % "Brantley Reservoir" )          ⎫⎫⎫
           ⎪    ⎪⎪ < ⎛ StorageTrigger ⎛ % "Brantley Reservoir" , ⎞ ⎞   ⎪⎪⎪
           ⎪    ⎪⎪   ⎜                ⎝        3.00000000         ⎠ ⎟   ⎪⎪⎪
           ⎨    ⎪⎨   ⎝ + SumRemainingCIDDiversion ( )              ⎠   ⎬⎪⎪
           ⎪    ⎪⎪ AND NOT SumnerBlockReleaseAt15Days ( )             ⎪⎪⎪
           ⎪    ⎪⎩ AND NOT TotalBlockReleaseDaysReached65 ( )         ⎭⎪⎪
           ⎪    ⎪ OR PreviousStorage ( % "Sumner Reservoir" )          ⎪⎪
           ⎪    ⎨    < StorageTrigger ⎛ % "Sumner Reservoir" , ⎞      ⎬⎪
           ⎪    ⎪                     ⎝       2.00000000        ⎠      ⎪⎪
           ⎪    ⎩ AND MonthIsSeptOrOct ( )                            ⎭⎪
           ⎪ AND PreviousStorage ( % "Santa Rosa Reservoir" )          ⎪
           ⎩    > StorageTrigger ⎛ % "Santa Rosa Reservoir" , ⎞       ⎭
                                 ⎝        1.00000000          ⎠
            BlockRelease ( % "Santa Rosa Reservoir" )
```

146

```
        ELSE
            IF ⎧ PreviousStorage ( % "Brantley Reservoir" )            ⎫ THEN
               ⎪  < StorageTrigger ⎛ % "Brantley Reservoir" ,  ⎞       ⎪
               ⎪                   ⎝ 0.00000000               ⎠       ⎪
               ⎪  AND PreviousStorage ( % "Sumner Reservoir" )         ⎪
               ⎨      < StorageTrigger ⎛ % "Sumner Reservoir" ,  ⎞      ⎬
               ⎪                       ⎝ 4.00000000             ⎠      ⎪
               ⎪  AND PreviousStorage ( % "Santa Rosa Reservoir" )     ⎪
               ⎪      > StorageTrigger ⎛ % "Santa Rosa Reservoir" , ⎞  ⎪
               ⎩                       ⎝ 0.00000000                ⎠  ⎭
                BlockRelease ( % "Santa Rosa Reservoir" )
            ENDIF
        ENDIF
    ENDIF
```

Execute Block Only When

IsBlockReleaseSeasonALTERNATIVES ( ) AND SantaRosaBlockReleaseOnPreviousDay ( )

RULE: Continue Sumner Block Release – WET Forecast

```
Sumner Reservoir.Outflow []
    = IF ( # Forecast time range
          ( @"Current Timestep"
            >= @"24:00:00 January 1, 1949" )
          AND # Wet forecast
              ( Forecast Info.LowerNearTermForecastProbabilityWET [ MostRecentForecastDate ( )]  )
                >= Forecast Info.WET threshold probability [] )                                    ) THEN
        # Lower threshold for stopping Block Releases
        IF ( ( PreviousStorage ( % "Brantley Reservoir" )
               < StorageTriggerWETforecast ( % "Brantley Reservoir" ,
                                             5.00000000 )
               AND PreviousStorage ( % "Sumner Reservoir" )
                   > StorageTriggerWETforecast ( % "Sumner Reservoir" ,
                                                 0.00000000 )
             AND NOT MonthIsSeptOrOct ( )
             OR ( PreviousStorage ( % "Brantley Reservoir" )
                  < ( StorageTriggerWETforecast ( % "Brantley Reservoir" ,
                                                  3.00000000 )
                    + SumRemainingCIDDiversion ( ) )
                  AND PreviousStorage ( % "Sumner Reservoir" )
                      > StorageTriggerWETforecast ( % "Sumner Reservoir" ,
                                                    0.00000000 )
                AND MonthIsSeptOrOct ( ) ) ) THEN
            BlockRelease ( % "Sumner Reservoir" )
        ENDIF
    ELSE
        # Original threshold
        IF ( ( PreviousStorage ( % "Brantley Reservoir" )
               < StorageTrigger ( % "Brantley Reservoir" ,
                                  5.00000000 )
               AND PreviousStorage ( % "Sumner Reservoir" )
                   > StorageTrigger ( % "Sumner Reservoir" ,
                                      0.00000000 )
             AND NOT MonthIsSeptOrOct ( )
             OR ( PreviousStorage ( % "Brantley Reservoir" )
                  < ( StorageTrigger ( % "Brantley Reservoir" ,
                                       3.00000000 )
                    + SumRemainingCIDDiversion ( ) )
                  AND PreviousStorage ( % "Sumner Reservoir" )
                      > StorageTrigger ( % "Sumner Reservoir" ,
                                         0.00000000 )
                AND MonthIsSeptOrOct ( ) ) ) THEN
            BlockRelease ( % "Sumner Reservoir" )
        ENDIF
    ENDIF
```

Execute Block Only When

```
IsBlockReleaseSeasonALTERNATIVES ( )
AND SumnerBlockReleaseOnPreviousDay ( )
AND NOT SumnerBlockReleaseAt15Days ( )
AND NOT TotalBlockReleaseDaysReached65 ( )
```

148

RULE: Continue Sumner Block Release – WET Forecast (Fish Counter)

FISH Rule Info.DaysInRecentSumnerBlockRelease []
= IF (# Forecast time range   THEN
       (@"Current Timestep"
         >= @"24:00:00 January 1, 1949")
       AND # Wet forecast
             (Forecast Info.LowerNearTermForecastProbabilityWET [MostRecentForecastDate ( )]
               >= Forecast Info.WET threshold probability [])
       # Lower threshold for stopping Block Releases
       IF ((PreviousStorage (% "Brantley Reservoir")   THEN
              < StorageTriggerWETforecast (% "Brantley Reservoir",
                                            5.00000000)
              AND PreviousStorage (% "Sumner Reservoir")
                  > StorageTriggerWETforecast (% "Sumner Reservoir",
                                                0.00000000)
              AND NOT MonthIsSeptOrOct ( ))
            OR (PreviousStorage (% "Brantley Reservoir")
                 < (StorageTriggerWETforecast (% "Brantley Reservoir",
                                                 3.00000000))
                   + SumRemainingCIDDiversion ( )
                 AND PreviousStorage (% "Sumner Reservoir")
                     > StorageTriggerWETforecast (% "Sumner Reservoir",
                                                   0.00000000)
                 AND MonthIsSeptOrOct ( ))
            FISH Rule Info.DaysInRecentSumnerBlockRelease [@"Previous Timestep"]
            + 1.00000000
       ENDIF
     ELSE
       # Original threshold
       IF ((PreviousStorage (% "Brantley Reservoir")   THEN
              < StorageTrigger (% "Brantley Reservoir",
                                 5.00000000)
              AND PreviousStorage (% "Sumner Reservoir")
                  > StorageTrigger (% "Sumner Reservoir",
                                     0.00000000)
              AND NOT MonthIsSeptOrOct ( ))
            OR (PreviousStorage (% "Brantley Reservoir")
                 < (StorageTrigger (% "Brantley Reservoir",
                                      3.00000000))
                   + SumRemainingCIDDiversion ( )
                 AND PreviousStorage (% "Sumner Reservoir")
                     > StorageTrigger (% "Sumner Reservoir",
                                        0.00000000)
                 AND MonthIsSeptOrOct ( ))
            FISH Rule Info.DaysInRecentSumnerBlockRelease [@"Previous Timestep"]
            + 1.00000000
       ENDIF
     ENDIF

FISH Rule Info.SumnerBlockReleaseDaysInCurrentYear []
= IF (# Forecast time range   THEN
       (@"Current Timestep"
         >= @"24:00:00 January 1, 1949")
       AND # Wet forecast
             (Forecast Info.LowerNearTermForecastProbabilityWET []
               >= Forecast Info.WET threshold probability []))
    # Lower threshold for stopping Block Releases
    IF ((PreviousStorage (% "Brantley Reservoir")   THEN
           < StorageTriggerWETforecast (% "Brantley Reservoir",
                                          5.00000000)
           AND PreviousStorage (% "Sumner Reservoir")
                 > StorageTriggerWETforecast (% "Sumner Reservoir",
                                               0.00000000)
           AND NOT MonthIsSeptOrOct ( ))
          OR (PreviousStorage (% "Brantley Reservoir")
               < (StorageTriggerWETforecast (% "Brantley Reservoir",
                                                3.00000000)
                   + SumRemainingCIDDiversion ( ))
               AND PreviousStorage (% "Sumner Reservoir")
                     > StorageTriggerWETforecast (% "Sumner Reservoir",
                                                    0.00000000)
               AND MonthIsSeptOrOct ( )))
        FISH Rule Info.SumnerBlockReleaseDaysInCurrentYear [@"Previous Timestep"]
        + 1.00000000
    ENDIF
  ELSE
    # Original threshold
    IF ((PreviousStorage (% "Brantley Reservoir")   THEN
           < StorageTrigger (% "Brantley Reservoir",
                              5.00000000)
           AND PreviousStorage (% "Sumner Reservoir")
                 > StorageTrigger (% "Sumner Reservoir",
                                    0.00000000)
           AND NOT MonthIsSeptOrOct ( ))
          OR (PreviousStorage (% "Brantley Reservoir")
               < (StorageTrigger (% "Brantley Reservoir",
                                    3.00000000)
                   + SumRemainingCIDDiversion ( ))
               AND PreviousStorage (% "Sumner Reservoir")
                     > StorageTrigger (% "Sumner Reservoir",
                                        0.00000000)
               AND MonthIsSeptOrOct ( )))
        FISH Rule Info.SumnerBlockReleaseDaysInCurrentYear [@"Previous Timestep"]
        + 1.00000000
    ENDIF
  ENDIF

Execute Block Only When
IsBlockReleaseSeasonALTERNATIVES ( )
AND SumnerBlockReleaseOnPreviousDay ( )
AND NOT SumnerBlockReleaseAt15Days ( )
AND NOT TotalBlockReleaseDaysReached65 ( )

150

FUNCTION: Most Recent Forecast Date

```
IF⎛ # March 1st Forecast                                              ⎞THEN
   ⎜⎛ @"Current Timestep" > @"24:00:00 March 1, Current Year"   ⎞⎟
   ⎝⎝ AND @"Current Timestep" < @"24:00:00 May 1, Current Year" ⎠⎠
     @"24:00:00 March 1, Current Year"
ELSE
   IF⎛ # May 1st Forecast                                           ⎞THEN
      ⎝( @"Current Timestep" < @"24:00:00 June 1, Current Year" )⎠
        @"24:00:00 May 1, Current Year"
   ELSE
      IF⎛ # June 1st Forecast                                          ⎞THEN
         ⎝( @"Current Timestep" < @"24:00:00 July 15, Current Year" )⎠
           @"24:00:00 June 1, Current Year"
      ELSE
         IF⎛ # July 15th Forecast                                              ⎞THEN
            ⎝( @"Current Timestep" < @"24:00:00 September 1, Current Year" )⎠
              @"24:00:00 July 15, Current Year"
         ELSE
            # September 1st Forecast
            @"24:00:00 September 1, Current Year"
         ENDIF
      ENDIF
   ENDIF
ENDIF
```

In addition to the rules and functions listed above, the following rules were turned off for the modification of block releases.

- Continue Santa Rosa Block Release – Alternatives & BO

- Continue Sumner Block Release – Alternatives & BO

- Continue Sumner Block Release – Alternatives & BO- Counter

Rules and Functions for Allotment Calculation Modifications

FUNCTION: Estimate CID Allotment

$$\text{Floor}\left[\frac{\text{Max}\left[10.00000000, \begin{array}{l} * \text{Max}\left[\text{Min}\left[\begin{array}{l}\text{DeliveryEfficiency}(\%\text{"CID Diversion"}) \\ * \left(\dfrac{\begin{array}{l}\text{BrantleyEffectiveEntitlementStorage}() \\ + \text{ForecastedAdditionalStorage}() \\ + \text{TotalDiversionToDate}(\%\text{"CID Diversion"}) \\ - \text{StorageToRetain}(\%\text{"CID Diversion Data"})\end{array}}{\text{IrrigableAcres}(\%\text{"CID Diversion"})}\right), \\ \text{MaxAllotment}(\%\text{"CID Diversion"})\end{array}\right], \\ \left(\begin{array}{l}\text{CID Diversion Data.LastEstimateCIDAllotment}[@\text{"Previous Timestep"}] \\ + 0.01000000[\text{"feet"}]\end{array}\right)\right] \end{array}\right], 1.00000000[\text{"feet"}]\right)}{10.00000000}\right]$$

FUNCTION: Forecasted Additional Storage

Forecast Info.ForecastPercentile [MostRecentForecastDate ( )]

FUNCTION: Most Recent Forecast Date

```
IF ( # March 1st Forecast
     ( @"Current Timestep" > @"24:00:00 March 1, Current Year"
       AND @"Current Timestep" < @"24:00:00 May 1, Current Year" ) ) THEN
     @"24:00:00 March 1, Current Year"
ELSE
  IF ( # May 1st Forecast
       ( @"Current Timestep" < @"24:00:00 June 1, Current Year" ) ) THEN
     @"24:00:00 May 1, Current Year"
  ELSE
    IF ( # June 1st Forecast
         ( @"Current Timestep" < @"24:00:00 July 15, Current Year" ) ) THEN
       @"24:00:00 June 1, Current Year"
    ELSE
      IF ( # July 15th Forecast
           ( @"Current Timestep" < @"24:00:00 September 1, Current Year" ) ) THEN
         @"24:00:00 July 15, Current Year"
      ELSE
         # September 1st Forecast
         @"24:00:00 September 1, Current Year"
      ENDIF
    ENDIF
  ENDIF
ENDIF
```